

**MAGNETIC RESONANCE IMAGING AS A TOOL  
FOR THE DETECTION AND CHARACTERIZATION  
OF RAT PITUITARY LESIONS**

**Joop H.J. van Nesselrooij**

The cover shows a T1-weighted midline sagittal high resolution image of a normal (left) and hypertrophic (right) rat pituitary gland (chapter V, figures 1 and 2).  
The cover is designed by Al. van Nesselrooij.

MAGNETIC RESONANCE IMAGING AS A TOOL FOR THE  
DETECTION AND CHARACTERIZATION OF RAT  
PITUITARY LESIONS

*DETECTIE EN KARAKTERISERING VAN  
HYPOFYSELESIES BIJ DE RAT MET BEHULP  
VAN KERNSPIN TOMOGRAFIE*

(Met een samenvatting in het Nederlands)

PROEFSCHRIFT

ter verkrijging van de graad van doctor aan de Rijksuniversiteit te Utrecht  
op gezag van de Rector Magnificus Prof. Dr. J.A. van Ginkel ingevolge  
het besluit van het College van Dekanen in het openbaar te verdedigen op  
donderdag 7 mei 1992 des namiddags te 16.15 uur.

door

Johannes Henricus Joseph van Nesselrooij

geboren 24 juli 1946 te Utrecht

CIP-GEGEVENS KONINKLIJKE BIBLIOTHEEK, DEN HAAG

Nesselrooij, Johannes Henricus Joseph van

Magnetic resonance imaging as a tool for the detection and characterization of rat pituitary lesions / Johannes Henricus Joseph van Nesselrooij. - Utrecht : Universiteit Utrecht, Faculteit Diergeneeskunde  
Proefschrift Rijksuniversiteit Utrecht. - Met samenvatting in het Nederlands.

ISBN 90-393-0231-6

Trefw.: hersenziekten ; ratten.

**Promotores:**

Prof. Dr. V.J. Feron  
Prof. Dr. S.W.J. Lamberts  
Prof. Dr. R. Kroes

**Co-promotor:**

Dr. M.C. Bosland

Het drukken van dit proefschrift werd mogelijk gemaakt door financiële steun van de Nederlandse Kankerbestrijding (Dutch Cancer Society) en van het Instituut voor Toxicologie en Voeding TNO.

**Beoordelingscommissie:**

Prof. Dr. W. Misdorp  
Prof. Dr. A. Rijnberk  
Prof. Dr. E.J. Ruitenberg  
Prof. Dr. W. Seinen  
Prof. Dr. P.F.G.M. van Waas

## **PREFACE**

The studies described in this thesis were in part conducted at the Nuclear Magnetic Resonance Research Laboratory, Department of Radiology, State University of New York, Health Science Center at Syracuse, Syracuse NY 13210, USA, and in part at the TNO Toxicology and Nutrition Institute, Department of Biological Toxicology, Zeist, The Netherlands. They were financially supported by the Dutch Cancer Society (Nederlandse Kankerbestrijding, Stichting Koningin Wilhelmina Fonds, grant No CIVO 87-2) and the Netherlands Ministry of Welfare, Public Health and Culture.

## TABLE OF CONTENTS

<b>PREFACE</b> .....	<b>7</b>
<b>TABLE OF CONTENTS</b> .....	<b>8</b>
<b>ABBREVIATIONS</b> .....	<b>11</b>
<b>CHAPTER I</b> .....	<b>13</b>
General Introduction	
<b>CHAPTER II</b> .....	<b>19</b>
Correlations between presence of spontaneous lesions of the pituitary (adenohypophysis) and plasma prolactin concentration in aged Wistar rats. Veterinary Pathology, in press.	
<b>CHAPTER III</b> .....	<b>37</b>
Magnetic resonance imaging of estrogen-induced pituitary hypertrophy in rats. Magnetic Resonance in Medicine 11: 161-171, 1989.	
<b>CHAPTER IV</b> .....	<b>51</b>
Magnetic resonance imaging compared with hormonal effects and histopathology of estrogen-induced pituitary lesions in the rat. Carcinogenesis 12: 289-297, 1991.	
<b>CHAPTER V</b> .....	<b>63</b>
Gadolinium-DTPA enhanced and digitally subtracted magnetic resonance imaging of estrogen-induced pituitary lesions in rats: Correlation with pituitary anatomy. Magnetic Resonance Imaging 8: 525-533, 1990.	



<b>CHAPTER VI</b> .....	<b>75</b>
Pathogenesis of blood-filled cavities in the anterior pituitary gland of estrogen-treated male rats. Toxicologic Pathology, in press.	
<b>CHAPTER VII</b> .....	<b>89</b>
Magnetic resonance image analysis of estrogen-induced pituitary lesions in rats using T1 and T2 weighted intensities. Magnetic Resonance in Medicine, submitted.	
<b>CHAPTER VIII</b> .....	<b>101</b>
Rat pituitary changes observed with magnetic resonance imaging following removal of estrogen stimulus: Correlation with histopathology and immunohistology. Carcinogenesis 13: 277-282, 1992	
<b>SUMMARY AND CONCLUSIONS</b> .....	<b>111</b>
<b>SAMENVATTING</b> .....	<b>119</b>
<b>DANKWOORD/ACKNOWLEDGEMENTS</b> .....	<b>127</b>
<b>CURRICULUM VITAE</b> .....	<b>131</b>



## ABBREVIATIONS

---

ACTH	Adrenocorticotroph hormone
CS	Compressed sinusoid
CSF	Cerebro-spinal fluid
E2	Oestrogen
FOV	Field of view
FSH	Follicle stimulating hormone
Gd-DTPA	Gadolinium diethylenetriaminepentaacetic acid
GH	Growth hormone
HE	Hematoxylin and eosin
IU	International units
iv	Intravenous
LH	Luteinizing hormone
MRI	Magnetic resonance imaging
MR	Magnetic resonance
ms	Milliseconds
$\mu\text{m}$	Micrometer
ng	Nanogram
NIAMDD	National Institute of Arthritis, Metabolism and Digestive Disease
NMR	Nuclear magnetic resonance
NO	Not observed
PRL	Prolactin
RER	Rough endoplasmic reticulum
RF	Radio frequency
RIA	Radioimmunoassay
ROI	Regions of interest
sc	Subcutaneous
SD	Standard deviation
SE	Spin echo
SEM	Standard error of the mean
TE	Time of echo
TR	Time of repetition
TSH	Thyroid stimulating hormone



# CHAPTER I

## GENERAL INTRODUCTION



## GENERAL INTRODUCTION

Magnetic Resonance Imaging (MRI) is a new very powerful non-invasive method for the detection and characterization of neoplasia and other disease states that involve local tissue changes. MRI is exquisitely suitable for the early detection of small tissue lesions because of its high resolution, yielding images superior to those obtained by X-ray and CAT scanning methodologies. Clinical studies of intracranial disease processes have particularly benefitted from MRI techniques (1,2,3). These methods have also shown great promise as a tool for experimental studies on the development of intracranial neoplasia (4,5,6).

MRI can be defined as the application of nuclear magnetic resonance (NMR) methods for the imaging of human and animal tissues in which the distribution and dynamic properties of protons in tissues can be displayed. The principal aim of MRI techniques is to produce, non-invasively, a two- or three-dimensional image of the spatial distribution of resonant nuclei in living tissue. Any nucleus such as a proton (hydrogen nucleus) which possesses a magnetic moment, attempts to align itself with the local magnetic field within which it is placed. Application of a radio frequency (RF) pulse of a specific frequency displaces the net magnetic moment by an amount determined by the strength and duration of the pulse. This frequency is directly proportional to the strength of the magnetic field, and is known as the resonance frequency. After the pulse, the protons can emit an RF signal as they return to their original orientation along the Z axes. When a gradient is introduced into the magnetic field, the resonant frequency of protons in a tissue placed in the gradient will vary with their position. Thus, the frequency of the signals emitted by protons after applying a RF pulse will reflect their position. The signal is recorded and stored by the computer and later converted into an image.

The overall objective of the research described in this thesis was to evaluate MRI as a method for the early detection and characterization of tumor development in the rat pituitary as a model for human intracranial neoplastic disease. Specifically, estrogen-induced anterior pituitary tumors in male rats were studied as a model for spontaneous neoplasia of the pituitary gland. Pituitary tumors are frequent in aging humans and rats (7,8,9), and the majority of these tumors consists of prolactin (PRL)-secreting cells (8,9,10).

Therefore, elevation of plasma concentrations of PRL is often used as a diagnostic indicator of pituitary tumors in man, although there is considerable doubt about the reliability of this parameter (11,12,13). Thus, such tumors often present serious diagnostic problems, for which the advent of MRI has been an important solution (14).

The feasibility of MRI for the detection of spontaneous and estrogen-induced pituitary tumors in the rat has been demonstrated previously (4,5,6,15,16). However, the **development** of rat pituitary tumors and their putative precursor lesions, correlations between MR images and histomorphology of rat pituitary lesions, and the use of new contrast agents and computerized analysis methods to enhance MR images in this context have not been studied before. These issues comprise the principal focus of this thesis. The specific aims of the studies described herein were:

- To develop a biologically-based classification system for the entire spectrum of hypertrophic and proliferative lesions of the rat pituitary (**Chapter II**).
- To develop and apply MRI techniques for non-invasive visualization of estrogen-induced rat pituitary lesions as a model for spontaneous lesions (**Chapters III, IV, V, VII, VIII**).
- To compare MR images of the rat pituitary with the light microscopic morphology of estrogen-induced pituitary lesions and with information derived from plasma levels of pituitary hormones, (**Chapters IV, V, VIII**).
- To study by MRI the development of estrogen-induced pituitary lesions and their regression after withdrawal of the estrogen stimulus (**Chapters IV, VIII**), and
- To establish the histopathogenesis of blood-filled cavities in rat estrogen-induced pituitary tumors (**Chapter VI**) because of the possible role of these cavities in MR image enhancement by a magnetic relaxation contrast agent (**Chapter V**).

The following studies were conducted to accomplish these objectives. In **Chapter II**, a classification system is described for the entire spectrum of spontaneous focal hypertrophic and proliferative lesions of the rat pituitary. The morphologic criteria developed were shown to correlate well with the PRL immunoreactivity of the lesions and/or their ability to elevate plasma PRL levels. In **Chapter III**, MRI techniques were

applied to visualize estrogen-induced rat pituitary lesions with changes in pituitary anatomy apparent as early as 16 days after implantation of an estrogen pellet. Studies described in **Chapter IV** compared MRI-derived information on the development of estrogen-induced rat pituitary lesions with (i) plasma concentrations of pituitary hormones viz. PRL, growth hormone (GH), luteinizing hormone (LH), follicle stimulating hormone (FSH), thyroid stimulating hormone (TSH) as measured with RIA-techniques, and (ii) the light microscopic morphology of the induced lesions further characterized by immunohistochemical methods for the same pituitary hormones. **Chapter V** summarizes a study in which a magnetic relaxation contrast agent in combination with a digital subtraction technique was used to improve the MRI detection and characterization of rat pituitary lesions induced by estrogen. **Chapter VI** describes an ultrastructural study of sequential estrogen-induced morphological changes in the rat pituitary to establish the histopathogenesis of blood-filled cavities in pituitary tumors. In **Chapter VII**, the detection of subtle intensity changes on MR images of the rat pituitary using computer-generated two dimensional scatterplots is demonstrated. **Chapter VIII** deals with a study of the progression of estrogen-induced proliferative lesions in the rat pituitary and their regression after withdrawal of the estrogen stimulus after various times of exposure. Major findings and conclusions are high-lighted and put into perspective in **Summary and Conclusions**.

#### REFERENCES

1. Daniels D.L., Haughton V.M. and Naidich T.P. (Eds) Cranial and spinal magnetic resonance imaging; an atlas and guide. Raven Press, New York, 1987.
2. Brant-Zawadzki M., Norman D. (Eds) Magnetic resonance imaging of the central nervous system. Raven Press, New York, 1987.
3. Partain C.L., Price R.R., Patton J.A., Kulkarni M.V. and James Jr. A.E. (Eds) Magnetic resonance imaging. Vol 1&2, W.B. Saunders, Philadelphia, 1988.
4. Van Nesselrooij J.H.J., Szeverenyi N.M. and Ruocco M.J. (1998) Magnetic resonance imaging of estrogen-induced pituitary hypertrophy in rats. *Magn. Reson. Med.* 11, 161-171.
5. Van Nesselrooij J.H.J., Szeverenyi N.M., Tillapaugh-Fay G.M. and Hendriksen F.G.J. (1990) Gadolinium-DTPA enhanced and digitally subtracted magnetic resonance imaging of estrogen induced pituitary lesions in rats: Correlation with pituitary anatomy. *Magn. Reson. Imag.* 40, 525-533.
6. Van Nesselrooij J.H.J., Bruijntjes J.P., Garderen-Hoetmer A., Tillapaugh-Fay G.M. and Feron V.J. (1991) Magnetic resonance imaging compared with hormonal effects and histopathology of estrogen-induced pituitary lesions in the rat. *Carcinogenesis* 12, 289-297.
7. Gold E.B. (1981) Epidemiology of pituitary adenomas. *Epidemiol.Rev.* 3, 163-183.
8. Berkvens J.M., Van Nesselrooij J.H.J. and Kroes R. (1980) Spontaneous tumours in the pituitary gland of old Wistar rats: A morphological and immunocytochemical study. *J. Pathol.* 130, 179-191.
9. Trouillas J., Girod C., Claustrat B., Cure M. and Dubois M.P. (1982) Spontaneous pituitary tumors in the Wistar/Furth/Ico rat strain. *Am. J. Pathol.* 109, 57-70.
10. Hankins C.A., Zamani A.A. and Rumbaugh C.L. (1985) Prolactinomas: Clinical presentation, radiologic assessment and therapeutic options. *Invest. Radiol.* 20, 345-354.
11. Kleinberg D.L., Noel G.L. and Frantz A.G. (1977) Galactorrhea: A study of 235 cases including 48 with pituitary tumors. *N. Eng. J. Med.* 269, 589-600.
12. Malarkey W.B. and Johnson J.C. (1976) Pituitary tumors and hyperborean. 136, 40-44.
13. Kovacs K., Lloyd R., Horvath E., Asa E., Stefaneanu L., Killinger D.W. and Smyth H.S. (1989) Silent somatotrophic adenomas of the human pituitary; A morphologic study of three cases including immunocytochemistry, electron microscopy, in-vitro examination and in-situ hybridization. *Am. J. Pathol.* 134, 345-353.
14. Kulkarni M.V., Lee K.F., McArdle G.B., Yeakly J.W. and Haar F.L. (1988) 1.5-T MR imaging of pituitary microadenomas: technical considerations and CT correlation. *Am. J. Neuroradiol.* 9, 5-11.
15. Rudin M., Briner U. and Doepfner W. (1988) Quantitative magnetic resonance imaging of estradiol-induced pituitary hyperplasia in rats. *Magn. Reson. Med.* 7, 285-291.
16. Dixon D., Johnson G.A., Cofer G.P., Hedlund L.W. and Maronpot R.R. (1988) Magnetic resonance imaging (MRI): A new tool in experimental toxicologic pathology. *Toxicol Pathol.* 16, 386-391.







## **CHAPTER II**

### **CORRELATIONS BETWEEN PRESENCE OF SPONTANEOUS LESIONS OF THE PITUITARY (ADENOHYPHYSIS) AND PLASMA PROLACTIN CONCENTRATION IN AGED WISTAR RATS**

Joop H.J. van Nesselrooij, C. Frieke Kuper and Maarten C. Bosland.

Veterinary Pathology, in press.



## Correlations Between Presence of Spontaneous Lesions of the Pituitary (Adenohypophysis) and Plasma Prolactin Concentration in Aged Wistar Rats

Joop H.J. van Nesselrooij<sup>1</sup>, C. Frieke Kuper<sup>1</sup> and Maarten C. Bosland<sup>2</sup>

<sup>1</sup>Laboratory of Pathology, Department of Biological Toxicology, TNO Toxicology and Nutrition Institute, 3704 HE Zeist, The Netherlands.

<sup>2</sup>Institute of Environmental Medicine, New York University Medical Center, Tuxedo, New York 10987, USA.

### ABSTRACT

The predictive value of elevated plasma prolactin concentrations for the presence of spontaneous pituitary lesions was studied in 40 male and 38 female 30 months-old Wistar (Cpb:WU) rats. The pituitaries were examined by light microscopy and stained for prolactin by immunohistochemistry. Plasma prolactin concentrations were measured by radio-immunoassay. Pituitary lesions were classified on the basis of HE morphology as foci of hypertrophic or hyperplastic cells, and hemorrhagic, pleomorphic or spongicytic adenomas; no carcinomas were found. There were significantly ( $P=0.001$ ) more female than male rats with pituitary adenomas (58% of females; 33% of males) or without any pituitary lesions (21% females; 5% of males). However, there were less female (21%) than male rats (63%) with foci of hyperplastic and/or hypertrophic cells but no adenomas in the pituitary ( $P=0.001$ ). Elevation of plasma prolactin concentration above the upper 99th percentile value in age-matched rats without lesions was predictive, but not conclusively, of the presence of pituitary hemorrhagic adenomas in both sexes. It was, however, not predictive of the presence of foci of hypertrophic or hyperplastic cells. Elevation of plasma prolactin concentration above 10 ng/ml in male and 60 ng/ml in female rats was conclusive for the presence of hemorrhagic adenomas. Using multivariate analysis, significant positive correlations ( $P<0.01$ ) were found between plasma prolactin concentration and presence and size of hemorrhagic adenomas and their prolactin staining intensity (correlation coefficients between 0.392 and 0.652). Foci of hyperplastic cells stained positive for prolactin, whereas hypertrophic cell foci and pleomorphic and spongicytic adenomas did not stain for prolactin. There were no correlations (coefficients of less than + or - 0.189) between plasma prolactin concentration and

the presence of hypertrophic or hyperplastic cell foci and pleomorphic or spongicytic adenomas in the pituitary. The morphologic criteria developed to distinguish spontaneous hypertrophic, hyperplastic, and neoplastic lesions of the rat pituitary corresponded well with their prolactin immunoreactivity and/or ability to elevate plasma prolactin concentration. Therefore, these criteria constitute a biologically meaningful classification system for these rat pituitary lesions.

### INTRODUCTION

The anterior pituitary of aged rats frequently has hyperplastic and neoplastic lesions consisting of one or more of the hormone-producing cell types which are normally present in this gland (4, 10, 12, 16, 23, 27, 29, 35, 36, 44-47). These lesions consist predominantly of prolactin-containing cells as assessed by immunohistochemical methods (1, 29, 36). Elevation of plasma prolactin concentration is often used as a diagnostic indicator of pituitary tumors in humans (17, 19, 20), although there is considerable doubt concerning the reliability of this diagnostic parameter (1). Preliminary findings in male rats of the Wistar strain used in this study, which develops proliferative pituitary lesions in high incidence, indicated a correlation between specific types of pituitary tumors and elevated plasma prolactin concentrations (44). There was, however, no perfect consistency in this relationship, because some rats with pituitary tumors had the same plasma prolactin concentration as control rats, and some rats without tumors had slightly elevated plasma prolactin concentrations (44). The purpose of this study was to assess the predictive value of elevated plasma prolactin concentrations for the presence of tumors and non-neoplastic spontaneous lesions in the pituitary of aged Wistar rats. Correlations between plasma prolactin concentration and type, size, and prolactin

immunoreactivity of pituitary lesions were determined. Earlier mentioned preliminary data on pituitary tumors in aged male rats (44) were re-evaluated, together with observations on non-neoplastic pituitary changes that could be associated with tumor development, and they were compared with data on female rats. In addition, variables other than pituitary lesions that may influence plasma prolactin concentration (5, 13-15, 24, 30, 38, 40) were correlated with plasma prolactin concentration in an attempt to explain observed discrepancies between elevation of plasma prolactin concentration and the presence of pituitary lesions.

## MATERIALS AND METHODS

Weanling, random-bred Wistar rats (Cpb:WU), were obtained from the Central Institute for Breeding of Laboratory Animals TNO, Zeist, The Netherlands. Animals were used in a life-span study with sequential temporal kills in which the background lesions of this strain were documented. The animals were of weaning age at the start of the study, and no rats received any treatment. Groups of 200 male and 200 female rats were kept until about 80% had died, at which time the remaining 40 male and 38 female rats, 30 months of age, were killed and were used for the present study. Rats were housed under conventional conditions in a well-ventilated room at 23°C with 40-70% relative humidity and a 12-hour light/12-hour dark cycle. Male and female rats were separated, and housed, five to a cage, in stainless steel, wire-mesh suspended cages. The rats were fed an in house prepared powdered, natural ingredient diet (see reference 3, with minor modifications, including a vitamin A content of 6340 IU/kg diet and omission of choline suppletion). The animals had free access to food and tap water.

The animals were killed by decapitation between 9 and 12 a.m.; no anesthesia was used to avoid stress and anesthesia-induced prolactin release. Blood was sampled from the severed neck and plasma was separated and stored at -20°C. Plasma concentrations of prolactin, were measured by radioimmunoassay (RIA) according to Kwa et al. (25), using the antiserum obtained from NIAMDD, with an intra-assay variability of 7% and an inter-assay variability of 11%. Plasma concentrations of testosterone, 5-dihydrotestosterone, and estradiol-17 $\beta$  were measured by RIA using antisera raised in rabbits to testosterone-3(o-carboxymethyl) ether-bovine serum albumin (60% cross-reactivity with 5-dihydrotestosterone) and 17 $\beta$ -estradiol-6(o-carboxymethyl)ether-bovine serum albumin, after separation of testosterone and 5-dihydrotestosterone

by HPLC or purification of estradiol-17 $\beta$  by column chromatography. The intra-assay variability of these assays was 5-10%, and the inter-assay variability 10-15%.

A complete necropsy was performed on all animals. The pituitary, thymus, mammary gland and gonads were fixed in a 4% neutral buffered formaldehyde solution. These tissues were embedded in paraffin and sectioned at 5  $\mu$ m thickness. One of 3 step sections of the pituitary and single sections of the other tissues were stained with hematoxylin and eosin (HE) for routine evaluation. The remaining step sections were immunostained for prolactin (34), using rabbit anti-rat antiserum obtained from the National Institute of Arthritis, Metabolism and Digestive Disease (NIAMDD), Bethesda, MD. Swine anti-rabbit immunoglobulin (Sanbio, Nistelroode, The Netherlands) was used as a bridge between the primary antiserum and rabbit peroxidase-antiperoxidase (Dako, Amsterdam, The Netherlands). The 3,3-Diaminobenzidine-tetrahydrochloride (Sigma Chemical Co, St. Louis, MO, USA) was used as substrate to visualize the product. The sections were counter-stained with Gill's type II hematoxylin.

The following criteria were used to differentiate between foci of hypertrophic or hyperplastic cells, and tumors (4, 7) (see Results for description of lesions). Hypertrophic and hyperplastic cell foci were distinguished on the basis of cytoplasmic staining (HE), cell size, and nuclear density. In comparison with normal pituitary tissue, nuclear density was lower, cells were larger, and cytoplasm was hypochromatic in hypertrophic cell foci, whereas in hyperplastic cell foci, nuclear density was higher, cells were smaller, and cytoplasm was hyperbasophilic. Hyperplastic cell foci were distinguished from tumors on the basis of growth pattern and cytomorphology. Lesions with hemorrhagic areas and/or cellular and nuclear pleomorphism were classified as neoplasms, and lesions with neither pleomorphism nor hemorrhagic areas as hyperplastic or hypertrophic cell foci. Compression, demarcation, and encapsulation were not used as criteria to distinguish hyperplastic cell foci from tumors because the degree of demarcation was highly variable even for large lesions, and some compression was occasionally found for even very small lesions; capsule formation never occurred. Unequivocal carcinomas displaying clear-cut invasive growth or metastases were not found in the present study. Yet, some tumors had highly pleomorphic cells and atypical mitotic figures and would therefore qualify as carcinoma. However, these tumors were well

demarcated and not invasive, and they were therefore classified as adenomas. Pituitary adenomas were sub-classified in three types, as previously proposed (4), on the basis of the following criteria. Hemorrhagic adenomas were characterized by the presence of hemorrhagic areas, which were never found in the two other types; spongiocytic adenomas were characterized by abundant presence of intracytoplasmic vacuoles; and pleomorphic adenomas consisted entirely of pleomorphic cells that did not have conspicuous vacuoles.

The presence, number, size, and staining intensity for prolactin of the hypertrophic, hyperplastic, and neoplastic lesions were determined for each pituitary. The size of hypertrophic or hyperplastic cell foci, neither of which influenced pituitary size, was semi-quantitatively scored based on the area occupied by the lesion as small ( $\leq 15\%$  of the pars distalis), medium-sized (16-20%) or large (21-25%). The size of adenomas was semi-quantitatively scored on the basis of their largest diameter as small (1-3 mm), medium-sized (4-7 mm), or large (8-15 mm). Staining intensity for prolactin was assessed semi-quantitatively as absent, slight, moderate, or marked. All size and staining intensity assessments were made by the same pathologist.

Because the parameters examined in this study are not normally distributed, non-parametric methods were used throughout for statistical analysis (39). The predictive value of elevation of plasma prolactin concentrations for the presence of pituitary lesions was assessed by determining, using the rank correlation method of Spearman (39), correlations between on the one hand plasma prolactin concentration and on the other hand hypertrophic, hyperplastic and neoplastic pituitary lesions, scored either as the number of lesions per animal or as absent, small, medium-size or large, as well as their prolactin staining intensity (scored as none, slight, moderate or marked). Also, correlations were calculated between plasma prolactin concentration and variables other than pituitary lesions that possibly influence plasma prolactin concentrations, i.e., plasma concentrations of testosterone, 5-dihydrotestosterone, and estradiol-17 $\beta$ , and the presence of age-related lesions in the gonads, uterus, mammary gland, and thymus (5, 13-15, 24, 30, 38, 40). Correlation coefficients of 0.4 and higher had a P value less than 0.05 and were considered significant. In order to determine the additive predictive value of combinations of variables, discriminant analysis was carried out (2). Step-wise regression analysis was conducted to select the optimal set of variables

for performing this analysis, and parameters were excluded if only a single animal had a specific variable and/or an elevated plasma prolactin concentration (2). Differences in the incidence of lesions between males and females were analyzed using the Fisher exact test and the  $X^2$  test (39). Differences in prolactin concentrations between animals with and without the various pituitary lesions were analyzed using the Kruskal-Wallis one-way analysis of variance and the Mann-Whitney test (39).

## RESULTS

### Morphology of Pituitary Lesions

The cells that stained positively for prolactin were diffusely and randomly distributed throughout the pars distalis of normal pituitaries. This pattern was altered in pituitaries that had foci of hypertrophic or hyperplastic cells or adenomas. These lesions were more or less well demarcated, sometimes expansile, focal processes that differed from normal pituitary tissue in cytomorphology, prolactin staining properties, and/or growth pattern, but were never encapsulated. Invasive growth and metastases were never found. The morphology of each of these pituitary lesions is described in the following.

Foci of hypertrophic cells (Figs. 1a and b). Hypertrophic cell foci consisted of solid sheets of enlarged cells with clear cytoplasm and distinct eosinophilic cell boundaries (HE). Density of nuclei in these foci was lower than in normal pituitary tissue. The nuclei had no abnormalities and mitotic figures were not observed. Hypertrophic cells did not stain for prolactin. These foci were not always clearly demarcated, but compression of surrounding tissue by these foci was never observed. There was no specific area in the pars distalis where these foci were located. Foci occupied an area varying from 10 to 25% of the pars distalis.

Foci of hyperplastic cells (Figs. 2a and b). Cells in foci of hyperplastic cells were uniform and were mainly arranged in solid sheets. The cells in these foci were smaller in comparison with normal pituitary tissue, and the density of the nuclei was increased. Cytoplasm was hyperbasophilic and nuclei had prominent nucleoli (HE). Mitotic figures were not observed. All foci stained positive for prolactin. Most, but not all, foci were well circumscribed with little or no compression of the adjacent pituitary tissue. The localization of the foci of hyperplastic cells within the anterior

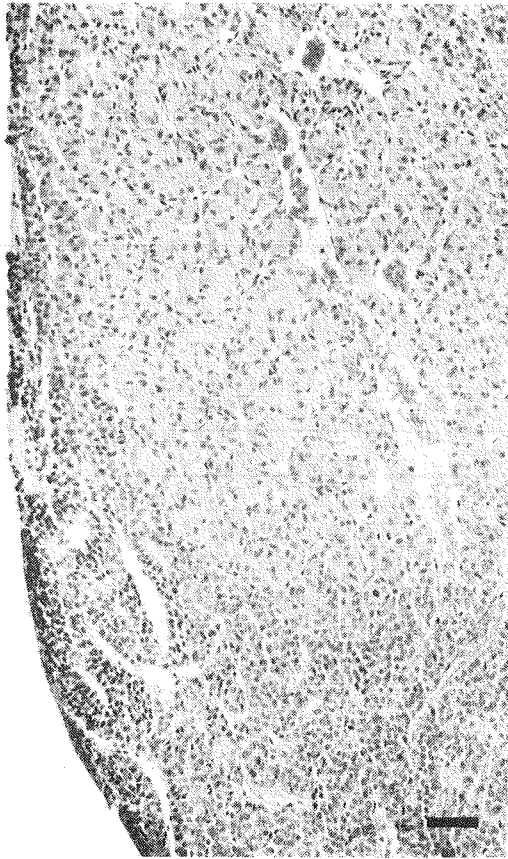
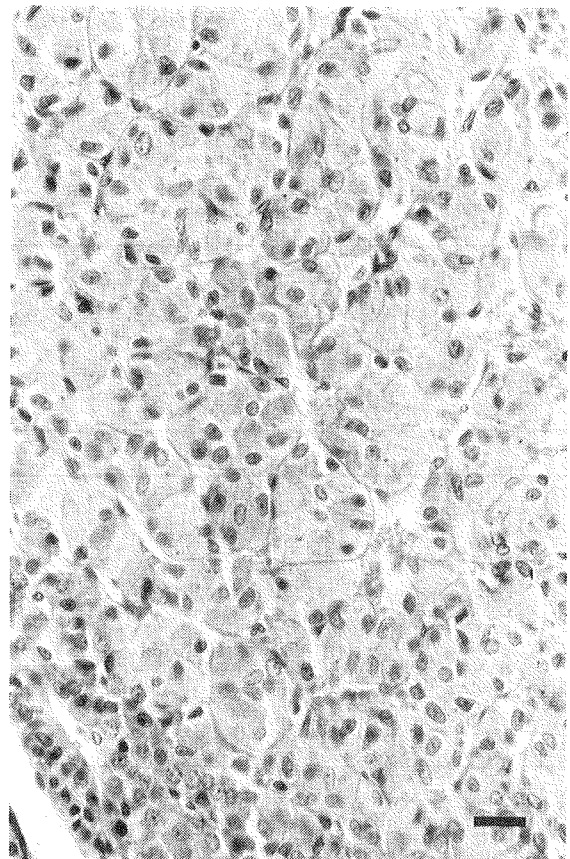


Fig. 1 -- Focus of hypertrophic cells.

a. On the top and right hand side a hypertrophic cell focus with no compression of surrounding tissue; on the bottom and left hand side normal pituitary cells. HE, bar = 50  $\mu$ m

pituitary was variable. The lesions occupied an area ranging in size from 10 to 25 % of the pars distalis. There was no correlation between size of the foci and the intensity of staining for prolactin.

Hemorrhagic pituitary adenomas (Figs. 3a, b and c). Hemorrhagic pituitary adenomas consisted of cells that were arranged in solid cords or trabeculae of one to up to several cell layers thick. These adenomas were characterized by the presence of smaller or larger hemorrhagic cavities or cysts. These cavities gave the adenomas the appearance of consisting cords of tumor cells with on one side cleft-like sinusoids covered with endothelial cells, and on the other side cyst-like spaces which were not lined with endothelial cells. These cavities were always filled with blood and occasionally contained some necrotic pituitary epithelial cells. The tumor cells had mostly pale cytoplasm and varied in size and shape, but the nuclei were rather uniform although their tinctorial properties varied (HE). This type of tumors always stained positively for prolactin, although to a variable



b. Higher magnification of a. showing enlarged cells with clear cytoplasm and distinct cell boundaries which were eosinophilic; in the lower left hand corner a small rim of normal cells is visible. HE, bar = 20  $\mu$ m

degree. Some adenomas had zones consisting of large, markedly pleomorphic cells arranged in solid fields with frequent, sometimes abnormal, mitotic figures. These pleomorphic zones did not stain for prolactin. The adenomas were well demarcated and no invasive growth was seen, but they were expansile and compressed surrounding normal pituitary tissue. These adenomas ranged from small focal lesions to large masses that occupied the entire pituitary. There was no correlation between tumor size and staining intensity for prolactin.

Pleomorphic pituitary adenomas (Fig. 4). Pleomorphic adenomas consisted of cells that were arranged in solid sheets or cord-like structures. Endothelium-lined sinusoids were present on both sides of the cords. The tumor cells were large and polygonal and markedly pleomorphic with considerable variation in size, shape and tinctorial properties of cell and nucleus. Atypical mitotic figures were frequent. These adenomas did not stain for prolactin. They were small to medium-



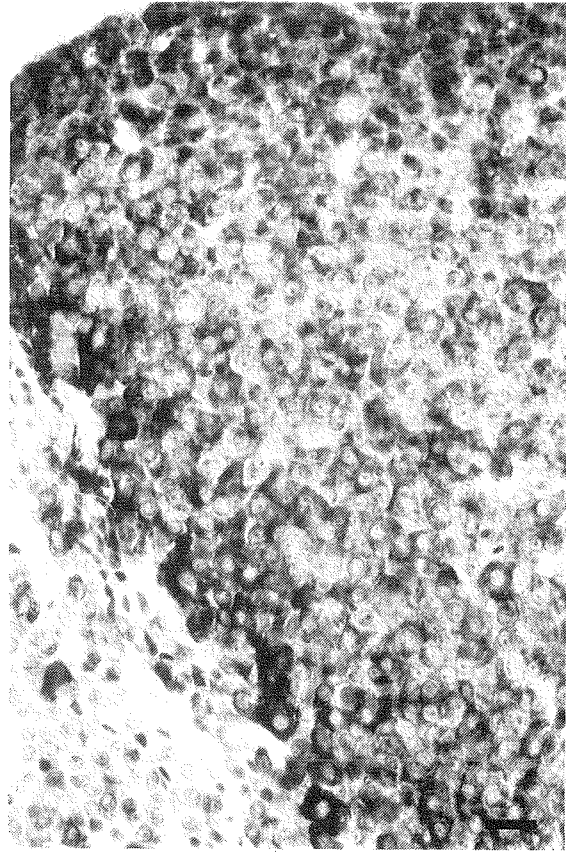
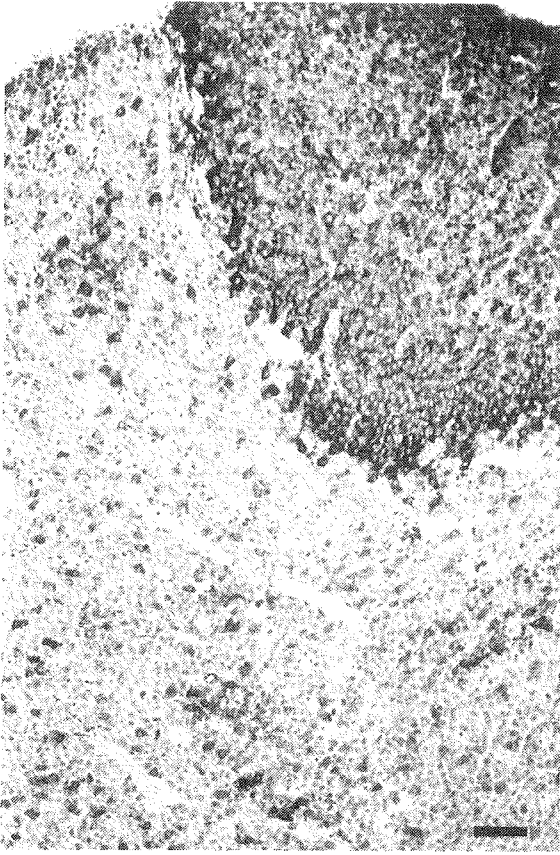


Fig. 2 -- Focus of hyperplastic cells.

a. In the upper right hand corner a prolactin-positive focus of hyperplastic cells with little or no compression of surrounding tissue; on the bottom and left hand side normal pituitary cells, some of which are prolactin positive. Staining for prolactin, bar = 50  $\mu$ m.

b. Higher magnification of a.; there is increased nuclear density and several nuclei have prominent nucleoli; most cells have immunoreactivity for prolactin, which is particularly strong in the cells of the rim of the focus. In the lower left hand corner are normal cells visible, most of which are prolactin-negative. Staining for prolactin, bar = 20  $\mu$ m.

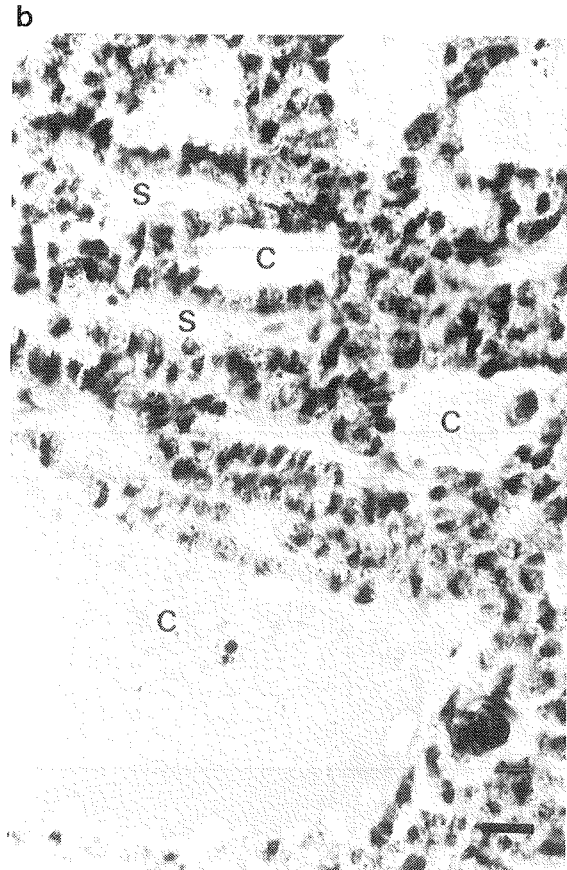
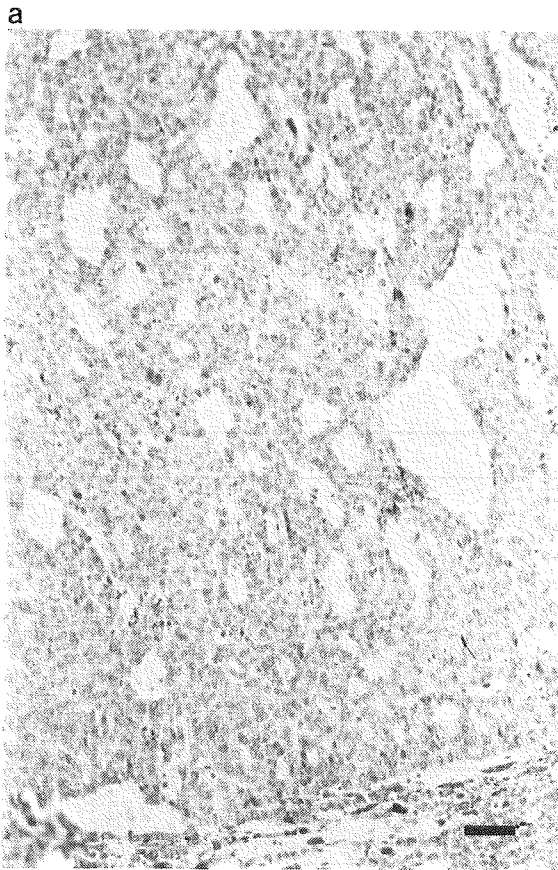
sized, and were well demarcated and caused compression of surrounding tissue.

Spongicytic pituitary adenoma (Fig. 5). One tumor was classified as a spongicytic adenoma (Table 1). This adenoma consisted of thin cords, 1-3 cell layers thick interspersed with endothelial-lined sinusoids. The tumor cells were uniformly round or oval with pale cytoplasm containing many small or large vacuoles. Nuclei varied in size, but mitotic figures were rare. The cells did not stain for prolactin. The adenoma was medium-sized and well demarcated.

#### Incidence of Pituitary Lesions and Plasma Prolactin Concentrations

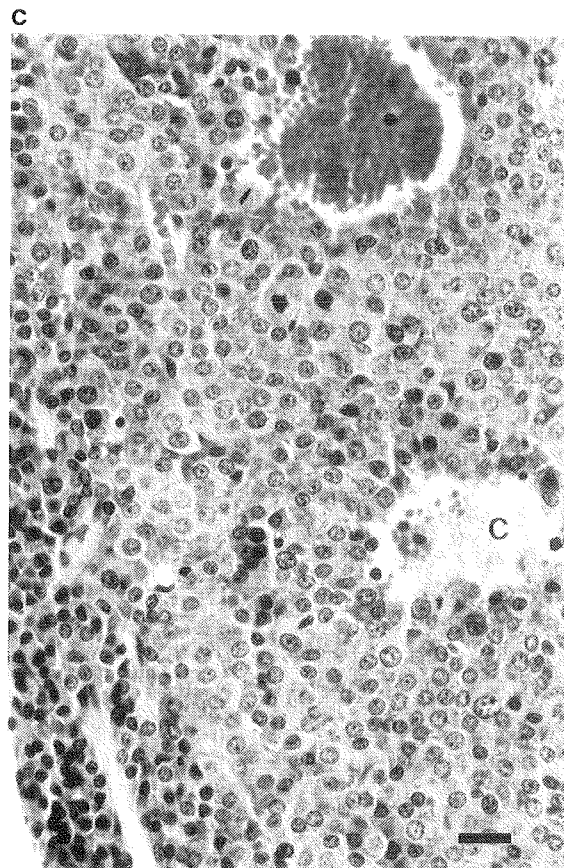
Many rats had multiple types of pituitary lesions. Several rats had multiple foci of hypertrophic or hyperplastic cells, and a few rats

had multiple adenomas. This lesion multiplicity complicated analysis of the data, in particular correlations between lesion occurrence and plasma prolactin concentration. Therefore, the data were reduced as follows. Rats were distinguished into five separate groups, 1) rats with pituitary adenomas, distinguishing the three morphologic sub-types of adenomas as indicated earlier, 2) rats with hypertrophic or hyperplastic cell foci but no adenomas, 3) rats with hyperplastic cell foci, irrespective of the presence of hypertrophic cell foci, but no adenomas, 4) rats with hypertrophic cell foci but neither hyperplastic cell foci nor adenomas, and 5) rats without any pituitary lesions. Within the groups with lesions, rats were ranked according to the largest lesion present, assuming that the largest lesion would have greatest potential impact on the plasma concentration of prolactin. The mean, median, range, and 95th and 99th percentile values of plasma prolactin concentrations for each of these groups were calculated by sex.



**Fig. 3 -- Hemorrhagic adenoma.**

- a. A hemorrhagic adenoma with many cyst-like spaces; on the bottom a small rim of normal pituitary cells is visible. HE, bar = 50  $\mu$ m.
- b. Higher magnification of a.. This adenoma consisted of prolactin-positive cells arranged in solid cords, one or a few cell layers thick; on one side of the cords there are cleft-like sinusoids (S) covered with endothelial cells (arrows) and at the other side cyst-like spaces (C) filled with blood and some necrotic cells. Staining for prolactin, bar = 20  $\mu$ m.
- c. This adenoma consisted of solid cords of cells, many cell layers-thick; otherwise it had the same morphology as the adenoma shown in a. and b.. There are some mitotic figures (arrow heads) and a small rim of normal pituitary cells at the bottom. HE, bar = 20  $\mu$ m.



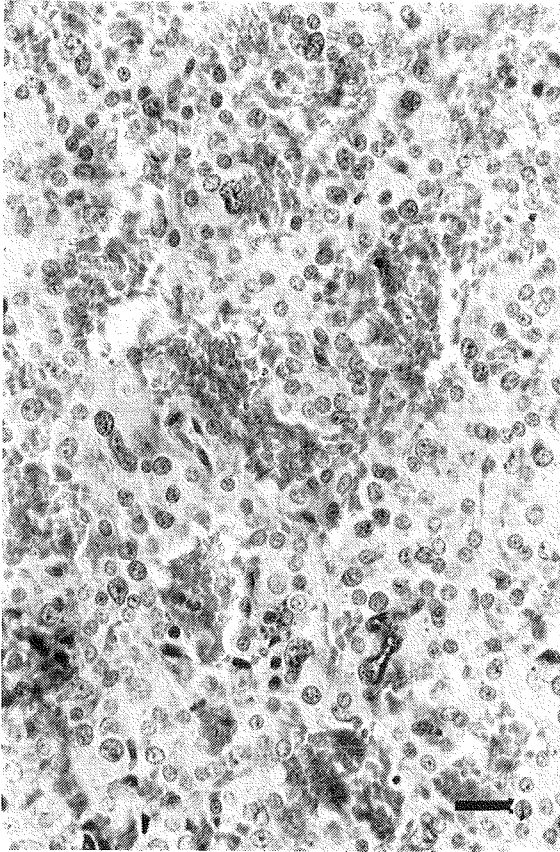


Fig. 4 -- Pleomorphic adenoma consisting of solid fields of large cells with moderate to marked nuclear and cellular pleomorphism. HE, bar = 20  $\mu$ m.

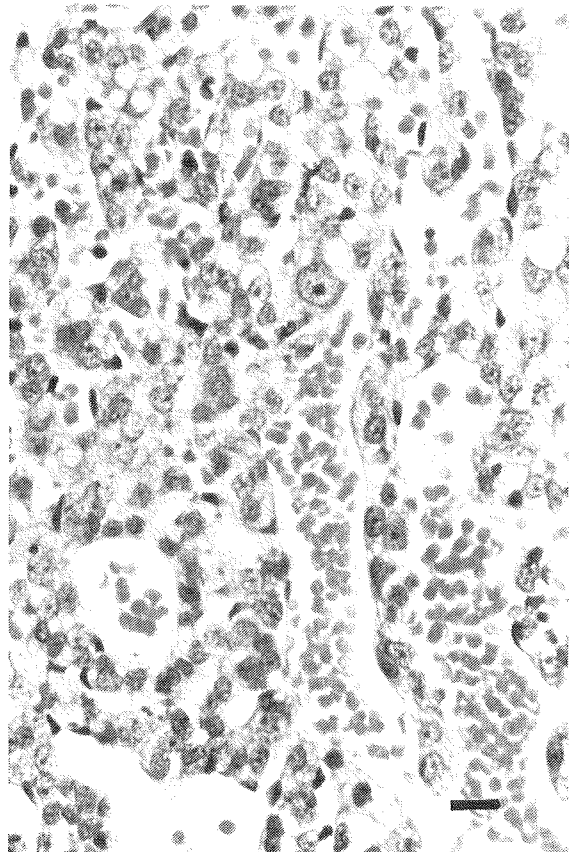


Fig. 5 -- Spongiocytic adenoma consisting of thin, 1-3 cell layers thick, cords of cells with small and large cytoplasmic vacuoles giving the cells a spongiocytic appearance. HE, bar = 20  $\mu$ m.

There were only two male rats without lesions. Therefore, their 95th and 99th percentile prolactin concentration values were calculated including values from animals with only foci of hypertrophic cells, whose plasma prolactin concentrations were completely within the range of values in the rats without lesions.

Table 1 presents the number and percentage of rats within each of the five above mentioned groups and the median plasma prolactin concentration for each group for male and female rats separately. Also, the 99th percentile values of the plasma prolactin concentration are presented for the rats without lesions. For the groups with lesions the range of concentrations is given to demonstrate possible overlap of the actual values in the latter groups with the 99th percentile interval in rats without lesions. Fig. 6 depicts the relation between plasma prolactin concentration and the largest pituitary lesion present for individual male and female rats, respectively, arranged in the above mentioned five groups. In addition, the staining intensity for prolactin of that most severe lesion is indicated for each rat. There were significantly

more female than male rats with pituitary adenomas or without lesions, and fewer female than male rats with only non-neoplastic lesions (see Table 1 for p-values). There were particularly fewer female than male rats with only hypertrophic cell foci. The numbers of male and female rats with no lesions, with only non-neoplastic lesions, or with adenomas were also significantly different when tested by a two-sided,  $2 \times 3$   $X^2$  test ( $P = 0.001$ ). Single or multiple foci of hypertrophic cells were present in 25 male rats (in total 34 foci) and single foci in seven female rats ( $P = 0.0004$  for male-female difference in incidence, two-sided  $X^2$  test). Single or multiple foci of hyperplastic cells were found in 15 male rats (16 foci) and 12 female rats (14 foci). Twelve male rats and 16 female rats had a single hemorrhagic adenoma, and two female rats each had two hemorrhagic adenomas. One male and three female rats with a hemorrhagic adenoma also had a smaller pleomorphic adenoma. Four male rats had a hemorrhagic adenoma with pleomorphic areas. Four female rats had a single pleomorphic adenoma, and one male rat had a single spongiocytic adenoma.

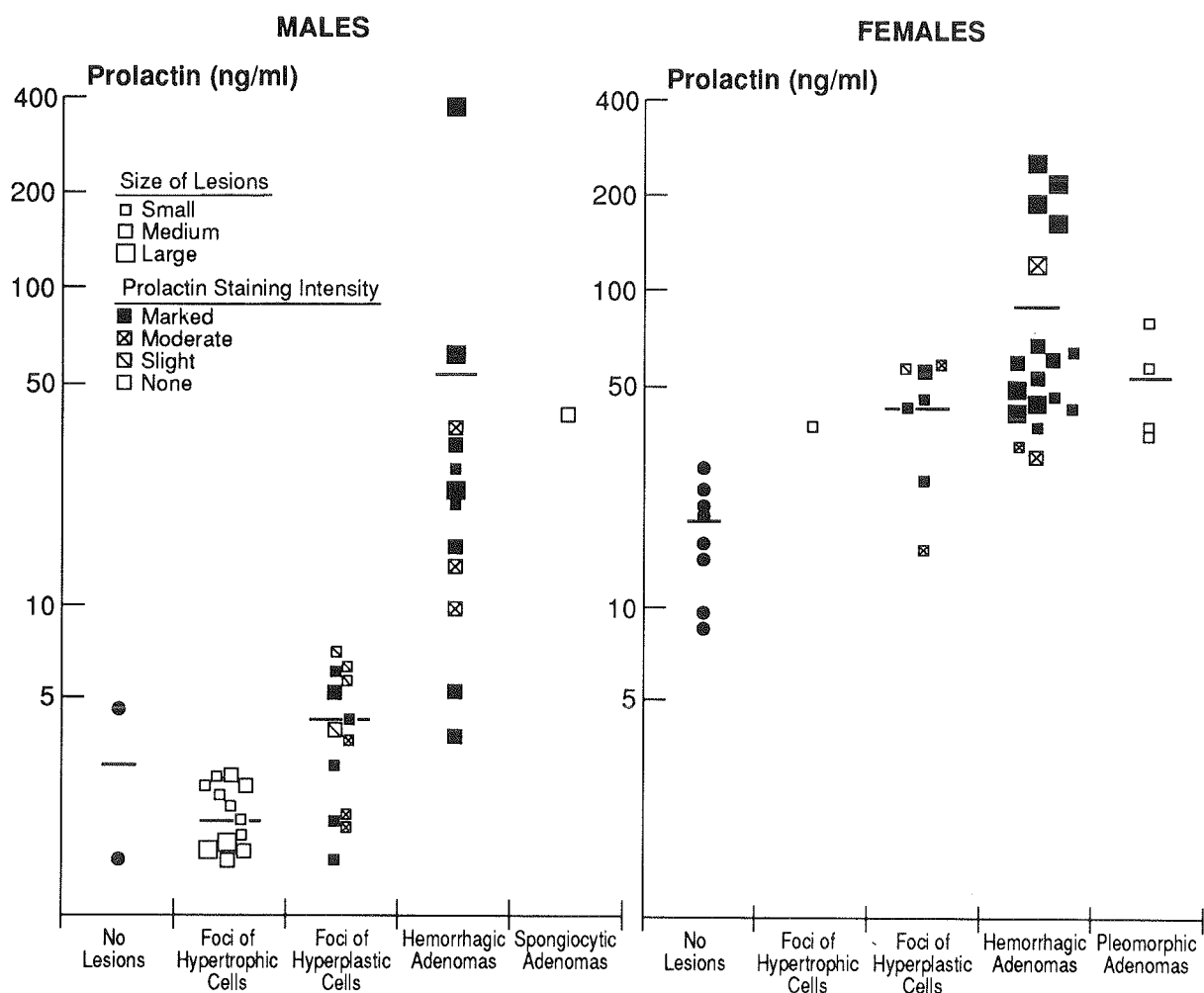


Fig. 6 -- Plasma prolactin levels in aged Wistar rats versus the presence, size, and intensity of prolactin staining of largest and most severe lesion (adenoma > hyperplastic cell focus > hypertrophic cell focus) in the anterior pituitary of each animal. Left panel, male rats (n=40), and right panel, female rats (n=38). The mean prolactin values are indicated by a horizontal line in each column.

Plasma prolactin concentrations were higher in female rats than in male rats, irrespective of the presence of pituitary lesions (Table 1, Fig. 6). Elevation of plasma prolactin concentrations above the 99th percentile of values of male rats without pituitary lesions was present in all, but one, male rats with adenomas and in 5 of 13 male rats (38%) with only foci of hyperplastic cells (Table 1, Fig. 6). The one male adenoma-bearing rat without such elevation had a plasma prolactin concentration of 3.7 ng/ml, which was just below the upper 95th percentile value (3.82 ng/ml). All female rats with adenomas and in 5 of 7 animals (71%) with only foci of hyperplastic cells had plasma prolactin concentrations above the 99th percentile of values in female rats without pituitary lesions (Table 1, Fig. 6). Males with only hypertrophic foci had

prolactin concentrations that fell within the range of values in male rats without lesions (Fig. 6). The one female rat with only a hypertrophic cell focus had a slightly higher prolactin concentration than rats without pituitary lesions (Fig. 6). There was a significant difference for both sexes in plasma prolactin concentration between rats without pituitary lesions, rats with pituitary adenomas, and rats with pituitary hypertrophic and/or hyperplastic cell foci but no adenomas ( $p < 0.0001$ , Kruskal-Wallis one-way analysis of variance). In males, plasma prolactin concentrations were significantly higher in rats with pituitary adenomas than in rats without pituitary lesions, or rats without adenomas but with any non-neoplastic pituitary lesion, hypertrophic cell foci, or hyperplastic cell foci (but no hyperplastic cell foci) (Mann-Whitney test, see

Table 1 for p-values). Plasma prolactin concentration was also significantly higher in male rats with hyperplastic cell foci than in rats with only hyperplastic cell foci (Table 1). There were no significant differences in plasma prolactin concentrations between male rats without lesions and rats with hyperplastic cell and/or hypertrophic cell foci (but no adenomas). In females, plasma prolactin concentrations were significantly higher in rats with pituitary higher in rats with hyperplastic cell and/or hypertrophic cell foci (but no adenomas) than in rats without pituitary lesions (Mann-Whitney test, see Table 1 for p values). There were no significant differences in plasma prolactin concentrations between female rats with pituitary adenomas and rats with hyperplastic cell and/or hypertrophic cell foci but no adenomas.

### **Correlation between Plasma Prolactin Concentration and Pituitary Lesions and Other Variables**

Correlations found by multivariate analysis between plasma prolactin concentrations and pituitary lesions and, if significant, other variables are presented in Table 2. There were significant positive correlations in both male and female rats between plasma prolactin concentrations and the presence and size of hemorrhagic adenomas as well as staining intensity for prolactin of these tumors. These correlations were stronger in female rats than in male rats. There was no correlation between prolactin concentration and number, size, and/or prolactin staining intensity of hyperplastic cell and hypertrophic cell foci. The number of foci of hypertrophic cells in females was excluded from the analysis, because only single foci occurred. A significant negative correlation was found in female rats between the number of corpora lutea in the ovaries and plasma prolactin concentrations. No correlation with plasma prolactin concentration was found for any of the other variables examined, which included plasma concentrations of testosterone and estradiol-17 $\beta$ , and the following age-related lesions: ovary: number of corpora lutea or follicles per animal, size of cysts, and presence of interstitial proliferation; testes: presence of atrophy or interstitial cell hyperplasias or tumors; uterus: degree of epithelial activity, dilation of mucosal glands, and presence of tumors (largely polyps); mammary gland: the presence of ductectasia, lobular hyperplasia, or tumors (largely fibroadenomas); and thymus: the presence of involution or epithelial proliferation. Ovarian tumors in female rats and spongiocytic adenomas in male rats were excluded from the multivariate

analysis because only a single rat had such a tumor. Testosterone and 5-dihydrotestosterone concentrations were elevated in only one female rat, and plasma 5-dihydrotestosterone concentration was elevated in only one male rat; these variables were therefore eliminated from the analysis. Discriminant analysis (data not shown) demonstrated that only the plasma prolactin concentration and none of the other variables provided useful information to discriminate between the various pituitary lesions, and that none of these other variables added significant information to this discriminative value of the plasma prolactin concentration.

### **DISCUSSION**

Elevation of plasma prolactin concentration in aged rats above the 99th percentile of values in aged-matched rats with morphologically normal pituitaries proved to be a good predictor for the presence of spontaneous tumors of the pituitary pars distalis, particularly hemorrhagic adenomas. This fact is underscored by the highly significant positive correlation found by multivariate analysis between plasma prolactin concentration and the presence and size of pituitary hemorrhagic adenomas, and by the positive correlation between plasma prolactin concentration and the intensity of immunohistochemical staining for prolactin in these tumors. However, false negatives can occur, because one male with a hemorrhagic adenoma in this study had a plasma prolactin concentration lower than the upper 95th percentile of normal values. Elevation of plasma prolactin concentrations above 10 ng/ml in males and 60 ng/ml in females was conclusively predictive of the presence of a pituitary hemorrhagic adenoma. These findings in Wistar rats are comparable to the following findings in humans. (1,6,11,18,19,41 1) A marked elevation of plasma prolactin concentration is conclusive for the diagnosis of a prolactin-secreting pituitary adenoma. 2) Only a proportion of patients with pituitary adenomas that positively immunostain for prolactin have elevated plasma concentrations of prolactin. 3) Microscopic-size adenomas that do not result in clinically detectable hyperprolactinemia or other symptoms are frequent. A few rats with hemorrhagic adenomas, which all stained positive for prolactin, had only slightly elevated or no elevated plasma prolactin concentrations. Possible explanations for this finding include obstruction of the pituitary blood supply due to compression of the pituitary stalk by the tumors (11, 32), and damage to hypothalamic

**Table 1.** Plasma prolactin concentrations and incidence of spontaneous lesions in the anterior pituitary of 30-month old Wistar rats.

	Males		Females	
	Number of rats with lesions*	Plasma prolactin concentration†	Number of rats with lesions*	Plasma prolactin concentration†
Number of animals examined	40		38	
Number of rats without lesions	2(5)	2.1 (1.5-4.5) (0.0,4.32)‡	8(21) <sup>#</sup>	18.2 (9.7-28.1) (0.0,27.7)‡
Number of rats with tumors:				
Any type of pituitary tumor	13(33)	23.0 <sup>ll</sup> (3.7-394)	22(58) <sup>§</sup>	57.6 <sup>¶</sup> (30.6-253)
Hemorrhagic tumor <sup>**</sup>	12(30)	22.15 <sup>ll</sup> (3.7-394)	18(47)	57.6 <sup>¶</sup> (30.6-253)
Spongiocytic tumor but no other tumor	1(3)	40.0	0	
Pleomorphic tumor but no other tumor	0		4(11)	49.2 <sup>¶</sup> (36.2-83.7)
Number of rats with non-neoplastic lesions but no tumor:				
Any non-neoplastic lesion	25(63)	2.6 (1.5-7.9)	8(21) <sup>#</sup>	46.6 <sup>††</sup> (15.8-59.7)
Hyperplastic cell foci +/- hypertrophic cell foci	13(33)	3.9 <sup>‡‡</sup> (1.5-7.9)	7(18)	47.4 <sup>††</sup> (15.8-59.6)
Hypertrophic cell foci but no hyperplastic cell foci	12(30)	2.1 (1.5-2.8)	1(3) <sup>##</sup>	38.5

\* The percentage of rats with(out) lesions is given in parentheses.

† Median prolactin concentration is given in ng/ml, and the range in parentheses.

‡ The 99th percentile limits of plasma prolactin concentration are given for rats without lesions.

#  $p = 0.0009$  (2-sided  $X^2$  test) for male-female difference.

ll  $p = \leq 0.025$  (1-sided) for difference with male rats without lesions;  $p < 0.01$  (2-sided) for difference with male rats with any non-neoplastic lesion (but no adenomas);  $p < 0.002$  (2-sided) for difference with male rats with hyperplastic cell foci (but no adenomas);  $p < 0.001$  (2-sided) for difference with male rats with hypertrophic cell foci (but no adenomas) (Mann-Whitney test).

§  $p = 0.0229$  (2-sided  $X^2$  test) for male-female difference in incidence.

¶  $p \leq 0.01$  (1-sided Mann-Whitney test) for difference with female rats without lesions.

\*\* The largest lesion per animal was taken as indicator lesion for that animal.

††  $p < 0.05$  (2-sided Mann-Whitney test) for difference with female rats without lesions.

‡‡  $p < 0.02$  (2-sided Mann-Whitney test) for difference with male rats without lesions.

##  $p = 0.0037$  (2-sided  $X^2$  test) for male-female difference.

neurons that produce secretory or inhibitory factors as reported in humans and animals with pituitary tumors (31, 33, 37, 43). Perhaps these tumors are comparable to the "silent lesions" described by Kovacs and co-workers (21) in humans, i.e., prolactin-positive staining pituitary adenomas that did not elevate plasma concentrations of prolactin (18, 28). Landolt (26) termed these lesions hyperplasias because of the lack of association with elevated plasma prolactin concentrations.

Pleomorphic adenomas and the spongiocytic adenoma did not stain for prolactin, and there was no statistical correlation between plasma prolactin concentration and their presence and size. Nevertheless, the four rats with a single pleomorphic adenoma and the one rat with a spongiocytic adenoma had slightly to moderately elevated plasma prolactin concentrations. There is no ready explanation for these observations. In only one of these five cases of a prolactin immunonegative adenoma were there prolactin positive foci of hyperplasia present which may have contributed to elevation of plasma prolactin concentration. However, we may have failed to detect hyperplasias or small hemorrhagic adenomas in the other four animals, because step sections rather than serial sections of the pituitaries were studied. Van Putten and van Zwieten (45) have also reported elevated prolactin concentrations in aged BN/BiRij and WAG/Rij rats with prolactin-negative, non-hemorrhagic, pituitary tumors. On the other hand, Trouillas et al. (42) did not find elevated plasma prolactin concentrations in Wistar/Furth/Ico rats with spongiocytic adenomas, which were prolactin immunonegative. There are disease conditions in man that can lead to hyperprolactinemia in the absence of a pituitary tumor (8, 11), but such conditions have not been described in rats, to our knowledge.

In contrast to hemorrhagic adenomas, there was no statistical correlation between plasma prolactin concentration and the presence of foci of hyperplastic cells and/or hypertrophic cells. Thus, elevation of plasma prolactin concentration was not predictive of the presence of these lesions. Nevertheless, plasma prolactin concentrations were slightly above the 99th percentile of normal values in a substantial proportion of male rats and, particularly, female rats with no adenomas but only hyperplastic lesions (with or without foci of hypertrophic cells). Male rats with only hypertrophic lesions did not have elevated plasma prolactin concentrations, but the plasma concentration of prolactin was slightly elevated in the one female rat with only such a lesion. Rats with only hyperplastic or hypertrophic cell foci that

had elevated plasma prolactin concentrations perhaps also had small hemorrhagic adenomas that we failed to detect.

Since the presence of prolactin positive or negative lesions in the pituitary did not entirely explain the observed elevations in plasma prolactin concentrations, correlations were determined between the prolactin concentrations and other parameters which may influence circulating prolactin (5, 13-15, 24, 30, 38, 40). Only for the number of ovarian corpora lutea per animal was there a significant, negative, correlation with plasma prolactin concentration, for which we do not have an explanation. Plasma prolactin concentration was not correlated with the plasma concentration of estradiol-17 $\beta$ . Elevated circulating levels of estrogens increase pituitary prolactin secretion and are suspected to be involved in the development of pituitary tumors in rats (24, 31, 46). However, the sampling of the blood in this study occurred when pituitary lesions already existed, whereas estradiol-17 $\beta$  in all likelihood plays a role in early stages of pituitary tumor development (33, 37, 46, 47). Nevertheless, the high estrogen levels in females may be related to the higher pituitary adenoma incidence and the lower frequency of non-neoplastic lesions in females than in males found in this study, perhaps due to enhancement of progression from precursor lesions to frank neoplasia.

In this study of 30 months-old Wistar rats, 95% of males and 79% of females developed hypertrophic, hyperplastic and/or neoplastic lesions of the anterior pituitary. Since no morphologic classification existed in the literature that included all these types of lesions, we expanded our previously proposed classification for pituitary tumors (4). The criteria that were used to distinguish hypertrophic, hyperplastic, and neoplastic lesions, and those used to subclassify different types of adenomas were entirely based on the light microscopic appearance of the lesions in HE-stained paraffin sections. The different types of lesions that were thus distinguished also appeared to differ in functional characteristics, i.e., immunostaining for prolactin and/or elevation of plasma prolactin concentration. Thus, foci of hypertrophic cells did not stain for prolactin, and their presence was not associated with elevation of plasma prolactin concentrations. In contrast, all foci of hyperplastic cells stained positive for prolactin, but there was no statistical correlation between plasma prolactin concentration and their presence or prolactin staining intensity. Hemorrhagic adenomas stained positive for prolactin and their presence, size, and prolactin

**Table 2.** Correlation between plasma prolactin levels and lesions in the anterior pituitary, uterus, gonads and thymus, and plasma sex steroid levels in 40 male and 38 female 30 month-old Wistar rats.

Variables	Correlation coefficient	
	Males	Females
Pituitary tumors:		
Number of tumors/animal	0.338	0.341
Hemorrhagic tumors*	0.494 <sup>†</sup>	0.652 <sup>‡</sup>
Pleomorphic tumors*	-0.023	0.038
Prolactin staining intensity	0.392 <sup>§</sup>	0.441 <sup>†</sup>
Hyperplastic cell foci:		
Number of foci/animal	-0.153	-0.117
Size of foci	-0.132	-0.108
Prolactin staining intensity	-0.155	-0.127
Hypertrophic cell foci:		
Number of foci/animal	-0.183	N.M.
Size of foci	-0.188	-0.172
Ovaries:		
Number of corpora lutea/animal	-0.491 <sup>†</sup>	

\* Presence and size of tumors was taken as variable.

<sup>†</sup> P = 0.003.

<sup>‡</sup> P < 0.00001.

<sup>§</sup> P = 0.006.

N.M. = not measured

staining intensity strongly correlated with plasma prolactin concentration. Pleomorphic adenomas and the one observed spongiocytic adenoma, on the other hand, did not stain for prolactin, and their presence and size did not correlate with plasma prolactin concentration, although rats with these types of tumors had mildly elevated plasma concentrations of prolactin. Spongiocytic adenomas are rare but have been described previously as prolactin immuno-negative tumors (9, 42). Furthermore, the morphology and prolactin immunoreactivity of spontaneous pituitary lesions in rats described previously by us and by others (4, 7,

12, 16, 27, 29, 36, 42, 45-47) are similar to the present observations. Therefore, the classification system that was used in this study 1) includes the entire spectrum of spontaneous focal hypertrophic, hyperplastic, and neoplastic lesions of the aging rat pituitary, 2) distinguishes lesions that are functionally different, 3) may be universal since it seems to apply to several rat strains, and 4) does not require special histological techniques, and therefore offers advantages for routine application over classifications that depend on immunohistochemical or ultrastructural characteristics (10, 12, 16, 29, 45).



The foci of hypertrophic cells that we observed have not been described previously as a separate lesion. Other reports on non-neoplastic pituitary lesions in aged rats did not distinguish hypertrophic from hyperplastic and/or neoplastic lesions (36, 42, 45, 46). At present, the origin and nature of these hypertrophic cells remains uncertain, but they are possibly precursors of the prolactin negative adenomas. Similarly, the prolactin-positive hyperplasias may be precursors of prolactin-secreting adenomas, as suggested by Kovacs et al. (22) and Landolt (26) for the human. Because of the scope of this study, the immunoreactivity of the observed lesions for pituitary hormones other than prolactin was not determined. The hypertrophic and hyperplastic lesions have been reported to be immunonegative for growth hormone, ACTH, LH and TSH in five other rat strains (36, 45). Non-hemorrhagic, prolactin negative, pituitary tumors have been reported immunonegative for ACTH and growth hormone in some rats strains (42, 45). However, there are also reports of rat pituitary tumors that were positive for ACTH, growth hormone, LH, or TSH, or for combinations of these hormones and prolactin (4, 10, 29, 36). Such tumors are far less frequent than tumors that are exclusively positive for prolactin (4, 10, 29, 36). The pleomorphic adenomas may represent a more advanced stage of the hemorrhagic adenoma phenotype, because some hemorrhagic adenomas contained solid pleomorphic areas, and because in a previous study of a closely related Wistar substrain some pleomorphic adenomas were faintly prolactin immunopositive and had hemorrhagic areas (4).

In conclusion, this study suggests that spontaneous pituitary lesions in aged rats provide a useful animal model for such lesions in the human pituitary, as previously proposed by others for pituitary tumors in other rat strains (26, 42). In particular, spontaneous prolactin-secreting adenomas of the Wistar rat pituitary appeared to share the limited predictive value of elevation of plasma prolactin concentration as a diagnostic feature with human prolactinomas. The morphologic criteria that we developed to distinguish the various spontaneous hypertrophic, hyperplastic, and neoplastic lesions of the Wistar rat pituitary appeared to correspond well with their prolactin immunoreactivity and their ability to elevate plasma prolactin concentration, and thus constitute a classification system for these lesions that is biologically meaningful.

## ACKNOWLEDGEMENTS

This work was supported in part by Grant No. CIVO 87-2 from the Dutch Cancer Society and by Grants No. ES00260 and CA13343 from the US National Institutes of Health. The authors wish to thank Dr. JTNM Thissen for his helpful criticism on the statistical analysis and JP Bruyntjes for his technical contributions. We are grateful to Dr. S Riati of the NIAMDD Rat Pituitary Distribution Program for the rat prolactin antiserum and RIA kit.

## REFERENCES

1. Assies J: Sense and nonsense in diagnostic tests. *In: Trends in Diagnosis and Treatment of Pituitary Adenomas*, ed. Lamberts SWR, Tilders FJV, van der Veen EA, and Assies J, pp. 115-121. Free University Press, Amsterdam, The Netherlands, 1984
2. Baak JPA, Langley FA, Hermans J: Classification of new cases: some aspects of single and multivariate analysis. *In: Morphometry in Diagnostic Pathology*, ed. Baak JPA and Oort J, pp. 27-39. Springer Verlag, Berlin, Germany, 1983
3. Beems RB, van Beek L, Rutten AAJL, Speek AJ: Subchronic (106-day) toxicology and nutrition studies with vitamin A and  $\beta$ -carotene in Syrian hamsters. *Nutr Rep Int* 35:765-770 1987
4. Berkvens JM, van Nesselrooij JHJ, Kroes R: Spontaneous tumours in the pituitary gland of old Wistar rats: a morphological and immunocytochemical study. *J Pathol* 130:179-191 1980
5. Bonney RC, Franks S: The role of prolactin in the uterus. *In: Prolactin and Lesions in Breast, Uterus, and Prostate*, ed. Nagasawa H, pp. 97-106. CRC Press, Boca Raton, FL, 1985
6. Burrow GN, Wortzman G, Rewcastle NR, Holgate RC, Kovacs K: Microadenomas of the pituitary and abnormal sellar tomograms in an unselected autopsy series. *N Engl J Med* 304:156-158, 1981
7. Carlton WW, Gries CL: Adenoma and carcinoma, pars distalis, rat. *In: Endocrine System*, ed. Jones TC, Mohr U, and Hunt RD, pp. 134-145. Springer Verlag, Berlin, Germany, 1983.
8. Cook DM: Pituitary tumors: Diagnosis and therapy. *CA* 33:215-236, 1983
9. Dux C: Recherches microscopiques sur les adénomes hypophysiaires du rat. *Bull Ass Franc Cancer* 35:201-218
10. Fong ACO, Hardman JM, Porta EA: Immunocytochemical hormonal features of pituitary adenomas of aging Wistar male rats. *Mech Ageing Dev* 20:141-154, 1982
11. Frohman LA: The anterior pituitary. *In: Cecil Textbook of Medicine*, Volume 2, 18th ed., ed. Wyngaarden JB and Smith LH, pp. 1290-1305. Saunders, Philadelphia, PA, 1988

12. Furth J, Nakana PK, Pasteels JL: Tumours of the pituitary gland. *In: Pathology of Tumours in Laboratory Animals, Volume 1, Part 2, IARC Sci. Publ. No. 6, ed. Turusov VS, pp. 201-237. World Health Organization, Geneva, Switzerland, 1976*
13. Greenstein BD: Androgen receptors in the rat brain, anterior pituitary gland and ventral prostate gland: Effects of orchectomy and ageing. *J Endocrinol* **81**:75-81, 1979
14. Hall NRS, O'Grady MP: Regulation of pituitary peptides by the immune system. *BioEssays* **11**:141-144, 1989
15. Herbert DC, Cisneros PL, Rennels EG: Morphological changes in prolactin cells of male rats after testosterone administration. *Endocrinol.* **100**:487-495, 1977
16. Ito A, Moy P, Kaunitz H, Kortwright K, Clarke S, Furth J, Meites J: Incidence and character of spontaneous pituitary tumors in strain CR and W/Fu male rats. *J Natl Cancer Inst* **49**:701-711, 1972
17. Kellet J, Friesen HG: The endocrinology of prolactin secreting microadenomas. *In: Pituitary Microadenomas, ed. Faglia G, Giovanelli MA, and McLeod RM, pp. 265-275. Academic Press, London, UK, 1980*
18. Klibanski A: Nonsecreting pituitary adenomas. *Clin Endocrinol Metab* **16**:793-804, 1987
19. Klijn JGM, Lamberts SWJ, de Jong FH, Doctor R, van Dongen KJ, Birkenhagen JC: Relationship between pituitary tumor size, hormonal parameters and extrasellar extension in patients with prolactinomas. *In: Pituitary Microadenomas, ed. Faglia G, Giovanelli MA, and McLeod RM, pp. 303-311. Academic Press, London, UK, 1980*
20. Kleinberg DL, Noel GL, Frantz AG: Galactorrhea: A study of 235 cases, including 48 with pituitary tumors. *N Engl J Med* **296**:589-600, 1977
21. Kovacs K, Horvath E, Bayley TA, Hassaram S, Ezrin C: Silent corticotroph cell adenoma with lysosomal accumulation and crinophagy. A distinct clinicopathologic entity. *Am J Med* **64**:492-499, 1978
22. Kovacs K, Ilse G, Ryan N, McComb DJ, Horvath E, Chen HJ, Walfish PG: Pituitary prolactin cell hyperplasia. *Hormone Res* **12**:87-95, 1980
23. Kroes R, Garbis-Berkvens JM, de Vries T, van Nesselrooij JHJ: Histopathological profile of a Wistar rat stock including a survey of the literature. *J Gerontol* **36**:259-279, 1981
24. Kwa HG, Bulbrook RD, Wang DY: An overall perspective on the role of prolactin in the breast. *In: Prolactin and Lesions in Breast, Uterus, and Prostate, ed. Nagasawa H, pp. 3-22. CRC Press, Boca Raton, FL, 1989*
25. Kwa HG, van Gugten AA, Verhofstad F: Radioimmunoassay of rat prolactin. Prolactin levels in plasma of rats with spontaneous pituitary tumours, primary oestrone-induced pituitary tumours or pituitary tumour transplants. *Eur J Cancer* **5**:571-579, 1969
26. Landolt AM: Biology of pituitary microadenomas. *In: Pituitary Microadenomas, ed. Faglia G, Giovanelli MA, and McLeod RM, pp. 105-122. Academic Press, London, UK, 1980*
27. Lee AK, DeLellis RA, Blount M, Nunnemacher G, Wolfe HJ: Pituitary proliferative lesions in aging male Long-Evans rats. A model of mixed multiple endocrine neoplasia syndrome. *Lab Invest* **47**:595-602, 1982
28. Mashiter K, Adams E, Van Noorden S: Secretion of LH, FSH and prolactin shown by cell culture and immunocytochemistry of human functionless pituitary adenomas. *Clin Endocrinol* **15**:103-112, 1981
29. McComb DJM, Kovacs K, Beri J, Zak F: Pituitary adenomas in old Sprague-Dawley rats: A histologic, ultrastructural, and immunocytochemical study. *J Natl Cancer Inst* **73**:1143-1158, 1984
30. Meites J: Relation of prolactin to development of spontaneous mammary and pituitary tumors. *In: The prostatic cell: Structure and function, Pt. B, ed. Murphy GP, Sandberg AA, and Karr JP, pp. 1-8. , Liss, New York, NY, 1981*
31. Meites J: The neuroendocrinology of hypothalamic aging. *In: Neuroendocrine Perspectives, Vol. 5, ed. Muller EE and MacLeod RM. pp. 179-190. Elsevier, Amsterdam, The Netherlands, 1986*
32. Molitch ME: Nonsecreting adenomas. *In: The Pituitary Adenoma, ed. Post KD, Jackson IMD, Reichlin S, pp. 151-158. Plenum, New York, NY, 1980*
33. Morgan WW, Steger RW, Smith MS, Bartke A, Sweeney CA: Time course of induction of prolactin-secreting pituitary tumors with diethylstilbestrol in male rats: response of tuberoinfundibular dopaminergic neurons. *Endocrinol* **116**:17-24, 1985
34. Nakana PK, Pierce GB: Enzyme-labeled antibodies for the light and electron microscopic localization of tissue antigens. *J Cell Biol* **33**:307-318, 1967
35. Ross MH, Bras G, Ragbeer MS: Influence of protein and caloric intake upon spontaneous tumor incidence of the anterior pituitary gland of the rat. *J Nutr* **100**:177-189, 1970
36. Sandusky GE, Van Pelt CS, Todd GC, Wightman K: An immunohistochemical study of pituitary adenomas and focal hyperplasia in old Sprague-Dawley and Fischer 344 rats. *Toxicol Pathol* **16**:376-380, 1988
37. Sarkar DK, Gottschall PE, Meites J: Damage to hypothalamic dopaminergic neurons is associated with the development of prolactin-secreting pituitary tumors. *Science* **218**:684-686, 1982
38. Shaar CJ, Euker JS, Riegler GD, Meites J: Effects of castration and gonadal steroid on serum luteinizing hormone and prolactin in old and young rats. *J Endocrinol* **66**:45-51, 1975
39. Siegel S: *Nonparametric Statistics for the Behavioral Sciences, McGraw-Hill Kogakusha, Tokyo, Japan, 1956*

40. Spangelo BL, Ross PC, Judd, AM, MacLeod RM: Thymic stromal elements contain an anterior pituitary hormone-stimulating activity. *J Neuroimmunol* **25**:37-46, 1989
41. Spark RF, Wills CA, O'Reilly G, Ransil BJ, Bergland R: Hyperprolactinaemia in males with and without pituitary macroadenomas. *Lancet* **ii**:129-131, 1982
42. Trouillas J, Girod C, Claustrat B, Cure M, Dubois MP: Spontaneous pituitary tumors in the Wistar/Furth/Ico rat strain. *Am J Pathol* **109**:57-70, 1982
43. Van Loon GR: A defect in catecholamine neurons in patients with prolactin secreting pituitary adenoma. *Lancet* **ii**:868-871, 1978
44. Van Nesselrooij JHJ, Kuper CF, Bosland MC, Bruyntjes JP, Kroes R: Spontaneous pituitary lesions and plasma prolactin levels in rats. In: *Prolactinomas: an Interdisciplinary Approach*, ed. Auer LM, Leb G, Tscherne W, Urdl W, and Walter GF, pp. 85-87. de Gruyter, Berlin, Germany, 1985
45. Van Putten LJA, van Zwieten MJ: Studies on prolactin-secreting cells in aging rats of different strain. II. Selected morphological and immunohistochemical features of pituitary tumors correlated with serum prolactin levels. *Mech Ageing Dev* **42**:115-127, 1988
46. Van Putten LJA, van Zwieten MJ, Mattheij JAM, van Kemenade JAM: Studies on prolactin-secreting cells in aging rats of different strain. I. Alterations in pituitary histology and serum prolactin levels as related to aging. *Mech Ageing Dev* **42**:75-90, 1988
47. Wolfe JM, Bryan WR, Wright AW: Observations on the histologic structure of the anterior pituitaries of old female rats. *Proc Soc Exp Biol Med* **38**:80-82, 1983



## **CHAPTER III**

### **MAGNETIC RESONANCE IMAGING OF ESTROGEN-INDUCED PITUITARY HYPERTROPHY IN RATS**

Joop H.J. van Nesselrooij, Nikolaus M. Szeverenyi and Martin J. Ruocco.

Magnetic Resonance in Medicine 11: 161-171, 1989.



## Magnetic Resonance Imaging of Estrogen-Induced Pituitary Hypertrophy in Rats

JOOP H. J. VAN NESSELROOIJ,\*† NIKOLAUS M. SZEVERENYI,\*  
AND MARTIN J. RUOCCO\*

\*Nuclear Magnetic Resonance Research Laboratory, Department of Radiology, State University of New York, Health Science Center at Syracuse, Syracuse, New York 13210, and †Laboratory of Pathology, Department of Biological Toxicology, TNO-CIVO Toxicology and Nutrition Institute, 3704 HE Zeist, The Netherlands

Received July 27, 1988; revised October 27, 1988

Estrogen-induced pituitary hypertrophy has been studied using magnetic resonance imaging in a group of 15 control and 30 experimental rats. Following the subcutaneous implantation of an estrogen pellet, differences in the anatomical appearance of the pituitary gland of the implanted rats can be detected in as little as 16 days, when compared to the control animals. The gland in the experimental animals appears diffusely enlarged with rounded margins, when viewed in sagittal T1-weighted magnetic resonance images. Additionally, a uniform signal intensity is not detected in the hypertrophic pituitary glands of estrogen-implanted rats, while in the control rats this is a common finding. A satellite study of 300 animals (treated in a manner identical to that in the imaging study) demonstrates that the weights of excised pituitaries in estrogen-treated rats increases to a statistically significant level in the interval 18 to 35 days. Changes in the appearance and volume of the pituitary gland observed with magnetic resonance imaging seem to have promise for the early detection of pituitary lesions in rats. © 1989 Academic Press, Inc.

### INTRODUCTION

The purpose of this investigation was to evaluate the capability of magnetic resonance imaging (MRI) as a method for the early detection of pituitary hypertrophy in rats. Proliferative pituitary gland lesions (hyperplasias or tumors) occur relatively frequently in both aging man and animals (1-6). In human, such lesions may pose a serious diagnostic problem to the clinician (7-11), because biochemical tests measuring hormone levels often do not permit detection of pituitary hyperplasias and certain large pituitary tumors. Additionally, it is also very difficult for the radiologist to detect focal and diffuse hyperplasias or small pituitary adenomas with contrast enhanced computer tomography (11).

Estrogen-induced pituitary tumor in rats has been suggested as a relevant model for the human disease (4, 12-14), one that is both reliable and technically easy to implement (2-4, 15, 16). This is the model employed in the present study in order to determine if magnetic resonance imaging can permit the early detection of these estrogen-induced pituitary lesions in rats.

## MATERIALS AND METHODS

*Animals and Treatment*

Forty-five male weanling Sprague–Dawley (SD) rats were obtained from a commercial supplier (Harlan Sprague–Dawley, Inc., Indianapolis, IN). The animals were 3 weeks old upon arrival and were held in quarantine 1 week before this study was initiated. The rats were divided into two groups, one group of 30 rats served as the experimental group and the second group of 15 rats served as the control group. The rats were kept in stainless-steel wire-mesh cages (3 animals per cage; controls separated from experimental animals) in a well-ventilated area maintained at 20°C with relative humidity 40–70% and 12 h of lighting per day. Animals had free access to food (Purina Formulab Chow 5000, Purina Mills, Inc., St. Louis, MO) and tap water and were checked twice daily.

Under ether anesthesia, each rat in the experimental group had a 25-mg estradiol-17 $\beta$  pellet (Organon, The Netherlands) implanted subcutaneously between their scapulae at the same time of day in 3 consecutive days. According to a technique devised in this laboratory, a small incision was made through the skin in the region of the lumbar spine, and a cannula (2 mm i.d.) was passed subcutaneously to the cervical level. An estrogen pellet was pushed through the cannula with a blunt trocar and deposited subcutaneously, and the cannula and trocar were then withdrawn. Closure of the wound was not necessary, since the incision was small and the estrogen pellet was located at such a distance from the incision that the pellet could not be expelled.

The control rats were sham operated in an identical manner but without the deposition of a pellet. All animals were treated under a protocol and housing arrangement approved by the institutional committee for the humane use of animals (CHUA).

*Imaging*

Sets of one control and two estrogen-implanted rats were examined and then sacrificed at 15 points in time: 2, 4, 8, and 24 h; 2, 4, 8, and 16 days; and then approximately every 16th day up to 4 months after implantation of the estrogen pellets. Sagittal T1-weighted MR images of the head were obtained with a 30-cm horizontal-bore diameter, 2-T, chemical-shift/imaging (CSI) instrument (General Electric, Fremont, CA).

T1-weighted spin-echo imaging parameters were single sagittal midline slice, 2 mm slice thickness, repetition time (TR) 450–500 ms, echo time (TE) 24 ms, two excitations, 40-mm field of view, 425 Hz/mm read gradient, a 2.5-ms sinc pulse (having two side lobes on either side of the center lobe) for excitation, 256 complex sampling points, and 128 or 256 phase-encoding increments. In order to minimize animal motion during the image data acquisition, rats were anesthetized with sodium pentobarbital (Nembutal, Abbott Laboratories, North Chicago, IL) 5 mg/100 g body wt ip.

The rats were immobilized in a plexiglass cradle during the imaging experiment. A homemade NMR probe, consisting of a 30-mm-diameter by 32-mm-long saddle coil with a (1–30 pF parallel) tuning capacitor and two distributed (0.8–10 pF series)



## MRI OF RAT PITUITARY HYPERTROPHY

matching capacitors (Johanson Dielectrics, Burbank, CA), was attached to one end of the cradle. This probe design was found experimentally to optimize image signal-to-noise ratio from the head of the animal and also to facilitate the positioning and observation of the animal. This coil was sufficiently flexible to accommodate differences in head size. Birdcage resonator designs were evaluated and found to have superior radiofrequency (rf) homogeneity, but did not significantly improve imaging sensitivity in the region of the pituitary and were not as convenient for positioning and observing the animal.

### *Gross Pathology*

Following MR imaging, rats were sacrificed by decapitation with a guillotine while still under anesthesia. After the roof of the skull was removed, the brain and pituitary were examined grossly for pathological changes. Each gland was then removed and fixated in a phosphate-buffered 4% formaldehyde solution for further histological examination of size and growth pattern.

### *Satellite Study*

The purpose of this separate study was to provide data on weights of pituitary glands, plasma levels of pituitary hormones, and the morphology of pituitary lesions from a large number of rats treated in a manner identical to that as in the MRI study. This satellite study was performed in The Netherlands by the TNO-CIVO group. Three hundred male weanling Sprague-Dawley rats were obtained from a commercial supplier (Harlan Sprague-Dawley, Inc., Zeist, The Netherlands) and divided into two groups. One group of 150 rats served as control animals and the other group of 150 rats as experimental animals. The rats were treated with estrogen and sham operated in a manner identical to that for the animals used in the MR imaging study. They were housed under the same conditions as described previously and fed a powdered stock diet. Ten control and ten experimental rats were sacrificed at 15 points in time: 2, 4, 8, and 24 h; 4, 7, 11, 18 days; and then approximately every 16th day up to 4 months. Animals were sacrificed at the same time each day, between 9 and 12 a.m., except for the animals composing the first three time points. Blood was sampled to measure plasma levels of the pituitary hormones: prolactin (PRL), growth hormone (GH), luteinizing hormone (LH), follicle-stimulating hormone (FSH), thyroid-stimulating hormone (TSH), and adrenocorticotrophic hormone (ACTH). Pituitary wet weights were recorded before the glands were fixated. Step sections stained with hematoxylin and eosin were examined under light microscopy for morphological changes. Immunoperoxidase staining techniques (for the hormones mentioned above) were used to visualize the distribution of hormone-producing cells and to further characterize the induced lesions.

## RESULTS

A midline sagittal T1-weighted image proved to be the most effective and reproducible technique to display the anatomy of the pituitary gland region. In this image plane, the normal pituitary appeared triangular with sharply defined margins. On the

early time point images of both the control and the implanted rats (2, 4, 8, and 24 h and 2, 4, and 8 days) the intensity of the pituitary varied relative to surrounding brain tissue, but was uniform within the gland. The first changes became visible on the Day 16 images which demonstrated the entire pituitary gland to be enlarged in the two implanted rats compared to the images of the pituitary in the control rat. Also, the margins of the pituitary glands were slightly rounded compared to those of the control rat (Figs. 1 and 2).

As a result of this enlargement, the subarachnoid space between the pituitary gland and the diencephalon, and the space between the pituitary gland and the pons, was compromised when viewed in these sagittal images (arrow in Fig. 2). During the time between Day 16 and Month 4 postimplantation, a small space was still present dorsal to the pituitary, but areas of contact between the pituitary gland and the brain tissue could be detected due to enlargement of the pituitary gland.

Already after Day 16 postimplantation, images revealed a difference in signal intensity of the pituitary gland between the control and the experimental animals. Pituitary tissue of the control rats exhibited a uniform signal intensity on T1-weighted MR images which was equal to or greater than that of the surrounding brain tissue, while the enlarged pituitary glands of the estrogen-implanted rats demonstrated a mottled

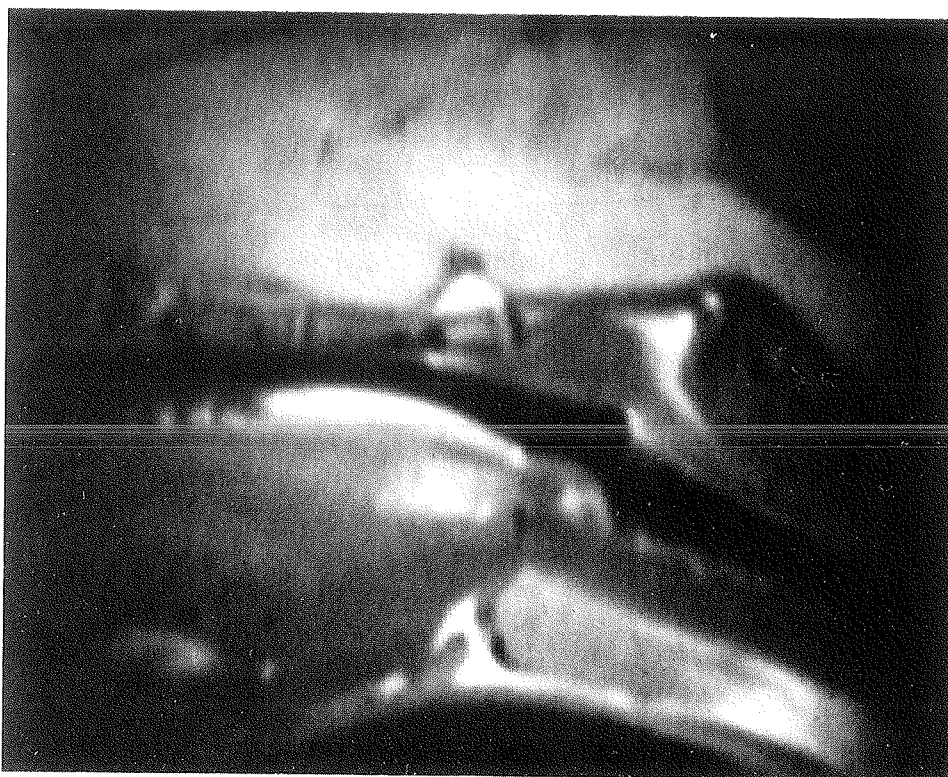


FIG. 1. A T1-weighted midline sagittal image of a control rat at Day 16 having a normal pituitary gland. Note the triangular structure.

## MRI OF RAT PITUITARY HYPERTROPHY

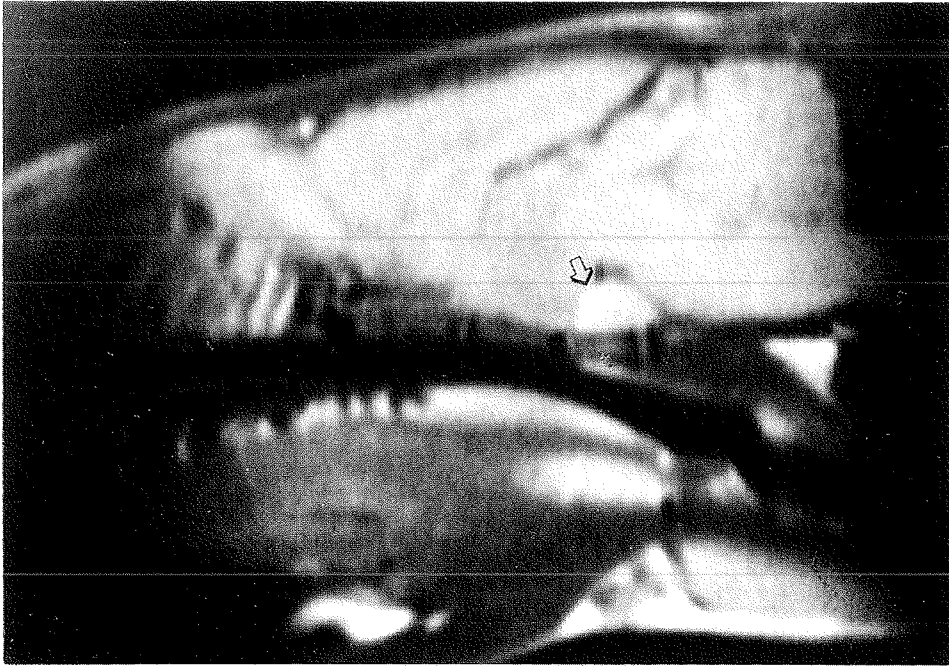


FIG. 2. A T1-weighted midline sagittal image of an experimental rat having an estrogen pellet implanted 16 days prior to imaging. The pituitary gland is enlarged and displays slightly rounded margins.

heterogeneous appearance and often appeared hypointense compared to surrounding brain tissue. Upon gross examination of the skull at autopsy, enlargement of the entire pituitary gland of the implanted animals was observed from Day 16 on (Figs. 3 and 4).

The satellite study revealed a slight fluctuation in pituitary weights for the early time point measurements (2, 4, 8, and 24 h) in the control animals (Fig. 5). This may reflect a circadian rhythm which could be expressed in the secretory pattern for PRL, with secretion of this hormone increasing in the afternoon and decreasing in the evening. This rhythm was not observed in the experimental animals and may be the first indication of metabolic change. The Day 4, 7, 11 weight measurements revealed no statistically significant changes. There is a significant (based on a Mann/Whitney *U* test [two sided]) weight increase in the pituitaries in the implanted rats relative to the control rats on the first day and for time points after Day 18 (Table 1).

## DISCUSSION

The first evidence of the rat pituitary enlargement became visible on Day 16 in this MRI study, suggesting that the gland must have hypertrophied a significant amount during the 8-day period between time points of this period. The satellite study, however, did not reveal a statistically significant difference in the relative weights of the

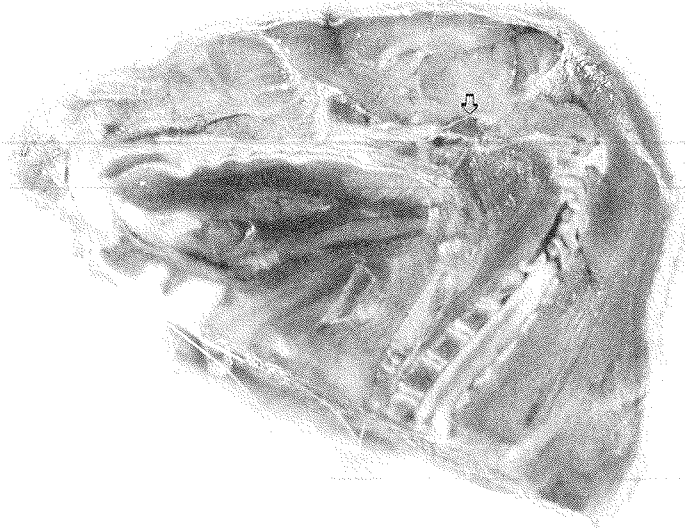


FIG. 3. A macroscopic photograph of a sagittal cut through the head of a control rat displaying a normal pituitary gland at Day 16 of the experiment.

pituitaries until after Day 18 postimplantation. We suggest that the weight increase observed on the first day is an acute effect of the estrogen which returns to normal after the first day. The weight gain observed after Day 18 is possibly due to dilation of the sinusoids and the resulting increased blood volume. The pathogenesis of the estrogen-induced pituitary lesion involving the development of hypertrophic pituitary cells was seen on histological sections to occur prior to the dilation of the sinusoids. This exaggerated growth would seem, therefore, to be the first contribution to the enlargement of the entire pituitary gland. These findings suggest that MRI may be a more sensitive method for detection of pituitary hypertrophy than the weight of the organ. MRI is sensitive to soft tissue changes and additionally has the advantage of being noninvasive, allowing repeated *in vivo* measurements. Although volume changes were not detected using the pituitary wet weight measurements for the period between Days 8 and 16, a significant diagnostic indicator of pituitary hypertrophy may be the rounded margins of the pituitary observed in the midsagittal MR images at these time points. This finding was not observed in the control animals and may be associated with tissue changes in the gland which actually precedes any volume increase.

Extrapolation of these observations directly to humans is not straightforward. The normal human pituitary gland has a rounded or oval configuration when viewed in the sagittal plane, and blunting of a triangular margin of the pituitary as occurs in the rat cannot be used to detect a tissue change in humans. Although Wiener *et al.* (17)

#### MRI OF RAT PITUITARY HYPERTROPHY



FIG. 4. A macroscopic photograph of a sagittal cut through the head of an experimental rat displaying pituitary hypertrophy at Day 16 of the experiment.

state that the height of the pituitary gland is the most important measurement in the detection of an intrasellar mass, Sekiya *et al.* (18) found a significant overlap between the heights of normal glands and glands with microadenomas. Generalized pituitary hypertrophy is not a common finding in humans, whereas it is in the estrogen-treated rat. Many factors influence the volume of the normal pituitary gland in humans (19). The gland enlarges during pregnancy, but returns to normal after lactation. Enlargement of the pituitary is associated with early development, as the infant matures, in both humans and rats. In the normal rat the margins are triangular and remain triangular during this time (Figs. 6 and 7).

The bright signal intensity of pituitaries in the control rats on T1 images is possibly caused by fat or lipids in the pituicytes of the pars nervosa. Characteristic lipid droplets have been shown in these (human) cells according to Wolpert *et al.* (20). Also, signal intensities of the pituitary on T1-weighted images appear to be brighter in infants than in older children. The signal intensity of the posterior pituitary gland was observed to be higher than that of the anterior pituitary gland, with either portion of the gland having higher image intensity than the surrounding brain. This intensity difference between pituitary and brain appears to be age related and becomes smaller in older children and adults. In our rat studies we are quite certain that this hyperintensity is not due to a flow entrance phenomenon. Congruent images through the rat pituitary in both the alive and the dead animal display identical signal behavior. The high signal intensity of the rat pituitaries reported in our investigation are similar to signal intensities found in human infants. The rats were weanlings in our study.

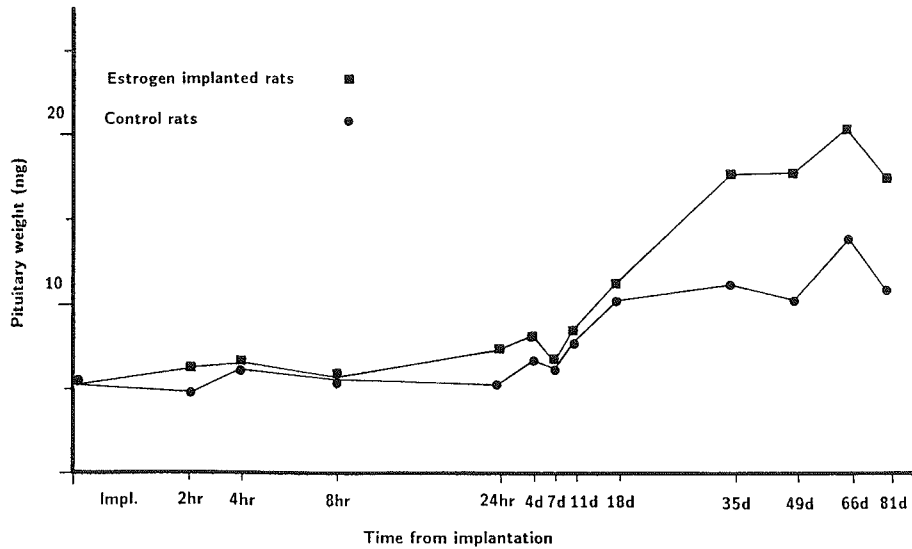


FIG. 5. A plot of the control and experimental animal pituitary weight as a function of time. The data were obtained from a satellite study using 20 rats per time point (10 control and 10 experimental).

Comparisons of MR signal intensity for normal and pathological pituitary tissue in humans have been reported by several investigators. Pojunas *et al.* (21) report a uniform signal intensity for normal pituitary tissue on T1-weighted images, whereas tumorous pituitary tissue gives rise to lower signal intensity due to longer T1 relaxation times. This observation was also described by Fink *et al.* (22). Dwyer *et al.* (23) studied different types of pituitary tumors and found that the detectability of a pituitary lesion with MR depends not only on the size but also on the histology of the lesion. The pituitary tumors observed by Dwyer *et al.* exhibit the following characteristics: tumors with cystic degeneration were bright on T2 and dark on T1, tumors with necrosis were bright on T1 and bright on T2, and solid tumors appeared isointense on both T1- and T2-weighted images in the four patients with this type of tumor. Three of these four isointense solid lesions were less than 4 mm in diameter and were detected only after Gd-DTPA contrast agent was injected. Microadenomas have

TABLE I

Rat Pituitary Wet Weights (mg) as a Function of Time Postimplantation of an Estrogen Pellet

		Day 1	Day 11	Day 18	Day 35	Day 49
Control rats	Mean	5.47	7.80	10.1	11.2	11.0
	SD	1.36	1.16	1.70	1.33	1.63
	<i>n</i>	40	10	10	10	10
Estrogen rats	Mean	6.40*	8.40	11.3	17.6**	16.9***
	SD	1.37	1.28	1.27	2.61	2.62
	<i>n</i>	40	10	10	10	10

Note. Mann/Whitney *U* test (two-sided). Statistical significance: \*  $P < 0.05$ , \*\*  $P < 0.02$ , \*\*\*  $P < 0.002$ .

## MRI OF RAT PITUITARY HYPERTROPHY



FIG. 6. A 2-week-old control rat displaying a normal pituitary gland.

signal intensities which are hardly predictable according to Pojunas *et al.* They describe microadenomas as having a variety of relaxation properties. Most have prolonged T1 and T2 relaxation times; however, some have short T1 or T2 values, or both short T1 and T2 values. Also, some have the same relaxation behavior as normal pituitary tissues. Lee and Deck (24) found that microadenomas that do not enlarge the sella could not be detected with MRI. Davis *et al.* (25) describe pituitaries as hyperintense relative to the cortex on T2-weighted images in only two out of four patients with proven microadenomas. In these two patients, T1 images present the pituitary as hypointense in one patient and hyperintense in the other patient. Kulkarni *et al.* (26) report the most consistent presentation of microadenomas on MR. They find on either a spin-echo or an inversion-recovery sequence that seven of a group of eight patients with microadenomas showed hypointense pituitaries on T1-weighted images. One microadenoma was seen as a hyperintense lesion on both T1- and T2-weighted images. The 6-mm microadenoma was removed and found to test immunohistochemically positive for prolactin and contained a hemorrhagic area in the center of the lesion. These findings corroborate those of Dwyer *et al.* who also suggest that the histology of the pituitary is involved in the appearance of the pituitary on MR images. Controversy still exists in the current literature as to how one can detect pituitary microadenomas. Just *et al.* (27) describe a tissue characterization method which makes it possible to differentiate between adenomatous tissue and normal pituitary tissue by the tissue relaxation parameters. Microadenomas can be discriminated from macroadenomas and from pituitary tissue through the use of proton density and strongly T2-weighted images.

Animal induction models or spontaneous pituitary lesions in animals, which can be as high as 70% in certain rat strains, are good for studying focal hyperplasias or microadenomas for human neoplastic diseases. Observations made in our animal

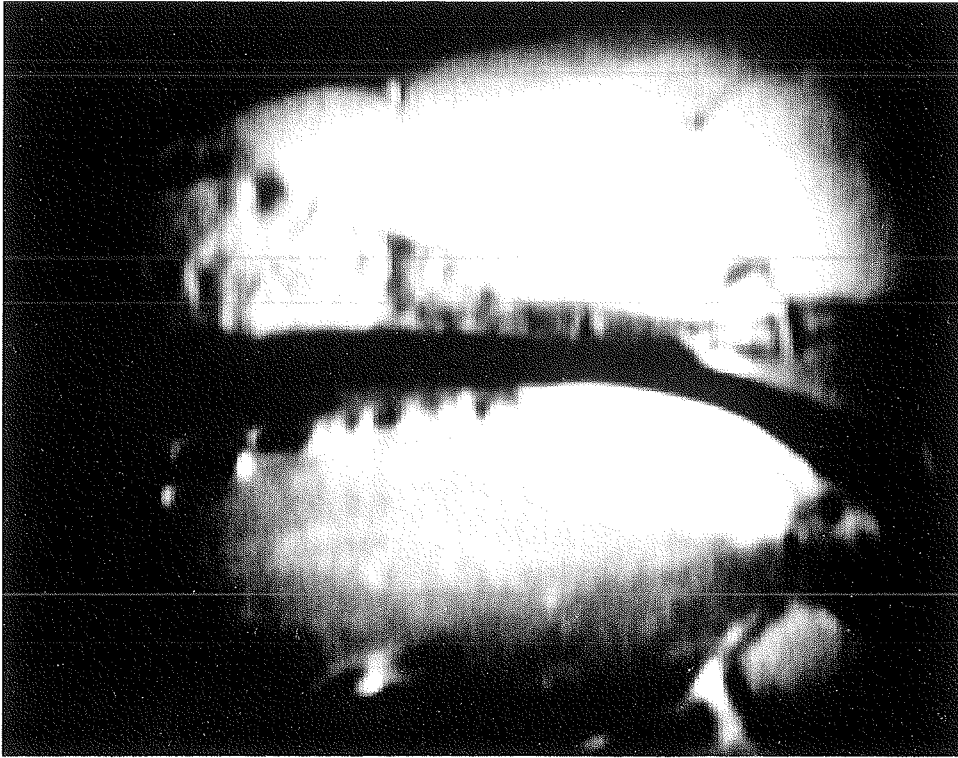


FIG. 7. A 2-month-old control rat. The pituitary is twice the size of the 2-week-old rat.

study, however, suggest that signal intensity of the pituitary is not a conclusive diagnostic indicator of pituitary hypertrophy in the rat. Volume changes may be a better indicator. Volume increase in the pituitary appears to be normal in the early development of the rat, but this change does not involve the blunting of the sharp triangular structure of the pituitary. We observe blunting of the margins in the hypertrophic rat as well as a volume increase. This blunting may provide the basis of a standard technique in the detection of rat pituitary hypertrophy. This rat model is also suggested by Rudin *et al.* (28) to be a useful analog of clinical situations. Rudin *et al.* also use MRI to examine the regression of the estrogen-induced pituitary hypertrophy following drug treatment. Further investigations into the changes of the pituitary as the young rat becomes an adult seem to be necessary. These studies would further correlate the changes seen on the MR image and volume measurements to the pathology of the pituitary.

#### CONCLUSION

Midline sagittal T1-weighted images prove to be the most effective and reproducible technique to display the anatomy of the pituitary gland region in rats. Volume changes of the pituitary gland appear to be normal during the development of the adolescent rat, but these changes do not involve the blunting of the sharp triangular structure of this structure. The findings of our study suggest that the changes in ap-



## MRI OF RAT PITUITARY HYPERTROPHY

pearance and volume of the pituitary gland as evaluated by MRI may provide the standard technique in detecting pituitary hypertrophy. In the estrogen-induced hypertrophy rat model, the pituitaries of the control animals and implanted animals have MRI intensity behavior similar to that of normal pituitary and pituitary lesions in humans.

### ACKNOWLEDGMENTS

We thank Gwen Tillapaugh-Fay and Annemarie van Garderen-Hoetmer for their skillful assistance with this project and Dr. M. C. Bosland for his helpful comments. This work was supported in part by Grant CIVO 87-2 from the Netherlands Cancer Foundation (KWF).

### REFERENCES

1. E. B. GOLD, *Epidemiol. Rev.* **3**, 163 (1981).
2. D. J. MCCOMB, K. KOVACS, J. BERI, AND F. ZAK, *JNCI* **73**, 1143 (1984).
3. J. H. J. VAN NESSELROOIJ, C. F. KUPER, M. C. BOSLAND, J. P. BRUYNTJES, AND R. KROES, in "Prolactinomas: An Interdisciplinary Approach" (L. M. Auer, Ed.), p. 85, de Gruyter, Berlin/New York, 1985.
4. J. H. J. VAN NESSELROOIJ AND C. F. KUPER, in "Proceedings, Second Meeting of the European Neuroendocrine Association," p. 208, 1985.
5. J. M. BERKVEN, J. H. J. VAN NESSELROOIJ, AND R. KROES, *J. Pathol.* **130**, 179 (1980).
6. R. KROES, J. M. BERKVEN, T. DE VRIES, AND J. H. J. VAN NESSELROOIJ, *J. Gerontol.* **36**, 259 (1981).
7. R. C. HAWKES, G. N. HOLLAND, W. S. MOORE, R. CORSTON, D. M. KEAN, AND B. S. WORTHINGTON, *AJNR* **4**, 221 (1983).
8. J. KELLET AND FRIESEN, in "Pituitary Microadenomas" (G. Faglia, M. A. Giovanelli, and R. M. McLeod, Ed.), p. 256, Academic Press, London, 1980.
9. J. G. M. KLIJN, S. W. J. LAMBERTS, F. H. DE JONG, R. DOCTER, K. J. VAN DONGEN, AND J. C. BIRKENHAGER, in "Pituitary Microadenomas" (G. Faglia, M. A. Giovanelli, and R. M. McLeod, Ed.), p. 303, Academic Press, London, 1980.
10. T. H. NEWTON AND I. RICHMOND, in "Pituitary Microadenomas" (G. Faglia, M. A. Giovanelli, and R. M. McLeod, Ed.), p. 256, Academic Press, London, 1980.
11. G. H. SCHNEIDER, in "Prolactinomas: An Interdisciplinary Approach" (L. M. Auer, Ed.), p. 91, de Gruyter, Berlin/New York, 1985.
12. F. CASANUEVA, D. COCCHI, V. LOKATELLI, C. FLAUTO, F. ZAMBOTTI, G. BESTETTI, G. L. ROSSI, AND E. E. MULLER, *Endocrinology* **110**, 590 (1982).
13. W. W. MORGAN, R. W. STEGER, M. S. SMITH, A. BARTKE, AND C. A. SWEENEY, *Endocrinology* **116**, 17 (1985).
14. D. K. SARKAR, P. E. GOTTSCHALL, AND J. MEITES, *Science* **218**, 684 (1982).
15. B. CORENBLUM, K. KOVACS, G. PENZ, AND C. EZRIN, *Endocrinol. Res. Commun.* **7**, 137 (1980).
16. H. M. LLOYD, J. D. MEARES, AND J. JACOBI, *Nature (London)* **225**, 497 (1975).
17. S. N. WIENER, M. S. RZESZOTARSKI, R. T. DROEGE, A. E. PEARLSTEIN, AND M. SHAFRON, *AJNR* **6**, 717 (1985).
18. T. SEKIYA, Y. FUKUDA, H. KOBAYASHI, Y. HATA, AND S. TADA, *Radiation* **3**, 131 (1985).
19. C. A. HANKINS, A. A. ZAMANI, AND C. L. RUMBAUGH, *Invest. Radiol.* **20**, 345 (1985).
20. S. M. WOLPERT, M. OSBORNE, M. ANDERSON, AND V. M. RUNGE, *AJNR* **9**, 1 (1988).
21. K. W. POJUNAS, D. L. DANIELS, A. L. WILLIAMS, AND V. M. HAUGHTON, *AJNR* **7**, 209 (1986).
22. U. FINK, B. MAYR, H. K. RJOSEK, R. OECKLER, K. VON. WERDER, AND D. HAHN, *Digit. Bilddiag.* **5**, 123 (1985).
23. A. J. DWYER, J. A. FRANK, J. L. DOPPMAN, E. H. OLDFIELD, A. M. HICKEY, G. B. CUTLER, D. L. LORIAUX, AND T. F. SCHIABLE, *Radiology* **163**, 421 (1987).
24. B. C. LEE AND M. D. F. DECK, *Radiology* **157**, 143 (1985).
25. P. C. DAVIS, J. C. HOFFMAN, T. SPENCER, G. T. TINDALL, AND I. F. BRAUN, *AJNR* **8**, 107 (1987).
26. M. V. KULKARNI, K. F. LEE, C. B. MCARDLE, J. W. YEAKLEY, AND F. L. HAAR, *AJNR* **9**, 5 (1988).
27. M. JUST, H. P. HIGER, M. SCHWARZ, J. BOHL, G. FRIES, P. PFANNENSTIEL, AND M. THELEN, *Magn. Reson. Imaging* **6**, 463 (1988).
28. M. RUDIN, U. BRINER, AND W. DOEPFNER, *Magn. Reson. Med.* **7**, 285 (1988).



## **CHAPTER IV**

### **MAGNETIC RESONANCE IMAGING COMPARED WITH HORMONAL EFFECTS AND HISTOPATHOLOGY OF ESTROGEN-INDUCED PITUITARY LESIONS IN THE RAT**

Joop H.J. van Nesselrooij, Joost P. Bruijntjes, Annemarie van Garderen-Hoetmer,  
Gwen M. Tillapaugh-Fay and Victor J. Feron.

Carcinogenesis 12: 289-297, 1991.



## Magnetic resonance imaging compared with hormonal effects and histopathology of estrogen-induced pituitary lesions in the rat

Joop H.J. van Nesselrooij<sup>1,2</sup>, Joost P. Bruijntjes<sup>1</sup>,  
Annemarie van Garderen-Hoetmer<sup>1</sup>,  
Gwen M. Tillapaugh-Fay<sup>2</sup> and Victor J. Feron<sup>1</sup>

<sup>1</sup>Department of Biological Toxicology, TNO-CIVO Toxicology and Nutrition Institute, 3704 HE Zeist, The Netherlands and <sup>2</sup>Nuclear Magnetic Resonance Research Laboratory, Department of Radiology, State University of New York, Health Science Center at Syracuse, Syracuse, NY 13210, USA

Estrogen-induced pituitary lesions in rats were studied in time-sequence experiments using magnetic resonance imaging (MRI), hormone determinations and light microscopy. The main purpose of the study was to evaluate the usefulness of MRI in comparison with conventional biochemical and histopathological methods for detecting the pituitary lesions as early as possible and to follow their development. Measurements were made at 15 time points, ranging from 1 h to 272 days after s.c. implantation of the estrogen pellet. High-resolution T1 weighted sagittal images with 2 mm slice thickness were made with a 2 Tesla 30 cm small-bore MRI system. Radioimmunoassay (RIA) was used to determine the different pituitary hormones. Conventional histopathology and immunoperoxidase staining methods were used to characterize the pituitary lesions and visualize the hormone-producing pituitary cells respectively. The first histopathological pituitary changes (enlarged acidophilic cells with increased number of vacuoles) were seen at day 2 after initiation of the estrogen treatment, while at day 4 the first immunohistochemical changes (increased number of prolactin-positive cells) were encountered. Significantly increased prolactin levels in blood plasma occurred from day 9 onwards. Also at day 9, changes of the pituitary gland were first visible on MR images, showing rounding of the anterior edge of the gland. Gradual enlargement of the pituitary caused by hyperplasia of hypertrophic prolactin-positive cells could be followed by MRI, and later on pituitary tumors were recognized, their images being heterogeneous due to great differences in signal intensity ranging from hypo- or iso- to hyperintense. Signal intensities of hemorrhagic tumor areas varies widely due to variation in the blood flow maintained in these areas. It was concluded that MRI is a powerful tool for detecting enlargement and tumors of the pituitary gland in rats. This method allows the development of such lesions to be followed in one and the same animal, thereby reducing the need of interim kills and thus the number of animals to be used.

### Introduction

Proliferative pituitary lesions frequently occur in ageing humans and animals. In humans, the incidence of asymptomatic microadenomas discovered at necropsy has been reported to vary

\*Abbreviations: RIA, radioimmunoassay; MRI, magnetic resonance imaging; PRL, prolactin; GH, growth hormone; TSH, thyroid-stimulating hormone; FSH, follicle-stimulating hormone; LH, luteinizing hormone.

between 20 and 30% with no predilection for a specific age, group or sex (1–5).

Clinical tests such as radioimmunoassays (RIAs\*) often fail in humans because of silent adenomas without elevated pituitary hormone levels (6), or because certain pituitary lesions, e.g. focal hyperplasias or small tumors (<5 mm in diameter), only slightly elevate pituitary hormone levels. Results are also poor with magnetic resonance imaging (MRI) in detecting small pituitary lesions (7).

Spontaneous pituitary tumors have been described in ageing rats of many strains (8–11). Their incidence can be as high as 60% in rats that are >30 months old, while the incidence of all types of proliferative pituitary lesions together can even be >90% (8–13). It is often difficult, however, to establish the presence and development of spontaneous pituitary tumors.

Estrogen-induced pituitary tumors in rats have been extensively studied as models for spontaneous pituitary tumors in both man and rodents (14–16). In previous studies, MRI proved to be an effective technique with which to display the pituitary anatomy (17,18).

The main objective of the present investigation was to evaluate the usefulness of MRI as a non-invasive technique to detect estrogen-induced pituitary lesions in the rat as early as possible and to follow their development. To this end changes in plasma levels of pituitary hormones, pituitary morphology and pituitary MRI at various time points after the start of estrogen treatment were monitored and correlated.

### Materials and methods

#### Animals and diets

Fifty-five 3 week old male weanling Sprague–Dawley rats were obtained from Harlan Sprague–Dawley, Inc., Indianapolis, IN, USA. In addition, two batches each consisting of 300 3 week old male weanling Sprague–Dawley rats were obtained from Harlan Sprague–Dawley CPB, Inc., Zeist, The Netherlands; the second batch was received ~6 months later than the first batch.

The rats were kept in stainless steel wire-mesh cages (two or three animals per cage; controls separated from experimental animals) in a well-ventilated room maintained at 20°C with relative humidity 40–70% and 12 h of lighting per day.

Rats of experiment I (see experimental design) had free access to food (Purina Formulab Chow 5000, Purina Mills, Inc., St Louis, MO, USA) and tapwater and were checked twice daily. Rats of experiment II (see experimental design) were fed a powdered, natural ingredient diet prepared in-house. The animals had free access to food and tapwater.

#### Estrogen treatment

Under ether anesthesia, a 25 mg estradiol-17 $\beta$  pellet (Organon, Oss, The Netherlands) was implanted s.c. between the scapulae of each rat in the treated group. The controls were sham operated in an identical manner but without the deposition of a pellet. All animals were treated under a protocol and housing arrangement approved by both Institutional Committees for the Humane Use of Animals.

#### Imaging

Sagittal T1 weighted MR images of the head were obtained with a 31 cm horizontal bore diameter, 2 Tesla, chemical shift/imaging instrument (General Electric, Fremont, CA, USA). The rats were immobilized in a Plexiglas cradle, and a saddle-coil NMR probe was used both for transmit and receive. Imaging parameters for the T1 weighted spin-echo's were: single sagittal midline slice, 2 mm slice thickness, repetition time 450–500 ms, echo time 24 ms, number of excitations 2, 40 mm field of view, 425 Hz/mm read gradient, a 2.5 ms duration sinc pulse

(having two side lobes on either side of the center lobe) for excitation, 256 complex sampling points and 128 or 256 phase encoding increments. The rats were anesthetized with sodium pentobarbital (Nembutal, Abbott Laboratories, North Chicago, IL, USA) 5 mg/100 g body wt i.p. in order to minimize motion during imaging.

#### Determination of plasma hormone levels

Blood was sampled from the trunk of the animals following decapitation with a guillotine. This procedure was done without anesthesia nearly always between 9 and 12 a.m. Plasma was separated and stored at  $-80^{\circ}\text{C}$ . The plasma concentrations of prolactin (PRL), growth hormone (GH), thyroid-stimulating hormone (TSH), follicle-stimulating hormone (FSH), luteinizing hormone (LH) were measured by RIA, according to Kwa *et al.* (19) using antiserum obtained through the courtesy of Dr S. Raiti (National Institute of Arthritis, Metabolism and Digestive Disease, Bethesda, MD, USA). The sensitivity of the assays was PRL 0.4 ng/ml, GH 1.0 ng/ml, TSH 3.5 ng/ml, FSH 0.2 ng/ml, LH 0.2 ng/ml, with intra- and interassay coefficients of variation of 5–10% and 10–15% respectively.

#### Histopathology and immunohistochemistry

At necropsy, pituitary wet wts were recorded before fixation in a 4% buffered formaldehyde solution. The pituitaries were processed to paraplasm, and 10  $5\text{-}\mu\text{m}$  thick step sections of each pituitary were made, one section of which was stained with H&E while the others were used for immunohistochemistry. Using rabbit anti-rat antiserum (UCB Bioproducts, Brussels, Belgium) the immunoperoxidase technique was applied to stain sections for PRL, GH, TSH, FSH, and LH.

Swine anti-rabbit total immunoglobulin (Sanbio, Nistelroode, The Netherlands) was used as a bridge between the antiserum and the rabbit peroxidase-anti peroxidase (Dako, Amsterdam, The Netherlands). 3,3-Diamino benzidine tetrahydrochloride (Sigma Chemical Co, St Louis, MO, USA) was used as substrate to visualize the product. The sections were counterstained with hematoxylin.

From the rats of experiment IIb (see experimental design) the brain with the tumorous pituitary gland was dissected, fixed *in toto* and further worked up as the other pituitaries were.

#### Experimental design

Two separate experiments were carried out, one (experiment I) being focused on MRI and histopathology of the pituitary gland, and the other (experiment II) on hormone plasma levels, and on immunohistochemistry and histopathology of the pituitary.

Experiment I consisted of two parts—experiment Ia and Ib. For experiment Ia, 45 male rats were used; 30 rats with an implanted estrogen pellet and 15 untreated controls. They were subdivided into 15 sets of one control and two treated rats each of which were examined by MRI and then killed at 15 time points, namely 2, 8 and 24 h, and 2, 4, 9, 16, 32, 49, 114, 133, 150, 186 and 240 days after implantation of the estrogen pellet. All pituitaries were examined for histopathological changes. For experiment Ib, which was started ~6 months later than experiment Ia, 10 male rats were used, six with an implanted estrogen pellet and four controls. Except for one rat that died on day 29 after treatment, all rats were examined by MRI at time points comparable to those for the rats of experiment Ia, but none of the controls was killed and each of the treated rats was killed after examination by MRI 240, 247, 250, 257 and 267 days after pellet implantation respectively. Again all pituitaries were examined histopathologically.

Experiment II also consisted of two parts. In experiment IIa, 300 male weanling rats were used and divided into two groups. One group of 150 rats served as controls and the other group of 150 rats as experimental animals. The rats were treated with estrogen and sham operated in an identical manner, as were the animals used in the imaging study. At 15 time points, namely 2, 4, 8 and 24 h, 4, 7, 11, 18, 35, 49, 66, 81, 98, 114 and 133 days after implantation of the estrogen pellet, 10 controls and 10 treated rats were killed.

In experiment IIb, again 300 male weanling rats were used and divided into two groups. One group of 150 rats served as controls and the other group of 150 rats as experimental animals. At 15 time points—7, 9, 11, 13, 16, 25, 35, 81, 114, 133, 150, 168, 217, 241 and 272 days—10 controls and 10 treated rats were killed.

Hormone levels in blood plasma were determined of all rats used in experiments IIa and IIb, and the pituitaries of these rats were subjected to histopathological examination; immunohistochemical examinations were done when considered relevant.

## Results

### MRI (experiment I)

Pituitaries of control rats were invariably triangular in shape with sharply defined margins. The signal intensity of the pituitary was always fully homogeneous.

An abnormal MR image of the pituitary was first detected 9

days after implantation of the estrogen pellet. Thereafter, the images gradually showed more deviations from normality, indicating an increase in degree of pituitary lesions with time. The MR images obtained can be described as follows.

*At 2, 4, 8 and 24 h, and 2 and 4 days after pellet implantation.* MR pituitary images of estrogen-treated rats were indistinguishable from those of the controls at these time points (Figure 1a and b).

*At 9, 16, 32 and 49 days after pellet implantation.* At day 9, rounding of the edge of the anterior side of the pituitary was visible. No inhomogeneities were detected (Figure 2a and b). At day 16, the gland was enlarged and the edges of both the anterior and posterior side were rounded. The subarachnoid space between the pituitary and the diencephalon, and the space between the pituitary and the pons were smaller than in control rats. The glands had a mottled, heterogeneous appearance and were often hypointense compared to surrounding brain tissue (Figure 3a and b). At days 32 and 49, the MR images were similar to those obtained at day 16, but indicated an increase in size of the pituitary with time.

*At 98, 114, 133 and 150 days after pellet implantation.* From day 98 onwards the images invariably showed a severely enlarged pituitary gland, with a small space still visible dorsal to the gland. The images of the pituitaries were very bright, while signal intensity was not uniform (Figure 4a and b).

*At 186 and 240 days after pellet implantation.* At days 186 and 240, images demonstrated considerably enlarged pituitaries. There were great differences in signal intensity within the (tumorous) pituitaries, ranging from hypo-, iso- to hyperintense relative to surrounding brain tissue (Figure 5a and b).

### Histopathology and immunohistochemistry (experiments I and II)

The first histopathological changes were seen at day 2 and the immunohistochemical changes at day 4, after estrogen implantation. Some acidophilic cells were enlarged and contained an increased number of vacuoles; they were evenly distributed over the gland. The number of PRL cells was slightly increased, that of FSH and TSH cells slightly decreased (Figure 1c and d).

At day 9, acidophilic cells became hypertrophic and had large nuclei; mitotic figures were conspicuous and sinusoids were slightly distended. The hypertrophic cells appeared to be PRL positive (Table I), and rapid proliferation of these hypertrophic cells caused the enlargement of the pituitary glands (Figure 2c and d).

At day 11, a marked decrease in the number of FSH and TSH cells occurred as well as a slight decrease in LH cells. The number of GH cells was not different from that in controls, whereas the number of PRL cells was now markedly increased; this increase was maintained throughout the study.

At day 16, cord-like structures of hypertrophic cells lined by endothelial cells and distended sinusoids were common features. The hypertrophic acidophilic cells showed clear paranuclear areas. Some atypical mitotic figures were now seen (Figure 3c and d).

At day 49, no FSH and TSH cells were found in the pituitary of estrogen-treated rats; LH cells were markedly and GH cells slightly decreased in number (Table I).

At day 98, once again some TSH cells could be detected (Table I), and the hyperplastic, enlarged PRL cells were seen to form clusters. Moreover, the sinusoidal lining showed interruptions causing intraparenchymal hemorrhages that contained some necrotic cells (Figure 4c and d).

From day 186 and onwards the pituitaries became tumorous

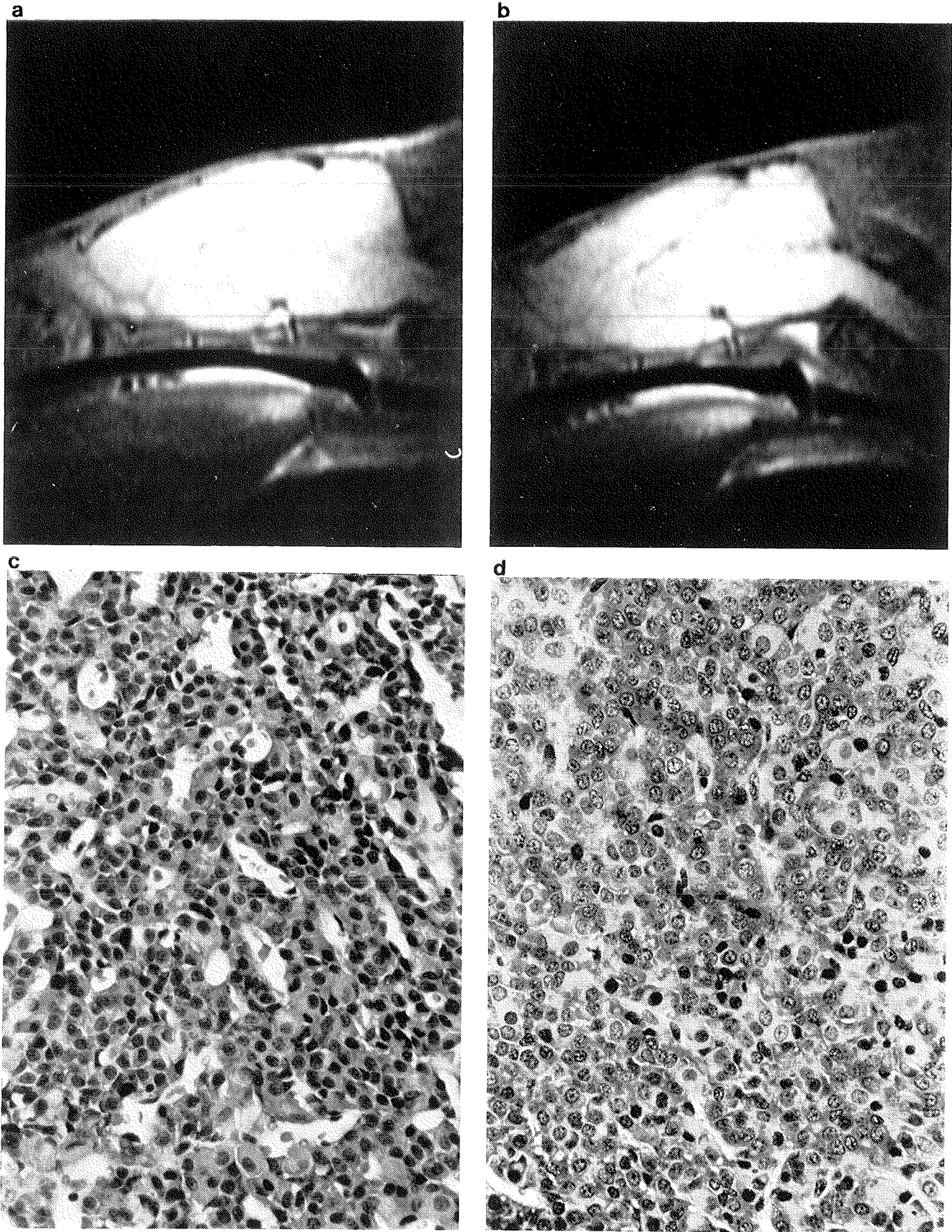


**Fig. 1.** (a) T1 weighted mid-sagittal image of a control rat at day 2, displaying a normal pituitary. (b) T1 weighted mid-sagittal image of an estrogen-implanted rat at day 2, no changes in size or signal intensity. (c) Control pituitary on day 2, normal distribution of the pituitary cells. H&E staining,  $\times 250$ . (d) Implanted rat at day 2, the pituitary shows a slight increase in intracellular vacuolization, some diffusely distributed hypertrophic cells. H&E staining,  $\times 250$ .

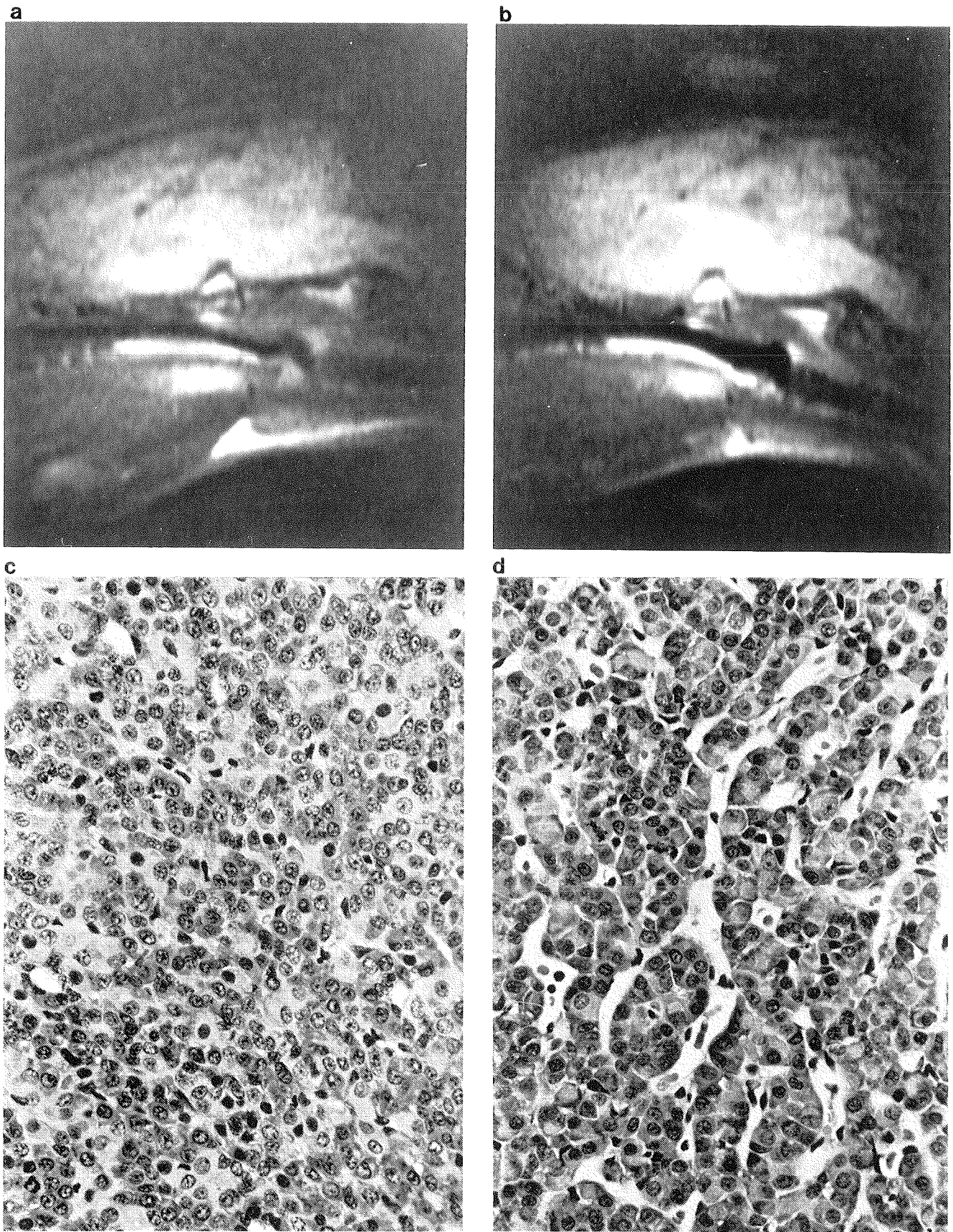


**Fig. 2.** (a) T1 weighted mid-sagittal image of a control rat at day 9, displaying a normal pituitary. (b) T1 weighted mid-sagittal image of an estrogen-implanted rat at day 9, on the anterior side of the pituitary rounding of the edge is visible. (c) Control pituitary on day 9, normal distribution of the pituitary cells. H&E staining,  $\times 250$ . (d) Implanted rat at day 9, hypertrophic pituitary cells and large nuclei. H&E staining,  $\times 250$ .



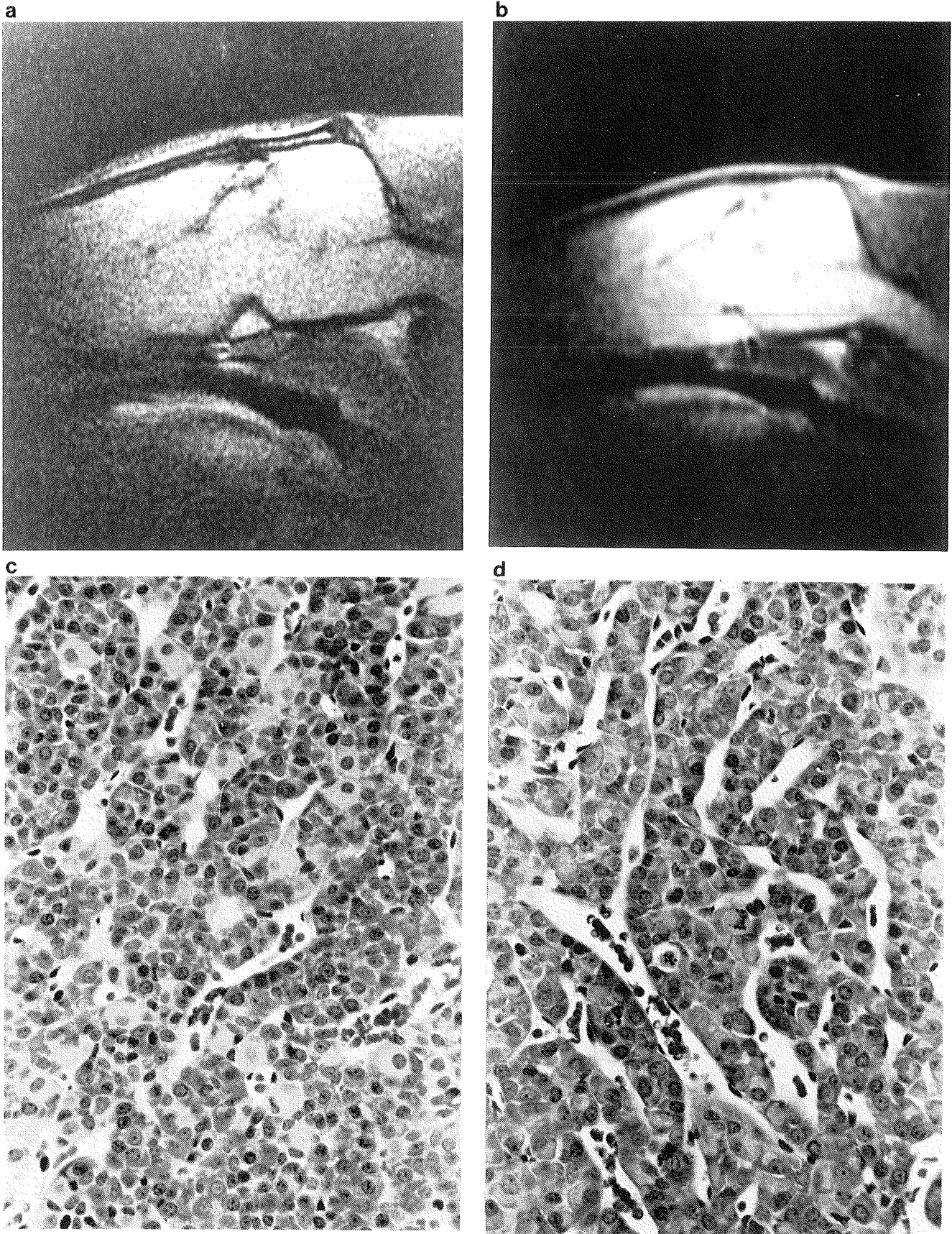


**Fig. 3.** (a) T1 weighted mid-sagittal image of a control rat at day 16, displaying a normal pituitary. (b) T1 weighted mid-sagittal image of an estrogen implanted rat at day 16, rounded margins on both sides anterior and posterior of the pituitary. (c) Control pituitary on day 16, normal distribution of the pituitary cells. H&E staining,  $\times 250$ . (d) Implanted rat at day 16, pituitary shows cord-like structures of hypertrophic pituitary cells lined by endothelial cells and markedly distended sinusoids. Some atypical mitoses. H&E staining,  $\times 250$ .

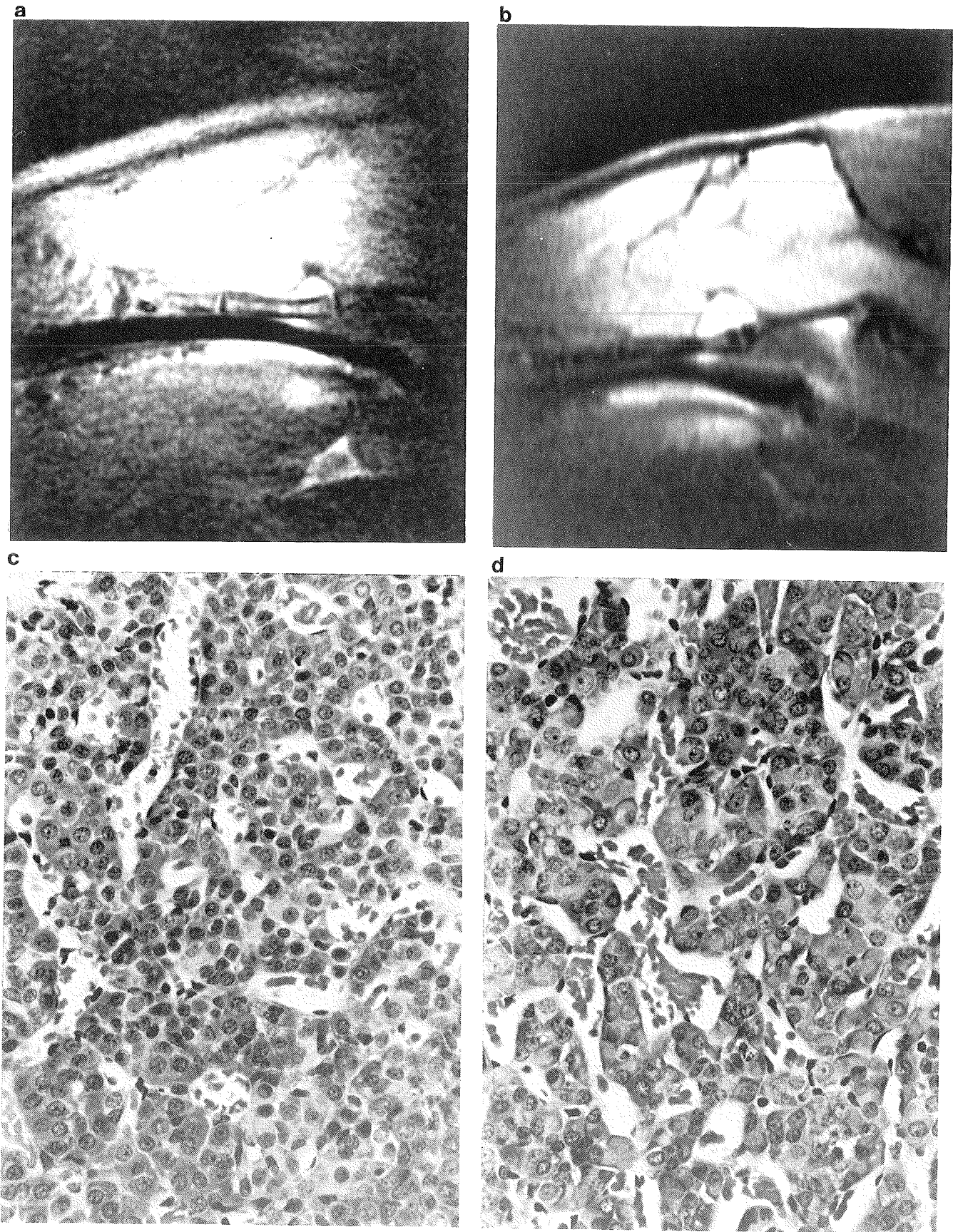
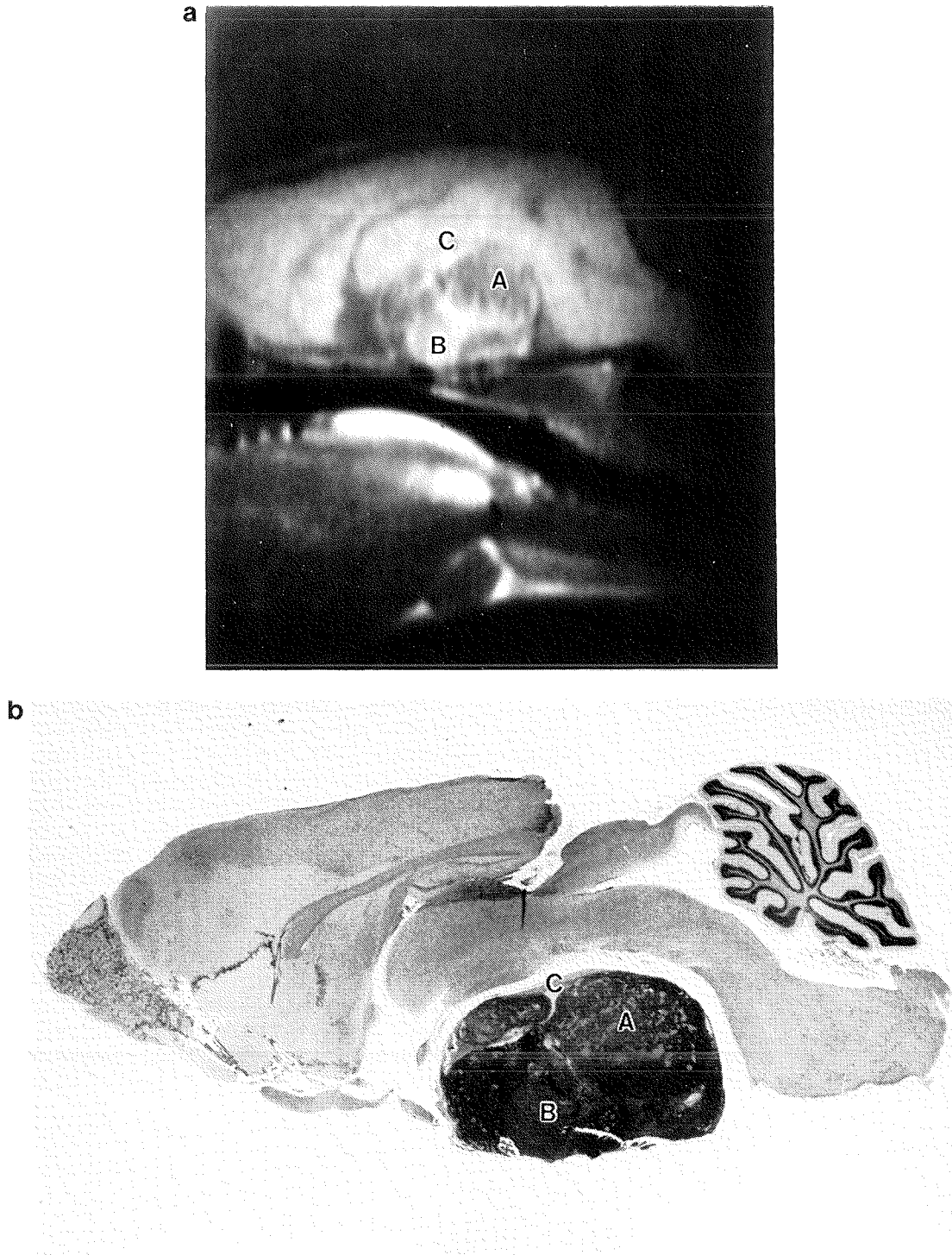


Fig. 4. (a) T1 weighted mid-sagittal image of a control rat at day 98, displaying a normal pituitary. (b) T1 weighted mid-sagittal image of an estrogen implanted rat at day 98, extensive growth of the pituitary. Dorsal to the pituitary, some space is left. (c) Control pituitary at day 98, normal distribution of the pituitary cells. H&E staining,  $\times 250$ . (d) Implanted rat at day 98, hypertrophic cells form clusters, some interruptions in the endothelial lining causes intraparenchymal hemorrhages. H&E staining,  $\times 250$ .



**Fig. 5.** (a) T1 weighted mid-sagittal image of an estrogen implanted rat at day 267, three different areas inside the tumor are visible with a hypointense (A), isointense (B) and hyperintense (C) signal intensity. (b) Implanted rat at day 267, corresponding to the same animal and anatomical plane as (a). The pituitary tumor displays a hemorrhagic area (A), a solid area (B) and a cystic area (C).

and contained areas that could be divided into different morphological entities. A combination of hemorrhagic areas, solid areas and colloid-filled cysts were found (Figure 5b). The hemorrhagic tumors were characterized by cells arranged in cord-like structures, one cell layer or several cell layers thick with cleft-like sinusoids on one side and cyst-like formations on the other side, both filled with blood. The solid tumors consisted of clusters of solid masses without a specific structure and were sparse of sinusoids. From day 240 and onwards the tumorous

pituitaries contained some GH and TSH cells, which were considered to be remnants of normal pituitary gland tissue (Table I). The same types of tumors can be found in human pituitaries (13).

#### *Plasma hormone levels (experiment II)*

During the first days the plasma PRL levels showed large variability both in the estrogen-implanted and in control rats. After day 5, however, there was a gradual elevation in the plasma PRL

level in the treated rats that became statistically significant at day 9 (Table II). For both control and implanted rats, GH levels showed a great variability during the entire period. Plasma levels of LH and FSH dropped at day 9 and these levels remained very low throughout the study. During the study a slight increase for TSH hormone level was visible for both control and implanted rats, while the TSH level of the implanted rats at the end of the study showed a slight decrease.

**Discussion**

In general, plasma hormone levels corresponded very well with the immunohistochemical findings in the pituitary gland: plasma PRL levels gradually increased, as did the number of enlarged PRL-positive pituitary cells. FSH, LH and TSH plasma levels as well as the number of FSH, LH and TSH cells in the pituitary gland decreased with time. GH being the exception, its blood plasma level nearly always being higher in treated rats than in control rats, whereas the number of GH pituitary cells in treated rats was decreasing with time. Clearly, the enlargement of the pituitary gland visible with MRI by 9 days after initiation of estrogen administration was exclusively due to hyperplasia of hypertrophic PRL cells.

Estrogen-induced hypertrophy and hyperplasia of the pituitary gland in rats have been previously reported (14–16) and were confirmed in the present study. However, tissue vascularization

as described in these previous papers was not seen in our study; we only observed distended sinusoids.

Estrogen-induced pituitary hypertrophy in rats is detectable with MRI in an early stage as we demonstrated in a previous study (17,18) and confirmed in the present study, rounding of the edges of the gland being seen as early as 9 days after estrogen implantation. Thus, rounding of the edges of the gland was seen early but none of the histological or immunohistochemical alterations, such as hypertrophy and hyperplasia of specific cells, distended sinusoids and intraparenchymal hemorrhages that developed during the first 5–6 months, could be specifically detected with MRI.

The sensitivity of MRI for small quantities of blood cells in the intraparenchymal hemorrhages or for the small number or size of these hemorrhages is apparently not sufficient to visualize these lesions with this technique. Nonetheless, the tiny white dots in the mottled images obtained from day 98 onwards might represent the microscopically detected intraparenchymal hemorrhages.

From day 186 the pituitaries became tumorous and areas that had obviously different signal intensities in the T1 weighted images appeared inside the tumors. When these areas were compared with light microscopical findings, hemorrhagic areas were found to be hypo-, hyper- or isointense; solid areas were invariably isointense and colloid-filled cysts appeared as hypo- or hyperintense signals. Comparison of these intensities with those of brain tissue indicates that hypointensity of hemorrhagic areas in tumorous tissue on T1 weighted imaging may be due to the hypoxic condition of tumorous tissue compared to normal tissue. Furthermore, the hemoglobin in hemorrhages in tumors may persist in the deoxyhemoglobin state for a relatively long period of time instead of the methemoglobin state which readily occurs in other types of hemorrhages (1,2,20–25). Hyperintensity of hemorrhagic areas is indeed known to be due to the conversion of the intracellular deoxyhemoglobin into methemoglobin by oxidative denaturation. Thereafter, red blood cell lysis and removal of the iron from the hemoglobin by macrophages starts; according to Bradley (21) this marks the beginning of the chronic phase of a hemorrhage. However, this explanation does not seem to be fully valid for the hemorrhages in the rat pituitary tumors, because these hemorrhages must have been in a chronic stage, most of them existing for at least 2 months. Moreover, in no case was red blood cell lysis observed. This may indicate that

**Table I.** Rat pituitary cellular hormone distribution as a function of the post-estrogen pellet implantation time

	I	Day 9		Day 49		Day 98		Day 240	
		A	B	A	B	A	B	A	B
PRL	I	×	++	×	++	×	++	×	++
GH	I	×	×	×	–	×	–	×	–
TSH	I	×	--	×	0	×	–	×	–
FSH	I	×	--	×	0	×	0	×	0
LH	I	×	–	×	--	×	--	×	0

A selection of the data from the satellite study was made to visualize the most advanced progression in the pathogenesis of the pituitary lesions. An immunoperoxidase staining for every specific hormone was used for the light microscopical evaluation of the pituitaries. A, control rats; B, estrogen-implanted rats. Cellular distribution: ×, equal to/or control; +, slight increase; ++, marked increase; 0, no hormone detectable; –, slight decrease; --, marked decrease.

**Table II.** Plasma hormone levels in male rats as a function of the post-estrogen pellet implantation time

Hormone (ng/ml)		Day 9	Day 49	Day 98	Day 240
PRL	A	8.4 ± 8.5	12.7 ± 8.5	12.9 ± 7.4	11.7 ± 5.1
	B	24.8 ± 9.1	97.0 ± 23.1	99.2 ± 43.0	323.0 ± 122
GH	A	4.2 ± 3.3	4.2 ± 2.1	14.2 ± 11.3	1.4 ± 0.4
	B	10.5 ± 4.9	17.3 ± 4.5	8.7 ± 2.1	4.9 ± 0.5
TSH	A	2.9 ± 1.0	3.9 ± 1.0	4.1 ± 0.9	3.7 ± 0.6
	B	2.3 ± 0.7	3.3 ± 0.3	2.9 ± 0.5	3.9 ± 0.5
FSH	A	21.0 ± 2.5	9.8 ± 0.8	9.6 ± 1.1	8.6 ± 1.1
	B	8.0 ± 0.6	5.1 ± 1.3	5.0 ± 0.7	5.1 ± 1.4
LH	A	0.61 ± 0.23	0.68 ± 0.09	0.78 ± 0.15	0.55 ± 0.18
	B	0.43 ± 0.10	0.50 ± 0.11	0.50 ± 0.06	0.39 ± 0.17

A, control rats; B, estrogen-implanted rats.

a certain blood flow was maintained in the hemorrhagic areas of the pituitary tumors, resulting in the absence of red blood cell lysis and in hemorrhagic conditions varying from acute, subacute to subchronic depending on the blood flow. The condition prevailing at the moment of making an MR image then determined whether an area was hypo-, iso- or hyperintense.

Pituitary tumors with colloid-filled cysts were found to be hyper- or hypointense in T1 weighted images. Dixon *et al.* (26) stated that in T1 weighted images, dark (hypointense) areas in the rat pituitary are consistent with fluid-filled cysts. Ishii *et al.* (27) found a round mass posterior to the pituitary with a very high signal intensity. Histological examination revealed that this mass represented a cyst filled with mucinous fluid and a wall composed of loose fibrous tissue lined by a single layer of ciliated cuboidal epithelium with some goblet cells. This cyst was diagnosed as a typical Rathkes cleft cyst. It is possible that cysts should be divided into three types, one of which is derived from Rathkes cleft and is hyperintense, another which originates from cleft-like cysts occurring in hemorrhagic tumors and which are hypointense in T1 weighted images, and common cysts which can be found in high numbers in fully normal pituitary glands of different strains of rats. These common cysts are lined by cuboidal cells and do not show up in MR images because they are isointense.

In conclusion, the present study confirmed that estrogen treatment of rats leads to hypertrophy and ultimately to hemorrhagic, solid and cystic pituitary tumors. MRI appears to be a powerful tool for detecting enlargement and tumors of the pituitary, allowing further development of such lesions to be followed in one and the same animal. Further studies are indicated to find out whether MRI of the pituitary in rats can be improved to such an extent that details of the pituitary lesions (intraparenchymal hemorrhages, hemorrhagic areas, cysts in tumors) can be unequivocally diagnosed by this technique.

### Acknowledgements

We wish to thank Drs M.C.Bosland, C.F.Kuper and N.M.Szeverenyi for their helpful comments. We are indebted to Professor Dr R.J.J.Hermus for critically reviewing the manuscript. This work was supported in part by Grant CIVO 87-2 awarded by the Dutch Cancer Society (Konigin Wilhemina Fonds).

### References

- Hankins,C.A., Zamani,A.A. and Rumbaugh,C.L. (1985) Prolactinomas: clinical presentation, radiologic assessment and therapeutic options. *Invest. Radiol.*, **20**, 345–354.
- McComb,D.J., Ryan,N., Horvath,E. and Kovacs,K. (1983) Subclinical adenomas of the human pituitary. *Arch. Pathol. Lab. Med.*, **107**, 488–491.
- Parent,D., Brown,B. and Smith,E.E. (1982) Incidental pituitary adenomas: a retrospective study. *Surgery*, **92**, 880–883.
- Taylor,C.R. and Jaffe,C.C. (1983) Methodological problems in clinical radiology research: pituitary microadenoma detection as a paradigm. *Radiology*, **147**, 279–283.
- Burrow,G.N., Wortzman,G., Rewcastle,N.B., Holgate,R.C. and Kovacs,K. (1981) Microadenomas of the pituitary and the abnormal sellar tomograms in an unselected autopsy series. *N. Engl. J. Med.*, **304**, 156–158.
- Kovacs,K., Lloyd,R., Horvath,E., Asa,S.L., Stefaneanu,L., Killinger,D.W. and Smyth,H.S. (1989) Silent somatotrophic adenomas of the human pituitary: a morphologic study of three cases including immunocytochemistry, electron microscopy, *in-vitro* examination and *in-situ* hybridization. *Am. J. Pathol.*, **134**, 345–353.
- Kulkarni,M.V., Lee,K.F., McArdle,G.B., Yeakly,J.W. and Haar,F.L. (1988) 1.5-T MR imaging of pituitary microadenomas: technical considerations and CT correlation. *Am. J. Neuroradiol.*, **9**, 5–11.
- Ito,A., Moy,P., Kaunitz,H., Kortwright,K., Clarke,S., Firth,J. and Meites,J. (1972) Incidence and character of spontaneous pituitary tumors in strain CR and W/Fu male rats. *J. Natl. Cancer Inst.*, **49**, 701–711.
- McComb,D.J., Kovacs,K., Beri,J. and Zak,F. (1984) Pituitary adenomas in old Sprague Dawley rats: a histologic, ultra structural and immunocytochemical study. *J. Natl. Cancer Inst.*, **73**, 1143–1166.
- Berkvens,J.M., Van Nesselrooij,J.H.J. and Kroes,R. (1980) Spontaneous tumours in the pituitary gland of old Wistar rats: a morphological and immunocytochemical study. *J. Pathol.*, **130**, 179–191.
- Kroes,R., Berkvens,J.M., de Vries,T. and Van Nesselrooij,J.H.J. (1981) Histopathological profile of a Wistar rat stock including a survey of the literature. *J. Gerontol.*, **36**, 259–279.
- Van Nesselrooij,J.H.J., Kuper,C.F., Bosland,M.C., Bruijntjes,J.P. and Kroes,R. (1985) Spontaneous pituitary lesions and plasma prolactin levels in rats. In Auer,L.M. (ed.), *Prolactinomas: An Interdisciplinary Approach*. de Gruyter, Berlin/New York, pp. 85–87.
- Trouillas,J., Girod,C., Claustrat,B., Cure,M. and Dubois,M.P. (1982) Spontaneous pituitary tumors in the Wistar/Furth/Ico rat strain. *Am. J. Pathol.*, **109**, 57–70.
- Lloyd,R.V. (1983) Estrogen-induced hyperplasia and neoplasia in the rat anterior pituitary gland, an immunohistochemical study. *Am. J. Pathol.*, **113**, 198–206.
- Wiklund,J., Wertz,N. and Gorsky,J. (1981) A comparison of estrogen effects on uterine and pituitary growth and prolactin synthesis in F34 and Holtzman rats. *Endocrinology*, **109**, 1700–1707.
- Hebert,D.C., Cisneros,P.L. and Rennels,E.G. (1977) Morphological changes in prolactin cells of male rats after testosterone administration. *Endocrinology*, **100**, 487–495.
- Van Nesselrooij,J.H.J., Szeverenyi,N.M. and Ruocco,M.J. (1989) Magnetic resonance imaging of estrogen-induced pituitary hypertrophy in rats. *Magn. Reson. Med.*, **11**, 161–171.
- Van Nesselrooij,J.H.J., Szeverenyi,N.M., Tillapaugh-Fay,G.M. and Hendriksen,F.G.J. (1990) Gadolinium-DTPA enhanced and digitally subtracted magnetic resonance imaging of estrogen induced pituitary lesions in rats: Correlation with pituitary anatomy. *Magn. Reson. Imag.*, **40**, 525–533.
- Kwa,H.G., van Gugten,A.A. and Vernofstad,F. (1969) Radioimmunoassay of rat prolactin. Prolactin levels in plasma of rats with spontaneous pituitary tumours, primary oestrone-induced pituitary tumours or pituitary tumour transplants. *Eur. J. Cancer*, **5**, 571–579.
- Atlas,S.W., Grossman,R.I., Gomori,J.M., Hackney,D.B., Goldberg,H.I., Zimmerman,R.A. and Bilaniuk,L.T. (1987) Hemorrhagic intracranial malignant neoplasms: spin-echo MR imaging. *Radiology*, **164**, 71–77.
- Bradley,Jr,W.G. (1988) MRI of hemorrhage and iron in the brain. In Stark,D.D. and Bradley,W.G. (eds), *Magnetic Resonance Imaging*. C.V.Mosby, St Louis, MO, pp. 359–374.
- Gomori,J.M., Grossman,R.I., Goldberg,H.I., Zimmerman,R.A. and Bilaniuk,L.T. (1985) Intracranial hematomas, imaging by high field MR. *Radiology*, **157**, 87–92.
- Gomori,J.M., Grossman,R.I., Ip-Yu,C. and Asakura,T. (1987) NMR relaxation times of blood: dependence on field strength, oxidation state, and cell integrity. *J. Comput. Assisted Tomography*, **11**, 658–690.
- Goldberg,H.I., Grossman,R.I. and Gomori,J.M. (1986) MRI diagnosis of cervical internal carotid artery dissecting hemorrhage. *Radiology*, **158**, 157–161.
- Unger,E.V., Cohen,M.S. and Brown,T.R. (1989) Gradient-echo imaging of hemorrhage at 1.5 Tesla. *Magn. Reson. Imag.*, **7**, 163–172.
- Dixon,D., Johnson,G.A., Cofer,G.P., Hedlund,L.W. and Maronpot,R.R. (1988) Magnetic resonance imaging (MRI): a new tool in experimental toxicologic pathology. *Toxicol. Pathol.*, **16**, 386–391.
- Ishii,T., Yamasaki,T., Tanaka,J., Tanaka,S., Hori,T. and Muraoka,K. (1987) Rathke's cleft cyst—report of three cases. *No Shinkei Geka*, **15**, 451–456 (English abstract).

Received on August 6, 1990; revised on October 8, 1990; accepted on November 1, 1990



## CHAPTER V

### **GADOLINIUM-DTPA ENHANCED AND DIGITALLY SUBTRACTED MAGNETIC RESONANCE IMAGING OF ESTROGEN-INDUCED PITUITARY LESIONS IN RATS: CORRELATION WITH PITUITARY ANATOMY**

Joop H.J. van Nesselrooij, Nikolaus M Szeverenyi, Gwen M. Tillapaugh-Fay and Ferry G.J. Hendriksen.

Magnetic Resonance Imaging 8: 525-533, 1990.





## GADOLINIUM-DTPA-ENHANCED AND DIGITALLY SUBTRACTED MAGNETIC RESONANCE IMAGING OF ESTROGEN-INDUCED PITUITARY LESIONS IN RATS: CORRELATION WITH PITUITARY ANATOMY

JOOP H.J. VAN NESSELROOIJ,\*† NIKOLAUS M. SZEVERENYI,\* GWEN M. TILLAPPAUGH-FAY,\*  
AND FERRY G.J. HENDRIKSEN†

\*Nuclear Magnetic Resonance Research Laboratory, Department of Radiology, State University of New York, Health Science Center at Syracuse, Syracuse, New York 13210, USA,

†Laboratory of Pathology, Department of Biological Toxicology, TNO-CIVO Toxicology and Nutrition Institute, 3704 HE Zeist, The Netherlands

Pituitary hypertrophy and tumors were induced in male Sprague Dawley rats using estradiol-17 $\beta$ . This tumor model generates a variety of pituitary lesions which are relevant to human pituitary disease. In order to characterize these lesions, gadolinium DTPA was injected intravenously into the tail vein of estrogen treated and control rats. High resolution  $T_1$ -weighted MR images, pre- and postenhancement, were obtained at 8 different time points spanning 300 days following the subcutaneous implantation of the estrogen pellets. Images with 2-mm slice thickness were made with a 2 Tesla small-bore MR imaging system.

Both normal and tumorous pituitaries were found to enhance with contrast agent, but contrast uptake was not uniform. Gd-DTPA distribution was sensitive to the different types of lesions generated in the course of this study. Digital subtraction of congruent images, pre- and postcontrast, provided difference images reflecting contrast concentration and allowed identification of subtle enhancement effects.

Hypertrophic pituitaries displayed uptake of contrast, but the distribution of contrast agent was nonuniform and appeared mottled. A bright rim enhancement was often seen anterior to the pituitary gland, most likely arising from the oculomotor nerves and arachnoid. Histological slices in the same anatomical plane as the MR images were obtained on the animals allowing identification of individual lesions. Cystic areas within tumors were found to give strong contrast enhancement in less than five min postinjection. Solid and hemorrhagic areas of the pituitary tumor were hypo- to isointense relative to surrounding brain and did not take up contrast agent. Significant perfusion in these areas apparently does not occur. Systemic treatment with a dopamine agonist may, therefore, not be effective for this type of tumor.

**Keywords:** Magnetic resonance imaging; Rat; Pituitary lesions; Gadolinium-DTPA; Digital subtraction; Pituitary anatomy.

### INTRODUCTION

The purpose of this study was to investigate the use of a magnetic relaxation contrast agent in combination with a digital subtraction technique to improve the detection and characterization of pituitary lesions in rats examined by MRI. The tumor model used in this study has been employed previously<sup>25</sup> and is believed to be a relevant model for human pituitary disease.

Gadolinium-DTPA (Gd-DTPA) is a very stable chelate complex and is widely used in clinical MRI. This compound is a paramagnetic relaxation agent and acts by enhancing  $T_1$  and  $T_2$  relaxation rates for water through a magnetic dipole-dipole interaction with the unpaired electrons of the gadolinium metal atom.<sup>4,7,12,18,23,24</sup> This complex has low toxicity and can be administered IV in concentrations sufficient to cause reduction of longitudinal magnetization relax-

---

RECEIVED 8/4/89; ACCEPTED 2/13/90.

*Acknowledgments*—We thank Annemarie van Garderen-Hoetmer for her skillful assistance with this project and Dr. M.C. Bosland for his helpful comments. This work was supported in part by Grant CIVO 87-2 from the Dutch Cancer Society (KWF).

Address correspondence to Joop H.J. van Nesselrooij, Nuclear Magnetic Resonance Research Laboratory, Dept. of Radiology, SUNY Health Science Center at Syracuse, Syracuse, NY 13210, USA.

ation times in specific tissues.<sup>5,8,11,22</sup> These tissues then appear with enhanced intensity on  $T_1$ -weighted images. The initial distribution of Gd-DTPA is related to blood flow and tissue perfusion and causes strong effects in the first few minutes after injection.<sup>20</sup> Gd-DTPA can be used as a probe of pituitary perfusion.<sup>9,21</sup>

To better visualize the structures that exhibit enhancement, a digital subtraction of congruent images pre- and postcontrast agent was carried out.<sup>15</sup> In the resulting difference images only regions having been affected by Gd-DTPA appear with significant intensity. Stationary tissue unaffected by contrast agent is cancelled and does not appear on the image.

## MATERIALS AND METHODS

### *Animal Handling*

A total of 21 male weanling Sprague-Dawley rats (Harlan Sprague Dawley, Indianapolis, IN) were used in this study to evaluate proliferative pituitary lesions induced by estrogen. The rats were three weeks old upon arrival and divided into two groups. Twelve rats served as experimental animals and nine as control. The experimental animals were implanted subcutaneously between the scapulae with 25-mg estradiol-17 $\beta$  (E2) pellets (Organon, The Netherlands), while the control rats were sham operated in the same manner without the deposition of a pellet. The operations were done under ether anesthesia.

Rats were housed in wire cages in a well ventilated room at 20°C with relative humidity 40–70% and lighting 12 hr a day. Animals had free access to food (Purina Formulab Chow 5000, Purina Mills, Inc., St. Louis, MO) and tap water and were checked twice daily. The animals were treated under a protocol and housing arrangement approved by our institutional Committee for the Humane Use of Animals.

### *Imaging*

Magnetic resonance images of the rats were obtained at various points in time after estrogen treatment. One control and two experimental animals were examined at the first three time points (16, 64, and 87 days), while one control rat and one experimental rat were examined at each of the later time points (112, 238, 240, 247, 280, and 300 days). Images were produced with a 31-cm horizontal bore diameter 2 Tesla spectroscopy/imaging system (General Electric, Fremont, CA). A homemade 3-cm diameter by 3.2-cm long saddle coil was used both for transmit and receive, as this arrangement was found to give adequate sensitivity and RF homogeneity to display the pituitary. Imaging parameters were as follows: single midsagittal slice, 2-mm slice thickness, repetition time (TR = 440–500

msec), echo time (TE = 24 msec), 2 excitations signal averaged, 40 mm  $\times$  40 mm field of view, 425 Hz/mm read gradient, 2.5 msec 3-lobed sync pulse, 128 phase-encoding increments, and 256 complex sampling points. For higher resolution images the phase-encoding increments were increased to 256 and the read points increased to 512 complex points. To minimize animal motion during the imaging procedure rats were anesthetized with sodium pentobarbital, 5 mg/100 g body weight, i.p. (Nembutal, Abbott Laboratories, North Chicago, IL).

MR images of the pituitary were obtained both pre- and postinjection of Gd-DTPA contrast agent. In order to compare congruent images, a technique was developed which permitted serial images of the same animal to be generated without repositioning the animal in the bore of the magnet. A heparinized needle, connected to a syringe via a thin plastic tubing, was inserted into a caudal vein of the rat tail prior to imaging. Injections of Gd-DTPA, 469 mg/ml (Magnevist, Berlex Laboratories, Inc., Wayne, NJ) were made while the animal was still anesthetized and in the bore of the magnet. There was no direct contact with the animal. Images (calculated in magnitude mode) obtained in this manner could be digitally subtracted and converted to magnitude mode to give "difference images." These images very much simplified the determination of which tissues were affected by contrast agent. Initially, the dose was varied over the range of 100–500 mg Gd-DTPA/kg bodyweight, but then 400 mg/kg was agreed upon as the effective dose in these experiments. This corresponds to approximately five times the dose used in human imaging and was found experimentally to best demonstrate the pituitary lesions. Images were always obtained at five min post-Gd injection, but in some animals where lesions did not display contrast uptake, additional images were obtained up to 50 min postinjection.

### *Microscopic Anatomy*

Following MR imaging rats were killed by decapitation while still under anesthesia. The heads were fixated in 4% formaldehyde solution for approximately one mo after which time the brain and pituitary were removed and sectioned for examination. Sections were cut 5  $\mu$ m thick and stained with hematoxylin and eosin. It was only possible to remove the brain and pituitary as an intact unit in the animals with large pituitary tumors.

The figures showing the normal anatomy of the rat pituitary in relationship to the brain were obtained from a previous study carried out at TNO-CIVO. These sections were prepared from the fixed heads of one-mo-old Sprague-Dawley rats, but were decal-

cified and embedded in paraplast before step sections were made of the intact pituitary/brain structure. The sections were 5  $\mu$ m thick and stained with hematoxylin and eosin. These sections proved to be valuable in identifying the structures observed on the MR images. Tumors were classified according to the morphological scheme presented by Berkvens et al.<sup>1</sup> This classification of tissue corresponds more closely to MRI appearance than when classification is based on tinctorial methods.

## RESULTS

The estrogen-induced pituitary tumor model ultimately gives rise to a variety of lesions containing solid, hemorrhagic, and cystic regions that could be identified on the basis of histology. Most pituitary tumors contained two or more of these growth patterns, each displaying a specific time dependence and intensity for enhancement with contrast agent in the MR imaging experiment. Although it was possible to detect regions of enhancement on  $T_1$ -weighted images of rats given Gd-DTPA contrast agent, the technique of digitally subtracting a pre- from a postcontrast-enhanced image of the same slice simplified the identification of these tissues.

Midsagittal images of the nine control animals displayed the pituitary as a triangular structure which was isointense or hyperintense relative to surrounding brain (Fig. 1(A)). A rapid enhancement of all or part of the pituitary was observed following the injection of Gd-DTPA contrast agent in each of these animals (Fig. 1(B)). Images obtained within five min postinjection already displayed enhancement of the pituitary as well as the infundibulum and pituitary stalk, provided that one was fortunate enough to select the exact plane containing these latter structures. The digitally subtracted image made it much easier to evaluate whether a region was really displaying enhancement as a result of contrast agent (Fig. 1(C)). In general no animals showed significant enhancement of the cerebrospinal fluid (CSF) or meninges around the brain. Digitally subtracted images in the control animals produced a bright rim enhancement extending around all three sides of the pituitary. When only partial enhancement of the gland was observed, the pars distalis was the region that contained the contrast agent.

At day 16 the experimental animals showed the first signs of pituitary hypertrophy which caused a slight bulging anterior in the normally sharply triangular gland when viewed in sagittal images. On day 64 this bulging was more pronounced and also affected the dorsal surfaces of the pituitary. Gadolinium enhancement was not noticeably different from the corre-

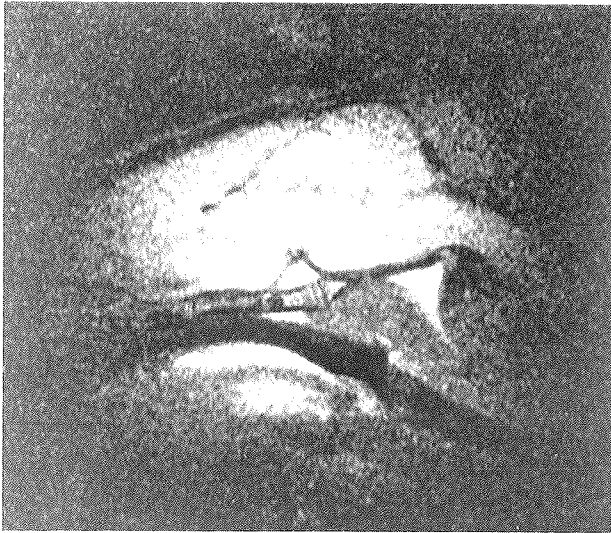
sponding control rats. Following 87 days of estrogen treatment, the pituitary of experimental animals was obviously hypertrophic and the normally triangular structure observed on sagittal MR images appeared to be significantly blunted (Fig. 2(A)). Gadolinium in these animals produced an enhancement of nearly the entire pituitary, although this enhancement was non-uniform (Fig. 2(B)). Again this effect was most easily evaluated on the difference image (Fig. 2(C)). The enhancement in hypertrophic pituitaries was already visible 5 min postinjection and disappeared after about 20 min. Enhancement of a rim around the pituitary was again found, but most often only at the anterior margin of the gland when viewed in a sagittal plane.

Between 112 and 238 days of development under estrogen stimulus, rat pituitary hypertrophy developed into a tumorous mass. Different regions in the pituitary tumor could now be identified on MR images and were more exactly classified based on histopathology. Figure 3(A) is the  $T_1$ -weighted image of a rat which was under estrogen stimulus for 240 days. The pituitary of this animal was grossly enlarged and displayed several tissues of differing MR image appearance. Gadolinium enhancement revealed several regions of strong contrast uptake (Fig. 3(B)) which could be readily identified on the difference image (Fig. 3(C)). A histological section obtained midsagittally through this rat pituitary (Fig. 3(D)) illustrates these different types of tumorous tissues. The solid area (s) consisted of a dense network of tumorous pituitary cells and lacked sinusoids. Hemorrhagic areas (h) contained cord-like formulations of pituitary tumor cells located between small isolated cystic pockets filled with red blood cells and sinusoids. Cystic regions (c) appearing as light colored areas on Fig. 3(D) were found to be filled with colloid and gave strong contrast enhancement on corresponding MR images. This observation is quite different than what is found in solid and hemorrhagic areas, which did not enhance with contrast even after 50 min postinjection.

## DISCUSSION

Paramagnetic contrast agents such as Gd-DTPA produce strong magnetic relaxation effects that directly influence signal intensity of water in MR images. Assuming that Gd-DTPA distributes primarily in the intravascular compartment and rapidly passes into the interstitial space, it is quite conceivable that this contrast agent would appear in the pituitary in a matter of minutes. The pituitary is an endocrine organ with a rich blood supply and is well vascularized with a dense network of sinusoids.<sup>5,6,13,14</sup>

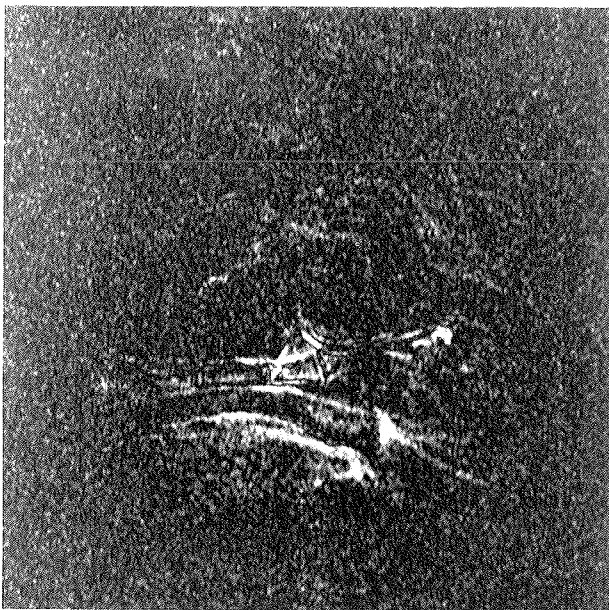
It is not surprising that in normal rats and rats that



A



B



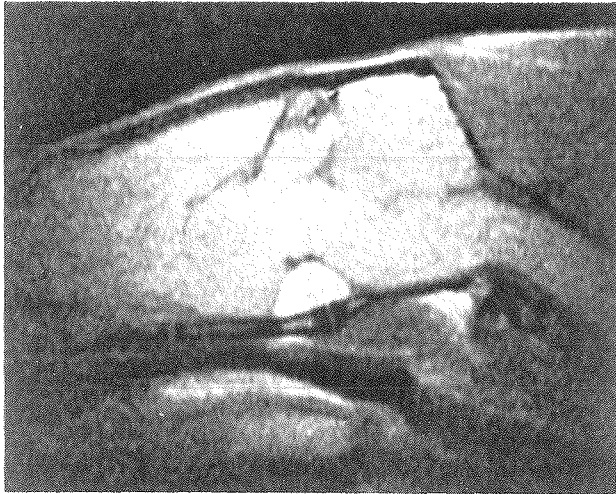
C

Fig. 1. (A)  $T_1$ -weighted midline sagittal high resolution image of a control rat at day 87 displaying a normal pituitary. Pre-Gd-DTPA. (B)  $T_1$ -weighted midline sagittal image of the same control rat as in Fig. 1, five min post-Gd-DTPA injection. The animal was not repositioned between images and all experimental conditions are identical to those of Fig. 1. (C) Digitally subtracted image (Fig. (B)-(A)). Enhanced rims are found around the pituitary, possibly arising from the oculomotor nerves and the surrounding arachnoid.

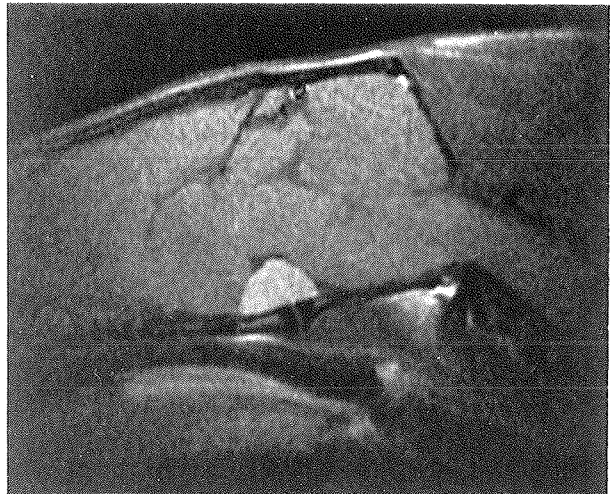
only had the estrogen implant for less than 87 days, the enhancement by Gd-DTPA was immediate. Starting with the 87 day rat, there was extensive hypertrophy involving changes in the histopathology of prolactin (PRL) cells that could be demonstrated microscopically. The endothelial cells of the sinusoids were interrupted, causing intraparenchymal hemorrhages. Gadolinium enhancement of the pituitary was still very rapid and occurred within minutes as was observed in the control rats. The distribution of gadolinium contrast in the control animals, day 16, and day 64 exper-

imental animals appeared to have the contrast agent concentrated in the ventral portion of the gland corresponding to the pars distalis. Figure 4(A) displays a histological slide of a normal rat pituitary viewed in the midsagittal plane. The pars distalis (d) forms the lower portion of the pituitary gland and is comprised of basophilic and acidophilic cells. As suggested by the staining, it is quite different both morphologically and histologically from the other sections of the pituitary (par nervosa and pars intermedia).

In the day 87 and day 112 animals the contrast en-



A



B



C

Fig. 2. (A)  $T_1$ -weighted midline sagittal high resolution image of an experimental rat having had an estrogen pellet implanted 87 days prior to imaging. The pituitary is hypertrophic and is enlarged relative to the control animal. The normally triangular shape of the gland is blunted. Pre-Gd-DTPA. (B) Same animal and conditions as (A), but five min post-Gd-DTPA injection. The pituitary appears mottled and hyperintense relative to surrounding brain. (C) Digitally subtracted image (Fig. (B)-(A)). There is an enhanced rim anterior to the hypertrophic pituitary most likely caused by the oculomotor nerve and/or arachnoid.

hancement appears to be more evenly distributed throughout the gland (Fig. 2(C)). The entire width of the normal pituitary is approximately 5 mm. As can be seen in the histological slide of a normal rat pituitary obtained in the axial plane (Fig. 4(B)), an image obtained with a slice thickness of 2 mm in the sagittal plane (indicated by the region between arrows) would have significant partial volume effects. If contrast agent were only localized in the pars distalis, midline images would exhibit enhancement primarily at the ventral portion of the gland, as is seen in images of the normal gland. As the pituitary hypertrophies, expan-

sion occurs in a dorsal direction, involving primarily the pars distalis. Images of such an animal would appear as if the entire enlarged pituitary contains contrast agent. This reasoning could explain the appearance of contrast in the day 87 rat (Fig. 2(C)).

Rats in this study started developing pituitary tumors between day 112 and day 238. The tumors generated in this model were only found in the pars distalis. Histologically the induced tumors showed a complex structure and growth pattern similar to the various spontaneous tumors described by Berkvens et al.<sup>1</sup> The MR images suggested a nonuniform distribution

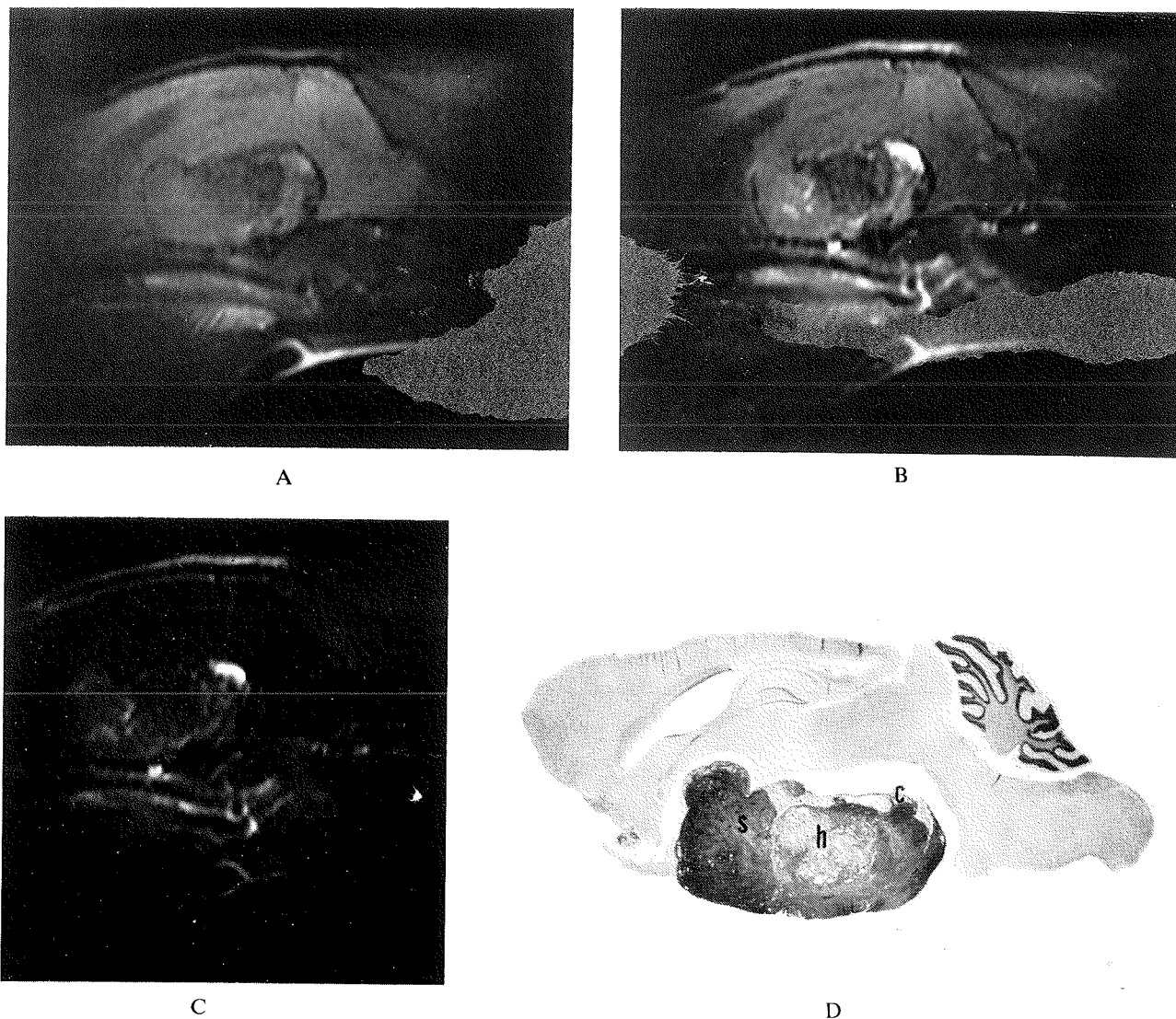


Fig. 3. (A)  $T_1$ -weighted midline sagittal high resolution image of a rat having had an estrogen pellet implanted 240 days prior to imaging. The pituitary is tumorous and displays regions that are hypo-, hyper-, and isointense compared to surrounding brain. Pre-Gd-DTPA. (B) Same animal and conditions as (A), but five min post-Gd-DTPA injection. Only one region inside the tumorous tissue of the pituitary is seen to be enhanced. (C) Digitally subtracted image (Fig. (B)-(A)). There is a variegated appearance of contrast within the tumor. The region showing very high intensity, when compared to the histological slide of the same animal (D), corresponds to a cystic area. (D) A histological slide of the tumorous pituitary corresponding to the same animal and anatomical plane as Figs. 3(A)-(C). The left side of the tumor displays a solid area (S), the central region corresponds to a hemorrhagic area (H), and the upper right corner contains a cystic area (C).

of Gd-DTPA in these different areas. No enhancement was seen in the hemorrhagic areas of the tumors even 50 min postgadolinium injection. This observation can be explained by a poor circulation and/or perfusion of tumorous hemorrhagic tissue. Hemorrhagic tumors consist of cells arranged in cord-like structures that are adjacent to both cleft-like sinusoids (covered with endothelial cells) and cyst-like formations (without endothelial lining) that are filled with

red blood cells and a small amount of necrotic tumor cells.<sup>1</sup> Histopathological observations in a study involving total body perfusion with a mixture of formaldehyde and mercury sublimate, demonstrated that the cyst-like formations in hemorrhagic tumors remained filled with blood, whereas the sinusoids were emptied.<sup>1</sup> These findings indicate that the sinusoids are not obstructed, consequently one would expect perfusion of contrast into and enhancement of the

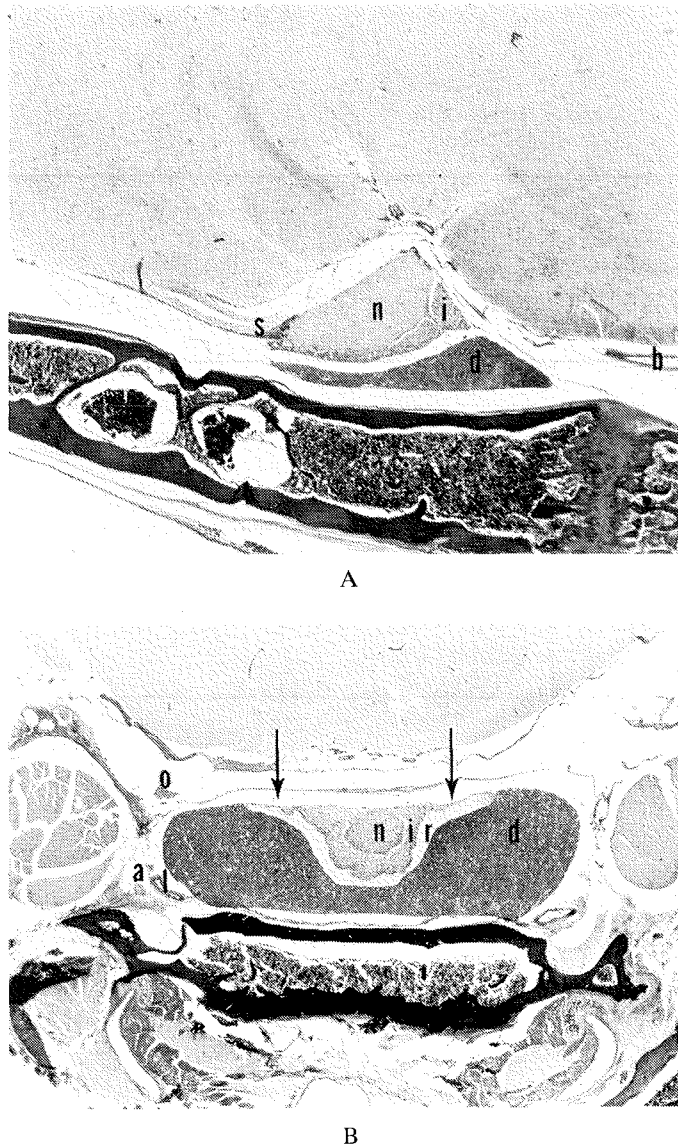


Fig. 4. (A) Midsagittal section of a rat skull. This photograph illustrates the anatomy of the pituitary and surrounding tissue. The pituitary consists of the pars nervosa (n), pars intermedia (i), and pars distalis (d). Also visible are the pituitary stalk and infundibulum (s), posterior the basilar artery (b), and the meninges covering the pituitary. (B) Axial cut of the rat skull displaying the abducent nerves (VI) (a) bilaterally, the internal carotid arteries (1) and oculomotor nerves (o), the pars nervosa (n), pars intermedia (i), pars distalis (d), and Rathke's cleft (r). The arrows correspond to the location and width of the 2-mm slice used in the midsagittal MR images.

sinusoids. These tissues were found to only display slight enhancement with contrast on the MR image. Since the cystic pockets account for the bulk of the volume in this tumorous tissue, it appears that contrast agent does not diffuse significantly into these surrounding tissues. Based on the histological observations that the red cells in the cystic pockets have a healthy appearance (not pineapples), there must be at least a minimal communication of nutrients to these

areas. The communication cannot be very effective, however, since contrast was not found to appear in hemorrhagic areas even 50 min postcontrast injection.

Solid tumors are more easily understood. Solid pituitary tumors in the rat lack sinusoids,<sup>1</sup> consequently little or no enhancement can be expected to occur in areas with a large cellular component and a small interstitial component. Relatively small amounts of Gd-DTPA were found to perfuse these areas and the signal

from this tissue was equally bright before and after contrast injection. Brant-Zawadzki<sup>3</sup> and Dwyer<sup>10</sup> arrived at the same conclusion regarding the solid areas in tumorous pituitaries in man.

Colloid-filled cysts in rat pituitary tumors reacted quite differently compared to the previously described areas. These regions already showed strong enhancement in 5 to 15 min postcontrast injection. This is in contradiction with the findings of Brant-Zawadzki,<sup>3</sup> but are in agreement with Dwyer.<sup>10</sup> Gadolinium-DTPA must reach the contents of these cysts and effect the intensity of the signal in the MR image. Perhaps this is due to the fluidity of the contents in this structure. The lining in these cysts were observed to be identical to the endothelial lining observed in the blood-filled hemorrhagic cysts.

There are several possible explanations for the enhanced rims that were observed around the pituitaries following injection of Gd-DTPA and digital subtraction. One possibility is an artifact caused by the slight movement of the animal after injecting the contrast agent. However, rims were found on three sides of the pituitary after subtraction and the consistency of this observation makes this explanation unlikely. A second possibility is that the gland had swollen postinjection. Only 0.5 ml of fluid was injected into the tail vein of the rat which would increase blood volume by 4%. A small change in blood volume alone would not account for the appearance of the bright rim on difference images. Since other pools of CSF elsewhere in the cranium did not display enhancement on images, CSF is also excluded as a source for the enhanced rims, unless flow is markedly lower in the area around the pituitary than elsewhere. Remarkably, Mark<sup>17</sup> found no CSF in the human pituitary fossa studied with cryomicrotomy.

Kilgore<sup>16</sup> describes that in humans the intracavernous segments of cranial nerves III–VI enhance significantly due to an incomplete blood-brain barrier. Perhaps this also occurs in the rat and causes the bright thin rim sometimes found in front of the pituitary on subtracted images.

Another explanation of the rim phenomenon is perhaps the slow flow rate of blood in arterial and venous system found in the subarachnoid space similar to that found around the human pituitary.<sup>2</sup> Page,<sup>19</sup> however, has found a very high blood flow posterior to the pituitary in sheep. Perhaps this flow rate was measured in the basilar artery and has no relation with the flow in the blood vessels directly covering the pituitary.

The most plausible explanation for the enhanced rims is a combination of enhancement of the capsule around the pituitary (the dura) which enhances quickly in man<sup>2</sup> and the contribution from the oculomotor

nerve (III) anterior to the pituitary.<sup>16</sup> If these enhanced rims are caused by the vascular system, it is conceivable that tumorous pituitaries would compress this network to the extent that these blood vessels would appear with smaller cross section, resulting in less rim enhancement. If flow is restricted, this could cause the delay or absence of enhancement in the various areas of the tumorous pituitaries. These hypotheses are consistent with the observations reported in this study.

## CONCLUSION

The blood-brain barrier that prevents the transport of Gd-DTPA to normal brain tissue is not operating in the pituitary, pituitary stalk, infundibulum, oculomotor nerve (III), and abducent nerve (VI). Thus, there is a rapid uptake of this material in this gland and associated tissue resulting in hyperintensity on  $T_1$ -weighted images. Uptake was seen to be nonuniform in both the control and experimental rats and is most likely related to the condition of the sinusoids and surrounding intercellular space. Following Gd-DTPA injection, normal pituitary tissue was found to enhance, whereas tumorous pituitary tissue in hemorrhagic and solid areas remained iso- or hypointense to surrounding brain.

These findings may have significant implications for the effectiveness of a dopamine agonist treatment in humans with large pituitary tumors containing hemorrhagic and solid areas. Perfusion in these tumors is likely to be very poor.

## REFERENCES

1. Berkvens, J.M.; Van Nesselrooij, J.H.J.; Kroes, R. Spontaneous tumors in the pituitary gland of old Wistar rats: A morphological and immunocytochemical study. *J. Pathol.* 130:179–191; 1980.
2. Berry, I.; Brant-Zawadzki, M.B.; Osaki, L.; Brash, R.; Murovic, J.; Newton, T.H. Gd-DTPA in clinical MR of the brain: 2. Extraaxial lesions and normal structures. *AJNR* 7:789–793; 1986.
3. Brant-Zawadzki, M.; Berry, I.; Osaki, L.; Brasch, R.; Murovic, J.; Norman, D. Gd-DTPA in clinical MR of the brain: 1. Intraaxial lesions. *AJNR* 7:781–788; 1986.
4. Brasch, R.C. Work in progress: Methods of contrast enhancement for NMR imaging and potential applications. *Radiology* 147:781–788; 1983.
5. Brasch, R.C.; Weinmann, J.H.; Wesbey, G.E. Contrast-enhanced NMR imaging: Animal studies using gadolinium-DTPA complex. *AJR* 142:625–630; 1984.
6. Carpenter, M.B.; Sutin, J. The hypothalamus. In: *Human neuroanatomy*. Baltimore, MD: Williams & Wilkins; 1983:pp. 552–578.



7. Claussen, C.; Laniado, M.; Schorner, W.; Niendorf, H.P.; Weinmann, H.J.; Fiegler, W.; Felix, R. Gadolinium-DTPA in MR imaging of glioblastomas and intracranial metastases. *AJNR* 6:669-674; 1985.
8. Davis, P.C.; Hoffman, J.C., Jr; Malko, J.A.; Tindall, G.T.; Takei, Y.; Avruch, L.; Braun, I.F. Gadolinium-DTPA and MR imaging of pituitary adenoma: A preliminary report. *AJNR* 8:817-823; 1987.
9. De Roos, A.; Doornbos, J.; Baleriaux, D.; Bloem, H.L.; Falke, T.H.M. Clinical applications of gadolinium-DTPA in MRI. In: Kressel, H.Y. (Ed.). *Magnetic resonance annual*. New York: Academic Press; 1988: pp. 113-145.
10. Dwyer, A.J.; Frank, J.A.; Doppman, J.L.; Oldfield, E.H.; Hickey, A.M.; Cutler, G.B.; Loriaux, D.L.; Schiavone, T.F. Pituitary adenomas in patients with Cushing disease: Initial experience with Gd-DTPA enhanced MR imaging. *Radiology* 163:421-426; 1984.
11. Goldstein, E.J.; Burnett, K.R.; Wolf, G.L.; Wortman, J. Contrast enhancement of spontaneous animal CNS tumors with gadolinium DTPA: A correlation of MRI with X-ray CT. *Physiol. Chem. Phys. Med. NMR* 17: 113-122; 1985.
12. Graif, M.; Bydder, G.M.; Steiner, R.E.; Niendorf, P.; Thomas, D.G.T.; Young, I.R. Contrast-enhanced MR imaging of malignant brain tumors. *AJNR* 6:858-862; 1985.
13. Green, J.D.; Harris, G.W. Observation of the hypophysoportal vessels of the living rat. *Physiol. London* 108:359-361; 1949.
14. Hebel, R.; Stromberg, M.W. Endocrine organs. In: Hebel, B. (Ed.). *Anatomy and embryology of the laboratory rat*. Worthsee FDR: Bio Med Verlag; 1986: pp. 89-96.
15. Hemminsson, A.; Bergstrom, K.; Ericsson, A.; Jung, B.; Sperber, G.; Thuomas, K.A. Structure enhancement by subtraction in magnetic resonance imaging. *Acta Radiol. Diagn.* 27:459-461; 1986.
16. Kilgore, D.P.; Breger, R.K.; Daniels, D.L.; Pojunas, K.W.; Williams, A.L.; Haughton, V.M. Cranial tissues: Normal MR appearance after intravenous injection of Gd-DTPA. *Radiology* 160:757-761; 1986.
17. Mark, L.M.; Pech, P.; Daniels, D.; Charles, C.; Williams, A.; Haughton, V. The pituitary fossa: A correlative anatomic and MR study. *Radiology* 153:453-457; 1984.
18. McNamara, M.T. Paramagnetic contrast media for magnetic resonance imaging of the central nervous system. New York: Raven Press; 1987: pp. 97-105.
19. Page, R.B.; Funsch, D.J.; Brennan, R.W.; Hernandez, M.J. Regional neurohypophysial blood flow and its control in adult sheep. *Am. J. Physiol.* 241:36-43; 1981.
20. Price, A.C.; Runge, V.M.; Alen, J.H. Tumor imaging with Gd-DTPA. In: Partain, C.L.; Price, R.R.; Patton, J.A.; Kulkarni, M.V.; Everette, J.A., Jr. (Eds.). *Magnetic resonance imaging*, Vol I. Philadelphia: W.B. Saunders; 1988: pp. 1969-181.
21. Runge, V.M.; Clanton, J.A.; Price, A.C.; Wehr, C.J.; Herzer, W.A.; Partain, C.L.; James, A.E., Jr. The use of Gd-DTPA as a perfusion agent and marker of blood brain-barrier disruption. *Magn. Reson. Imaging* 3:43-55; 1985.
22. Runge, V.M.; Price, A.C.; Clanton, J.A.; Weinmann, J.H.; Herzer, W.A.; James, A.E., Jr. The application of paramagnetic contrast agents to magnetic resonance imaging. *Noninvas. Med. Imaging* 1:137-147; 1984.
23. Strich, G.; Hagan, P.L.; Gerber, K.H.; Slutsky, R.A. Tissue distribution and magnetic resonance spin lattice relaxation effects of gadolinium-DTPA. *Radiology* 154: 723-726; 1985.
24. Tweedle, M.R.; Brittain, H.G.; Eckelman, W.C.; Gaughan, G.T.; Hagan, J.J.; Wedeking, P.W.; Runge, V.M. Principles of contrast-enhanced MRI. In: Partain, C.L.; Price, R.R.; Patton, J.A.; Kulkarni, M.V.; Everette, J.A., Jr. (Eds.). *Magnetic resonance imaging*, Vol I: Philadelphia: W.B. Saunders; 1988: pp. 793-809.
25. Van Nesselrooij, J.H.J.; Szeverenyi, N.M.; Ruocco, M.J. Magnetic resonance imaging of estrogen-induced pituitary hypertrophy in rats. *Magn. Reson. Med.* 11: 161-171; 1989.



## **CHAPTER VI**

### **PATHOGENESIS OF BLOOD-FILLED CAVITIES IN ESTROGEN-INDUCED ANTERIOR PITUITARY TUMORS IN MALE SPRAGUE-DAWLEY RATS**

Joop H.J. van Nesselrooij, Ferry G.J. Hendriksen, Victor J. Feron and Maarten C. Bosland.

Toxicologic Pathology, in press.



## Pathogenesis of Blood-Filled Cavities in Estrogen-Induced Anterior Pituitary Tumors in Male Sprague-Dawley Rats

Joop H.J. van Nesselrooij<sup>1</sup>, Ferry G.J. Hendriksen<sup>1</sup>, Victor J. Feron<sup>1</sup> and Maarten C. Bosland<sup>2</sup>

<sup>1</sup>Laboratory of Pathology, Department of Biological Toxicology, TNO Toxicology and Nutrition Institute, 3704 HE Zeist, The Netherlands.

<sup>2</sup>Institute of Environmental Medicine, New York University Medical Center, Tuxedo, New York 10987, USA.

### ABSTRACT

The formation of blood-filled cavities in developing tumors of the anterior pituitary of estrogen-treated male Sprague Dawley rats was studied in a serial sacrifice experiment. Two treated and 2 control rats were killed at each of 15 time points ranging from 7 to 272 days after s.c. implantation of an estradiol-17 $\beta$  pellet. The pituitaries were examined using light and electron microscopy. Changes at 7-9 days after implantation included epithelial cell swelling and trabecular arrangement. At 11-13 days, epithelial cells were further enlarged. Arrangement of epithelial cells in islands and endothelial degeneration were first seen at this interval. Also, any sinusoids were distended, whereas some were compressed by swollen epithelial cells. At 16-81 days, scattered necrotic and immature epithelial cells were present, and cell size decreased. Endothelial degeneration and both distended as well as compressed sinusoids were more prominent at this time. Loss of basement membrane was first seen during this interval. At 114-133 days, small hemorrhagic areas partially lined by epithelium were first seen; sinusoidal compression, endothelial necrosis, and loss of basement membrane were more frequent, but there was less sinusoidal distention. Between 150 and 272 days, epithelial cells were increasingly pleomorphic and arranged in nodules, and there was an increase in number and size of the hemorrhagic areas. Sinusoidal compression, endothelial necrosis, and loss of basement membrane were abundant, whereas sinusoidal distention had almost disappeared at this interval. Local compression of sinusoids and perhaps compression of pituitary surface veins due to epithelial cell swelling, were thought to play a primary role in the development of ischemic endothelial damage leading to loss of endothelial lining and basement membrane, and eventually to the formation of blood-filled spaces partially lined by epithelial cells.

### INTRODUCTION

Pituitary tumors are common in aged rats and humans (1, 2, 8, 12, 13, 16). Spontaneous rat pituitary tumors often contain abnormal vascularization (5, 6), and in particular blood-filled cavities. Therefore classification as hemorrhagic tumors has been proposed (1, 8, 16). Similar vascular abnormalities occur frequently in human pituitary adenomas (4, 6, 7, 14). Ischemia due to compression of pituitary stalk blood vessels by the tumor leading to hypoxic damage of endothelium has been suggested as a mechanism by which these vascular changes in human tumors develop (7, 14). The pathogenesis of hemorrhagic areas in spontaneous rat pituitary tumors is not known.

Estrogen-induced pituitary tumors in rats have been widely used as a model for spontaneous human and rodent pituitary neoplasms (3, 10, 18, 19).

In a previous study the first histopathological changes were seen at day 9 after estrogen implantation when acidophilic cells became hypertrophic. At day 16 cord-like structures of hypertrophic cells lined by endothelial cells and distended sinusoids were common features. At day 98 the sinusoidal lining showed interruptions causing intraparenchymal hemorrhages that contained some necrotic cells. From day 186 and onwards the pituitaries became tumorous and contained areas that could be divided into different morphological areas (20).

However, the development of pituitary vascular lesions in estrogen-treated rats has not been systematically studied. The purpose of this study was to establish sequential changes in the rat pituitary morphology following exposure to estrogen in an attempt to determine the histopathogenesis of blood-filled cavities in pituitary tumors. To this end, an experiment was conducted with serial sacrifices between 7 and 272 days after the start of estrogen treatment, and changes in pituitary morphology were examined at the light and electron microscopic levels.

## MATERIALS AND METHODS

Under ether anesthesia thirty 30 male Sprague-Dawley (Hsd/CPB:SD) rats (Harlan CPB, Zeist, The Netherlands), 4-5 weeks of age, were each s.c. between the scapulae implanted with a single pellet containing 25 mg estradiol-17 $\beta$  (Organon, Oss, The Netherlands). There was an equal number of control rats, which were sham operated in an identical manner but without the deposition of a pellet.

All 60 rats were kept in stainless wire-mesh cages (two or three animals per cage; controls separated from experimental animals) in a well ventilated room maintained at 20°C with relative humidity 40-70% and 12 h of lighting per day. Rats were fed the Institute's powdered, natural ingredient diet for rats. The animals had free access to food and tap water.

Two treated and two control rats were sacrificed by decapitation while under ether anesthesia at each of the following time points: 7, 9, 11, 13, 16, 25, 35, 81, 114, 133, 150, 168, 217, 241, and 272 days after the estradiol pellet implantation.

*All animals were treated under the protocol and housing arrangement approved by the Institutional Committee for the Humane Use of Animals.*

At necropsy, the pituitaries were carefully dissected and fixed in a 2.5% glutaraldehyde solution buffered with 0.1 M sodium cacodylate (pH 7.4), and post-fixed in a 1% osmium tetroxide solution in the same buffer. After rinsing, the pituitaries were dehydrated in a graded series of acetone, and embedded in a glycid ether 100/Araldite mixture. One  $\mu$ m-thick sections were stained with toluidine blue, and ultrathin sections with uranyl magnesium acetate and lead citrate. The periodic acid-silver methamine staining method for carbohydrates (9) was used to demonstrate basement membrane material. The ultrathin sections were examined using a Phillips EM401LS at 60 kV.

## RESULTS

The presence or absence, in comparison with controls, of alterations in the epithelial and perivascular compartments of the anterior pituitary, and a semi-quantitative assessment of their severity were recorded for each time point as determined by light and electron microscopy. The time points were grouped when no differences in alterations were observed between time points. The results of

this assessment are summarized in Table I, and the changes, in comparison with those of control tissue (Fig. 1), are briefly described below by time period.

### Days 7 and 9 Post-Implantation (Fig. 2)

The earliest change observed in epithelial cells was an increase in the size of many cells containing increased amounts of rough endoplasmic reticulum (RER), Golgi structures, and electron dense secretory vacuoles. The epithelial cells were arranged in more or less distinct trabeculae of a few cells thick lined by sinusoids, rather than more diffusely as seen in controls (Fig. 1).

The earliest vascular change was a slight distention of the pericapillary interstitial space containing collagen that appeared somewhat dispersed.

### Days 11 and 13 Post-Implantation (Fig. 3)

Some epithelial cells were now arranged in islands or foci, often surrounding a sinusoid, rather than in trabeculae. The RER proliferation and enlargement of epithelial cells were more marked than at 7-9 days, as was their arrangement in trabeculae.

Many sinusoids were now slightly distended, whereas a few displayed some compression of the lumen by enlarged epithelial cells (Fig. 3). Endothelial cells showing plasma membrane blebbing were now also regularly seen, and there were a few endothelial cells with prominent degenerative changes, particularly vacuolization, or frank necrosis. In addition, distention of pericapillary spaces and dispersion of collagen were more prominent than at days 7-9.

### Days 16, 25, 35, and 81 Post-Implantation (Fig. 4)

The epithelial cells appeared to contain less RER than at 11-13 days. These cells were also increasingly arranged in islands from 16 to 81 days post-implantation, whereas trabecular arrangement was decreasing in frequency. Occasional scattered necrotic and degenerated epithelial cells were observed from 16 days post-implantation onwards; the latter were characterized by cell swelling, RER degranulation, and swelling of endoplasmic reticulum and some mitochondria. The frequency of occurrence of these necrotic/ degenerated cells did not change much between 16 days and 272 days, which was the last time point in this study. There were also some scattered cells with an

**Table 1.** Presence and severity of epithelial and (peri)vascular alterations in rat pituitaries at different times after the start of estradiol treatment.

Alteration	Time-period (days after start of estradiol treatment)					
	7-9	11-13	16-81	114-133	150-217	241-272
<b>Epithelial compartment</b>						
Cell size	↑	↑↑	↑↑	↓↓	↓	
RER proliferation	+	++	+	----->		±
Degeneration/necrosis			+	+	+	+
Immature cells			+	++	++	+++
Lipid droplets				+	++	++
Cells directly on sinusoidal lumen				+	++	+++
Hemorrhagic areas				±	+	++/+++
<b>Growth pattern:</b>						
Trabecular	+	++	+			
Islands		+	++	+++	++	+/+++
Nodular					++	+++
<b>(Peri)vascular compartment</b>						
Distention of pericapillary spaces	+	++	++			
Collagen dispersion	+	++	++			
Sinusoidal distention		+	++	----->		±
Endothelial blebbing		+	++			
Endothelial degeneration and necrosis	±	+		++++	+++	
Localization of sinusoids within islands/nodules		+	++	----->		+++
Sinusoidal compression		±	+	++	++	++
Loss of collagen			±	+	++	+++
Loss of basement membrane			+	----->		++
Multiple basement membranes				+	++	+++
Change in cell size is indicated as:						
			↑ moderate, ↓ slight,	↑↑ marked increase ↓↓ moderate decrease		
The degree of severity of alteration is indicated:						
			±	minimal		
			+	slight		
			+/++	slight to moderate		
			++	moderate		
			++/+++	moderate to marked		
			+++	marked		
			----->	gradual change		

immature character, lacking secretory vacuoles and with few RER and Golgi structures.

Blebbing of endothelial cells was now very frequent, and from day 16 to day 81 post-implantation there were increasingly more degenerated/necrotic cells than at 11-13 days. There was also scattered loss of basement membrane material and some loss of pericapillary collagen. Distention of pericapillary spaces and dispersion of pericapillary collagen was similar in severity to what was seen at days 11-13. However,

both distention and compression of sinusoids were distinctly more prominent, as was the location of sinusoids within epithelial cell islands. The distended sinusoids were located in areas of epithelial cell trabeculae, whereas compressed sinusoids occurred in both islands and trabeculae of epithelial cells.

**Days 114 and 133 Post-Implantation (Fig. 5A,5B,6,7)**

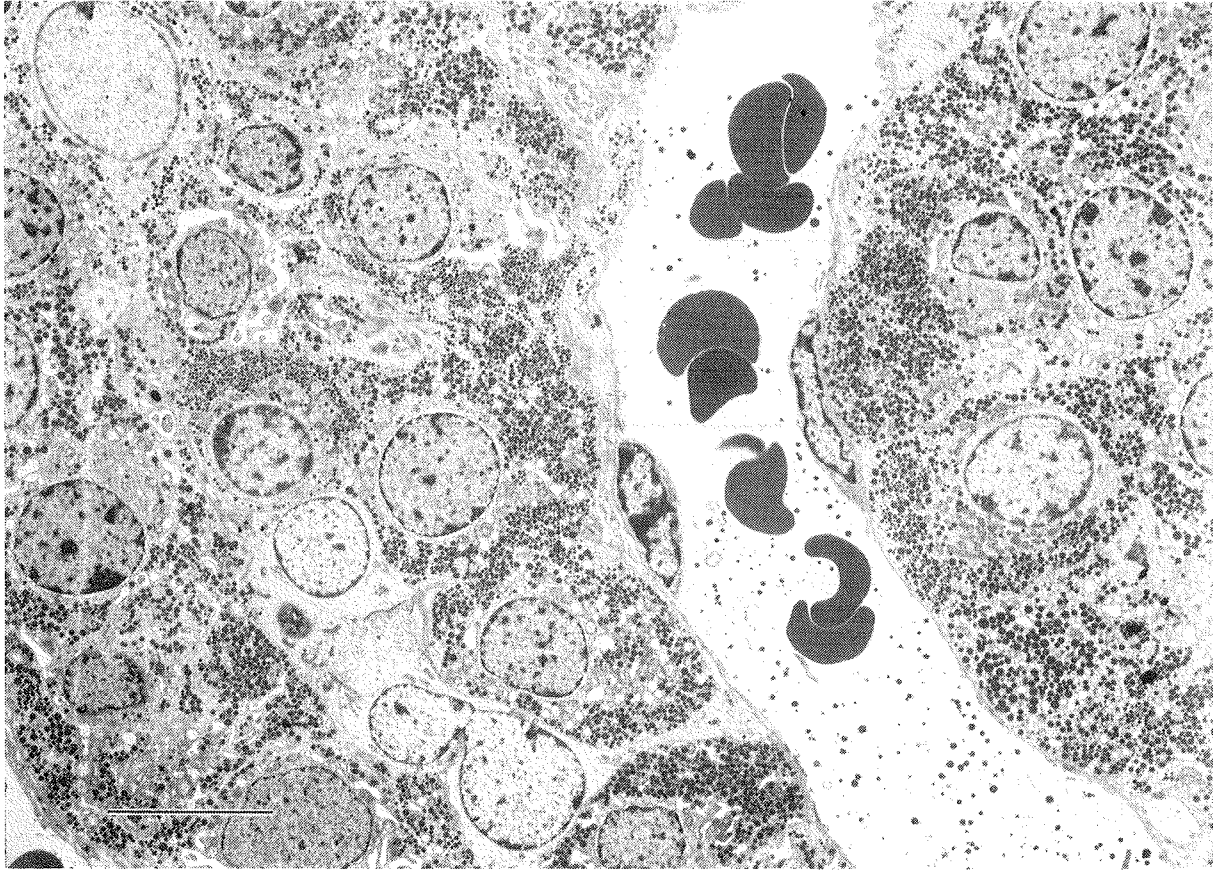


Fig. 1 -- Control pituitary; sinusoids are lined by epithelial cells on a single basement membrane.  
Bar  $\approx 10\mu\text{m}$ .

Some epithelial cells were now directly lining a sinusoid, due to the loss of endothelium and basement membrane, and there were some small hemorrhagic areas, i.e., distended, blood-filled areas lined with epithelial cells (Fig. 7). The epithelial cells were now decreasing in size and seemed to contain less RER as compared with days 16-81, whereas several cells now appeared to contain lipid droplets. There were more immature cells than seen at days 16-81, and their frequency of occurrence did not change much between days 114 and 217. Arrangement of epithelial cells in islands predominated, and many of these islands included one or a few sinusoids.

There were now many necrotic and degenerated endothelial cells, and blebbing endothelium without any more advanced degenerative changes was rare. Multiple basement membranes were occasionally observed for the first time (Fig. 6), but there was also somewhat more severe scattered loss of basement membrane than on days 16-81. Distention of sinusoids was somewhat less prominent than at earlier time points, whereas loss of pericapillary collagen was slightly more prominent (Fig. 5A,5B). Compression of sinusoids

was more frequent and severe than at days 16-81.

#### Days 150, 168, and 217 Post-Implantation (Fig. 8)

Several epithelial islands now contained cells that were slightly pleomorphic, i.e., showed variation in their size and in size and shape of their nucleus. These islands were demarcated from and caused compression of the surrounding islands that did not have pleomorphic cells, and they were therefore classified as nodules, perhaps representing early tumors. Approximately one third to half of the pituitary mass consisted of nodules. The decrease in epithelial cell size first seen between days 16 and 81 gradually continued, and the presence of lipid droplets was more prominent than earlier. There were more epithelial cells directly lining sinusoids and there were more and larger hemorrhagic areas, which were more frequent in nodular areas than in islands.

Necrosis and degeneration of endothelium were abundant, and there were more areas with multilayered basement membranes, as well as more loss of basement membrane material in other



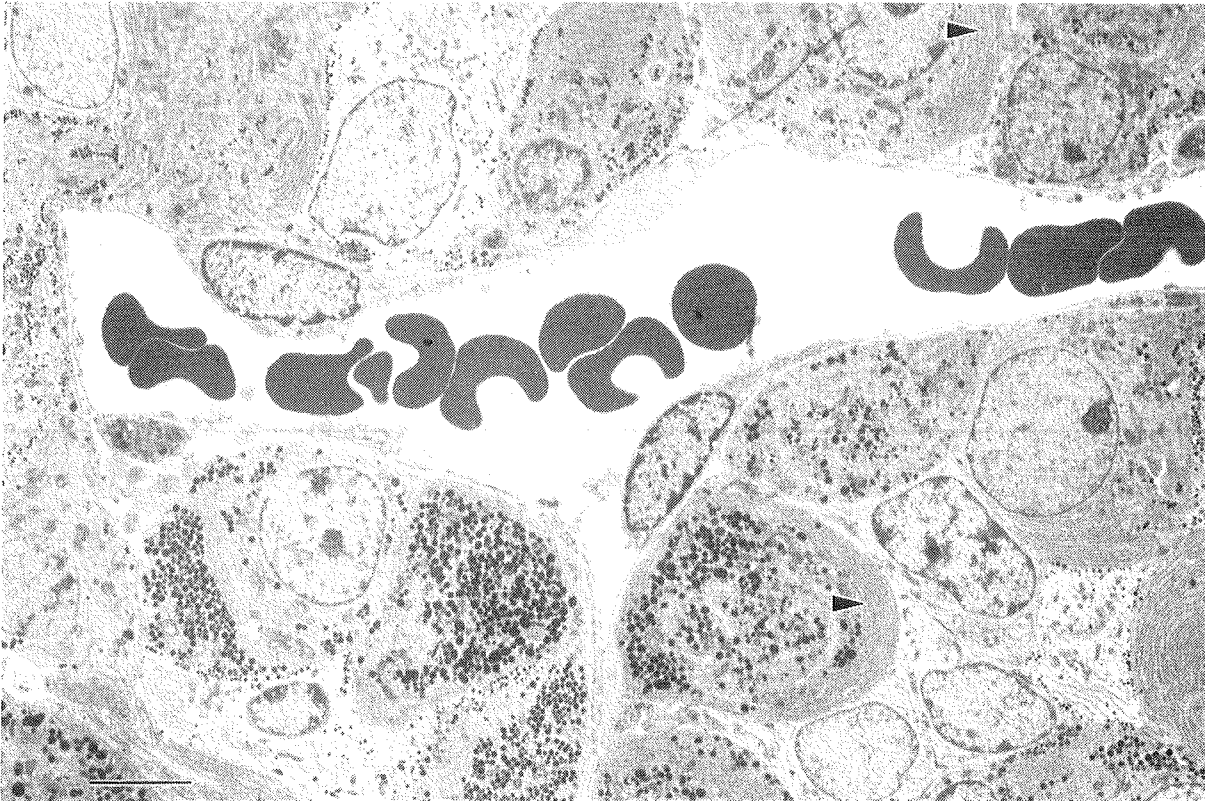


**Fig. 2** -- Pituitary after 7 days of estrogen treatment. Endothelial cells are increased in size and contain increased amount of rough endoplasmic reticulum (RER) arrowheads. Epithelial cells are arranged in more or less distinct trabeculae (not shown). Bar  $\approx 5\mu\text{m}$ .

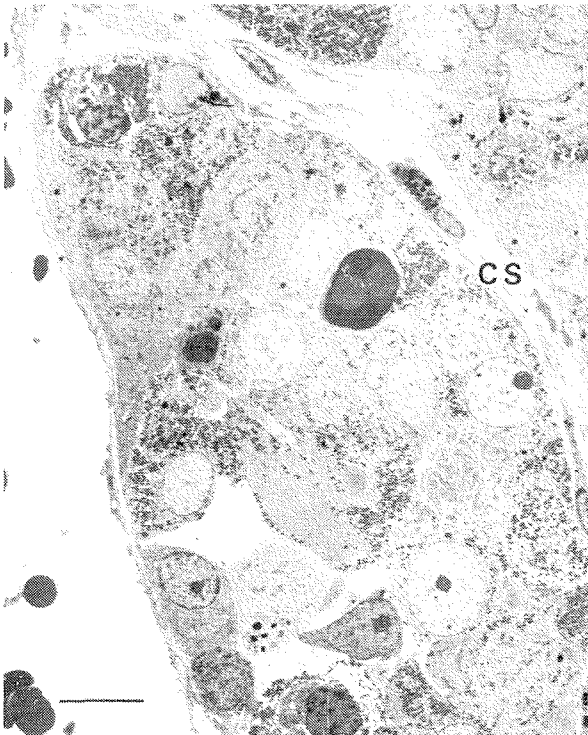


**Fig. 3** -- Pituitary after 11 days of estrogen treatment. Some cells are arranged in islands often surrounding a compressed sinusoid (CS). Other sinusoids are distended (lower left hand corner). Bar  $\approx 10\mu\text{m}$ .

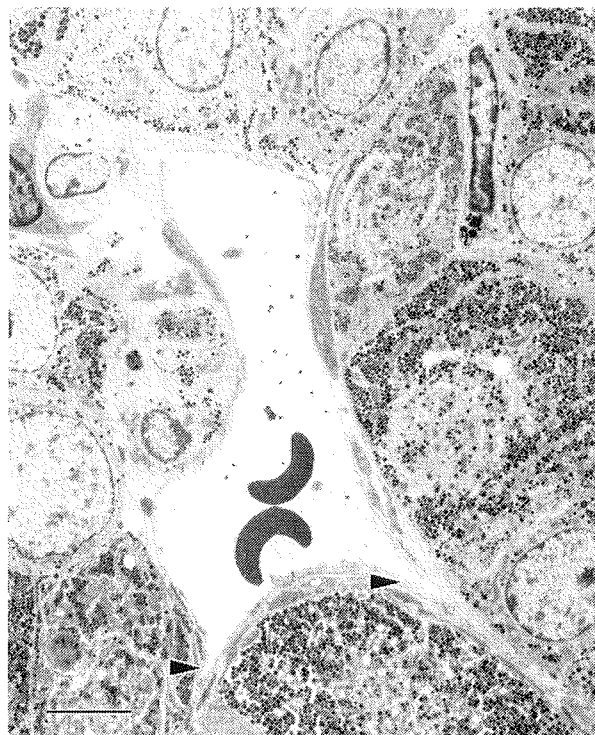


**Fig. 4** -- Pituitary after 16 days of estrogen treatment. A sinusoid with compression surrounded by epithelial islands (arrow heads). Bar  $\approx 5\mu\text{m}$ .



**Fig. 5A -- Control**

Pituitary after 114 days of estrogen treatment. Distention of sinusoids and loss of pericapillary collagen (compare arrow heads in A, control and B, estrogen-treated rat pituitary). Bar A  $\approx 2.5\mu\text{m}$ , and B  $\approx 2.5\mu\text{m}$ .

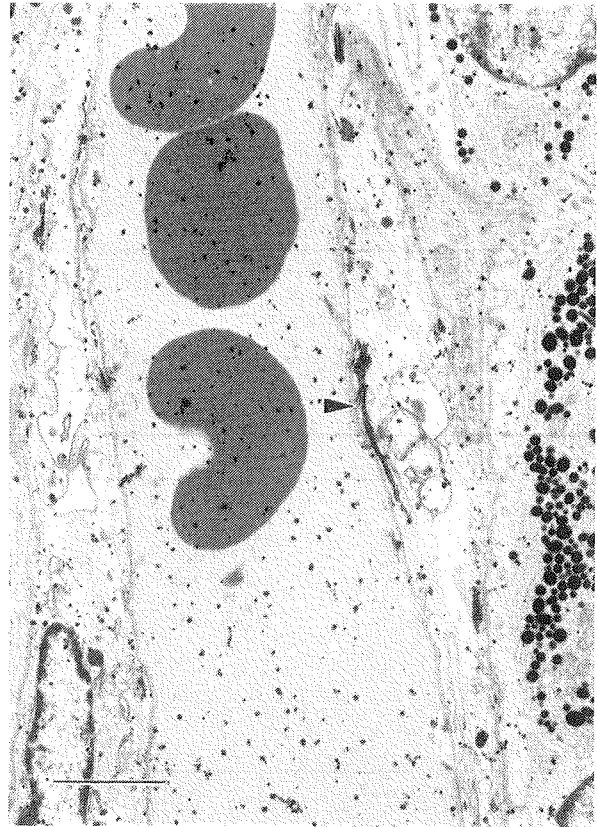


**Fig. 5B -- Estrogen-treated rat pituitary**

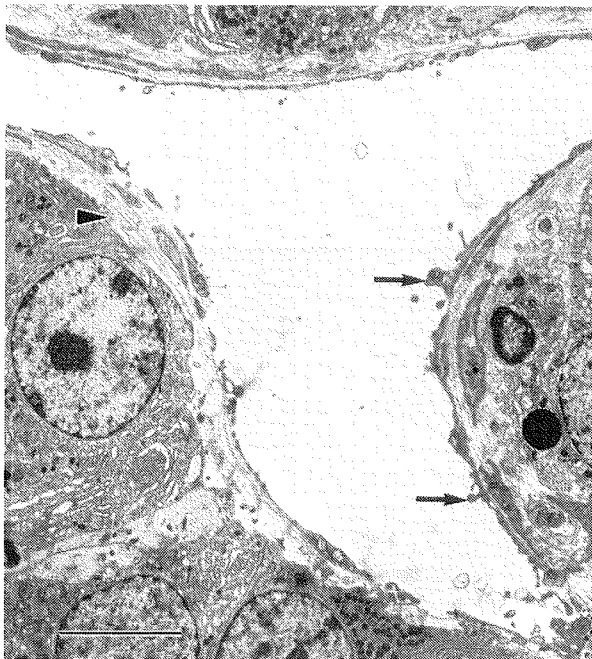


**Fig. 6 -- Pituitary after 114 days of estrogen treatment.** Compressed sinusoid lined with necrotic and degenerated endothelial cells and multiple basement membranes (arrowhead). Blebbing of endothelial cells (arrow) without more advanced degenerative changes was rare. Bar  $\approx 5\mu\text{m}$ .

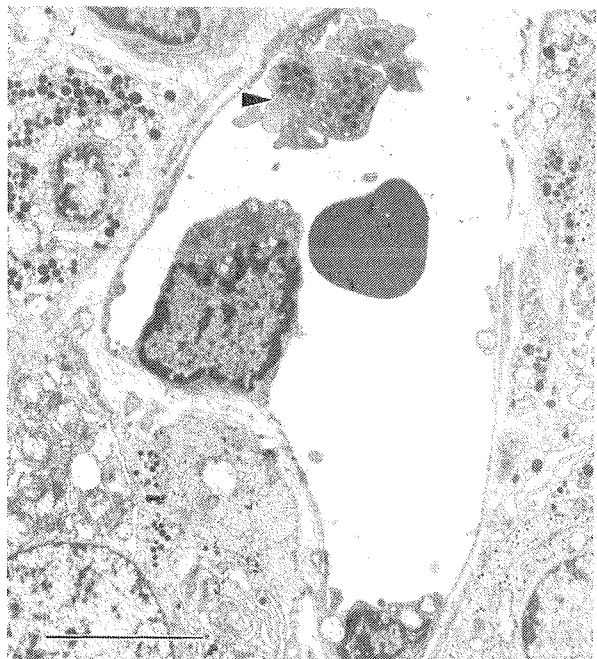


**Fig. 7 -- Pituitary after 114 days of estrogen treatment.** Some epithelial cells directly lining sinusoids, due to loss of endothelium and basement membranes (upper right corner). There are also some platelets sticking on a defect in endothelial lining (arrow head) and two nuclei of degenerating endothelial cells. Bar  $\approx 5\mu\text{m}$ .

locations than on days 114-133. Loss of pericapillary collagen and sinusoidal compression were more prominent than on days 114-133, and distention of sinusoids was less conspicuous.

#### Days 241 and 272 Post-Implantation (Figs. 9A,9B and 10)

The number and the size of nodules and hemorrhagic areas continued to increase. On day 272 approximately two thirds of the pituitary consisted of large nodules containing sinusoids, remnants of sinusoids, multiple basement membranes, and hemorrhagic areas. These hemorrhagic cavities were lined by epithelial cells and were filled with erythrocytes, a few macrophages, and some cellular debris. Immature cells were very frequent, occurring more often than at the previous time points, but there were no further changes in epithelial cell size or the amount of lipid droplets they contained.

There was a further increase in the extent of endothelial necrosis and loss of their basement membrane material, and, particularly on day 241, the presence of areas of multiple basement membranes. Loss of pericapillary collagen was progressive with virtually no collagen left on day 272. Sinusoidal compression and location of sinusoids within epithelial islands or nodules were very frequent, whereas distention of sinusoids was further reduced and almost absent on day 272.

## DISCUSSION

This study demonstrates that the development of hemorrhagic areas during estrogen-induced rat pituitary tumor formation is preceded by degenerative and necrotic changes in endothelium and loss of basement membrane and pericapillary collagen. Coinciding with these endothelial and pericapillary changes, some sinusoids are distended whereas others are compressed. Epithelial cell swelling and arrangement of these cells in trabeculae occurs prior to these sinusoidal changes. This sequence of events suggests that swelling of pituitary epithelium leads to interference with local circulation followed by ischemic injury to the endothelium. The result is loss of sinusoidal lining and degradation of basement membrane and pericapillary collagen. Ultimately, epithelial cells line sinusoidal lumina.

There are two potential mechanisms by which epithelial cell swelling can interfere with pituitary circulation. (i) The entire pituitary gland may enlarge which would result in compression of the

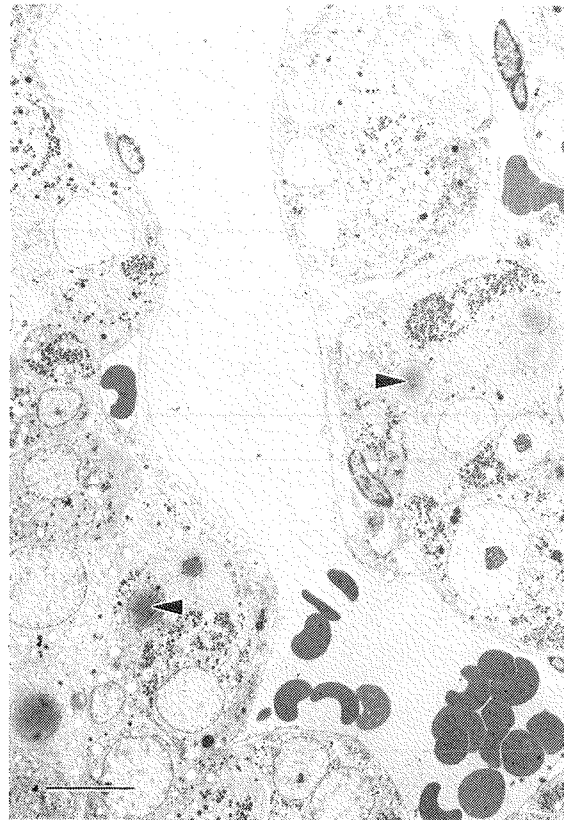


**Fig. 8** -- Pituitary after 150 days of estrogen treatment. Decrease in epithelial cell size and the presence of lipid droplets (arrow heads). Bar = 10 $\mu$ m.

draining venous system located at the pituitary surface (11). This leads to general pituitary congestion, subsequent distention of sinusoids, and finally compression of afferent stalk blood vessels. This process which would not result in sinusoidal distention. (ii) Sinusoids within the pituitary are locally compressed which may result in local reduction of blood flow and distention of proximal parts of the affected sinusoids. Stalk compression by the tumor and hypoxic endothelial damage due to reduced blood supply has been proposed as the mechanism for hemorrhagic lesions in human pituitary adenomas (7, 14). In the estrogen-induced pituitary tumor model used in this study, stalk compression is unlikely until 16 days following estrogen treatment. We have previously shown, using magnetic resonance imaging (MRI) techniques (20), that the subarachnoid space between the pituitary and the brain (diencephalon and pons) did not become smaller by that time. Swelling of the pituitary was first apparent by MRI on day 9 in that study. Distention of sinusoids was first seen on days 7 and 9 in the present study, together with the first signs of compression of sinusoids. Therefore, compression of draining

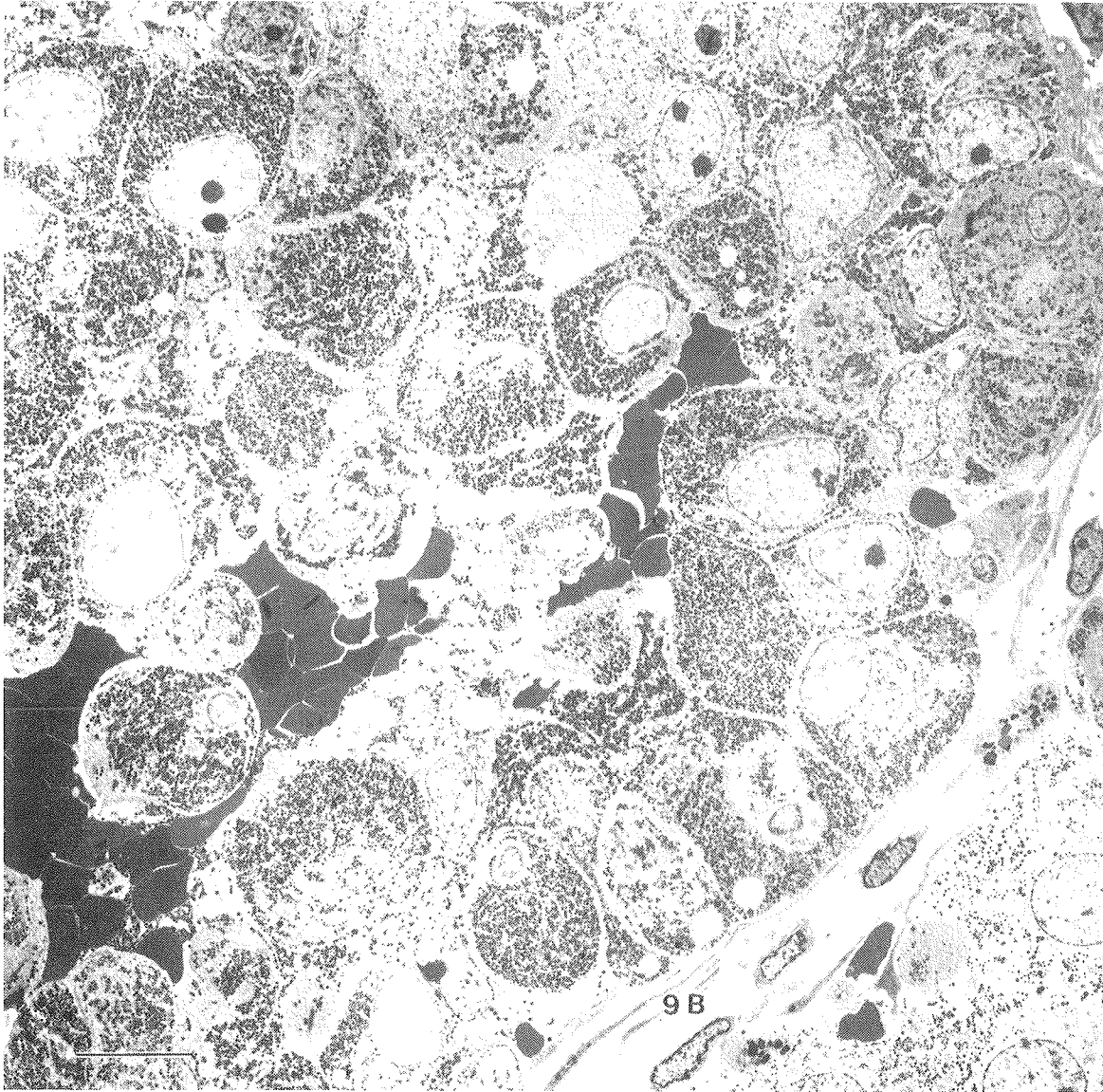


Fig. 9A -- Pituitary after 241 days of estrogen treatment. A nodule with hemorrhagic areas and multiple basement membranes (arrow head in Fig. 9B, detail of Fig. 9A). Bar A  $\approx 10\mu\text{m}$ , and B  $\approx 5\mu\text{m}$ .

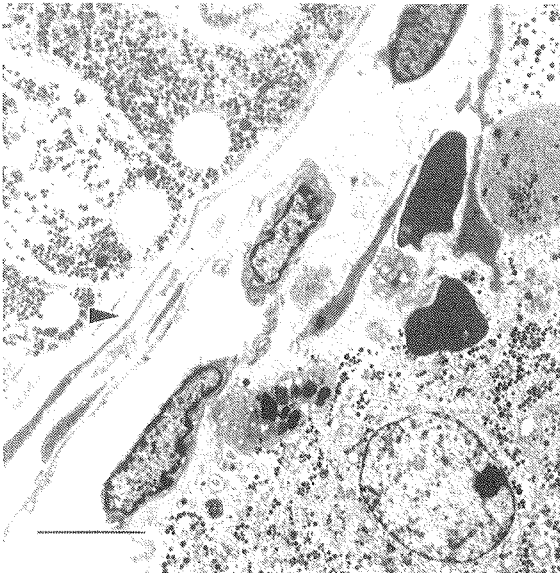
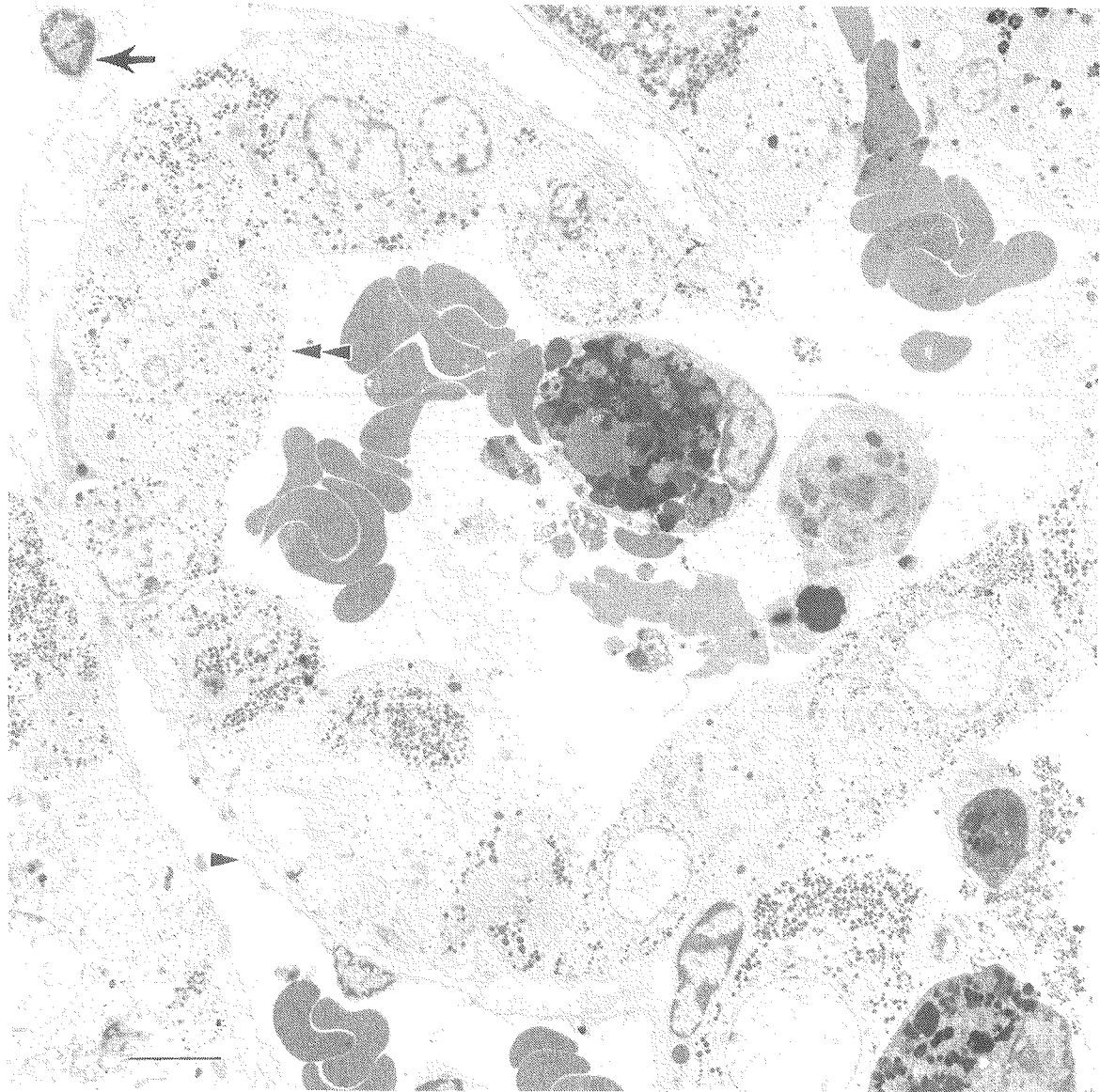


Fig. 9B -- detail of Fig. 9A



**Fig.10** -- Pituitary after 272 days of estrogen treatment. Nodule with hemorrhagic cavity filled with erythrocytes, a few macrophages and some cellular debris and lined by epithelial cells (double arrow head). The nodule is surrounded by sinusoids lined with endothelial cells (single arrow head) some of which are degenerate (arrow).  
Bar = 5 $\mu$ m.

veins on the surface of the pituitary and local compression of sinusoids, rather than stalk compression, may impair pituitary blood circulation and cause ischemia. The occlusion of sinusoids and pituitary circulatory congestion however, are not so severe that stasis occur, since no signs of coagulation or thrombus formation were found.

Hemorrhagic lesions are present in even very small spontaneous rat pituitary tumors (1, 16, 17) that cannot possibly cause compression of afferent or efferent blood vessels. This observation provides strong support for an important role of local ischemia due to local obstruction of blood flow in the pathogenesis of the hemorrhagic areas.

The estrogen-induced rat pituitary tumor model differs from spontaneous rat tumors in that the model produces enlargement and eventual tumor formation involving the entire pituitary, rather than the spontaneously occurring focal process. The tumorous nodules seen in the present study were however, morphologically indistinguishable from spontaneously occurring hemorrhagic tumors in aged rats described elsewhere (1, 8, 16, 17). Angiogenesis has been observed in the liver of estrogen-treated rats (21), and angiogenesis may occur in the pituitary of estrogen-treated rats (15). Signs of increased amounts of sinusoidal structures were not found in the present study. Regeneration

of endothelium following recurrent degeneration/-necrosis as indicated by the presence of multiple basement membranes, which did not occur until hemorrhagic areas were first encountered was observed however.

Contribution of central necrosis, in epithelial cell islands or tumorous nodules, to the development of hemorrhagic areas is theoretically also possible. Necrosis occurred in a scattered fashion (single cell necrosis) and no indications of central necrosis were observed until the last time point (272 days), when cellular debris and mononuclear inflammatory cells, predominantly macrophages, were observed in the hemorrhagic areas. There were no early signs of inflammatory reactions, and thus endothelial necrosis probably occurred gradually enough for vascular clearance of debris. Epithelial cells appeared less susceptible to the hypoxic conditions than endothelium probably because the former cells obtain oxygen from erythrocytes in several surrounding sinusoids, whereas endothelial oxygen supply is entirely derived from the blood in the sinusoid they line. As the epithelial cells apparently underwent a metabolic change with ongoing estrogen treatment, indicated by the decrease in cell size, change in RER content and the appearance of lipid vacuoles, they probably also became somewhat resistant to hypoxia.

In summary, this serial sacrifice study has provided morphologic evidence that local compression of pituitary sinusoids and probably also compression of pituitary surface veins, both due to epithelial cell swelling, play a primary role in the development of ischemic endothelial damage in the pituitary of estrogen-treated rats. This process in turn, causes loss of endothelial lining, basement membrane, and pericapillary collagen, thereby resulting in the formation of blood-filled spaces lined by epithelial cells in the developing tumors of the anterior pituitary.

#### ACKNOWLEDGEMENTS

This work was supported in part by Grant No. CIVO 87-2 from the Dutch Cancer Society, and the Netherlands Ministry of Welfare and Public Health.

#### REFERENCES

- Berkvens JM, Van Nesselrooij JHJ, and Kroes R (1980). Spontaneous tumours in the pituitary gland of old Wistar rats: A morphological and immunocytochemical study. *J. Pathol.* 130: 179-191.
- Burrow GN, Wortzman G, Rewcastle NB, Holgate RC, and Kovacs K (1981). Microadenomas of the pituitary and abnormal sellar tomograms in an unselected autopsy series. *N. Engl. J. Med.* 304: 156-158.
- Elias KA and Weiner RI (1984). Direct arterial vascularization of estrogen-induced prolactin secreting anterior pituitary tumors. *Proc. Natl. Acad. Sci. (US)* 81: 4549-4553.
- Erroi A, Bassetti M, Spada A, and Giannattasio G (1986). Microvasculature of human micro- and macroprolactinomas. A morphological study. *Neuroendocrinol.* 43: 159-165.
- Farquhar MG (1961). Fine structure and function in capillaries of the anterior pituitary gland. *Angiology (Balt.)* 12: 270-292.
- Hirano A, Tomiyasu U, and Zimmerman HM (1972). The fine structure of blood vessels in chromophobe adenoma. *Acta Neuropathol. (Berl.)* 22: 200-07.
- Kovacs K and Horvath E (1973). Vascular alterations in adenomas of human pituitary glands. An electron microscopic study. *Angiologica* 10: 299-309.
- Kroes R, Berkvens JM, de Vries T, and Van Nesselrooij JHJ (1981). Histopathological profile of a Wistar rat stock including a survey of the literature. *J. Gerontol.* 36: 259-279.
- Lewis PR and Knight DP (1982). Staining methods for sectioned material. In: *Practical Methods in Electron Microscopy*, AM Glauert (ed). North Holland, Amsterdam, pp. 110-101.
- Lloyd RV (1983). Estrogen-induced hyperplasia and neoplasia in the rat anterior pituitary gland, an immunohistochemical study. *Am. J. Pathol.* 113: 198-206.
- Murakami T (1975). Pliable methacrylate casts of blood vessels: Use in a scanning electron microscopic study of the microcirculation in the rat hypophysis. *Arch. Histol. Jap.* 38: 151-168.
- McComb DJ, Ryan N, Horvath E, and Kovacs K (1983). Subclinical adenomas of the human pituitary. *Arch. Pathol. Lab. Med.* 107: 488-491.
- Parent D, Brown B, and Smith EE (1982). Incidental pituitary tumors: A retrospective study. *Surgery* 92: 880-883.
- Schechter J (1972). Ultrastructural changes in the capillary bed of human pituitary tumors. *Am. J. Pathol.* 67: 109-126.
- Tiboldi T, Nemessanyi Z, Csernay L, and Kovacs K (1967). Effect of estrogen on pituitary blood flow in rats. *Endocrinol. Exp.* 1: 73-77.
- Trouillas J, Girod C, Claustrat B, Cure M, and Dubois MP (1982). Spontaneous pituitary tumors in the Wistar/Furth/Ico rat strain. *Am. J. Pathol.* 109: 57-70.

17. Van Nesselrooij JHJ, Kuper CF, Bosland MC, Buijntjes JP, and Kroes R (1985). Spontaneous pituitary lesions and plasma prolactin levels in rats. In: **Prolactinomas: An Interdisciplinary Approach**, LM Auer (ed). De Gruyter, Berlin/New York, pp. 85-87.
18. Van Nesselrooij JHJ, Szeverenyi NM, and Ruocco MJ (1989). Magnetic resonance imaging of estrogen-induced pituitary hypertrophy in rats. **Magn. Reson. Med.** 11: 161-171.
19. Van Nesselrooij JHJ, Szeverenyi NM, Tillapaugh-Fay GM, and Hendriksen FGJ (1990). Gadolinium-DTPA-enhanced and digitally subtracted magnetic resonance imaging of estrogen-induced pituitary lesions in rats: Correlation with pituitary anatomy. **Magn. Reson. Imaging** 8: 525-533.
20. Van Nesselrooij JHJ, Buijntjes JP, Van Garderen-Hoetmer A, Tillapaugh-Fay GM, and Feron VJ (1991). Magnetic resonance imaging compared with hormonal effects and histopathology of estrogen-induced pituitary lesions in the rat. **Carcinogenesis** 12: 289-297.
21. Widmann J and Dariush Fahimi H (1976). Proliferation of endothelial cells in estrogen-stimulated rat liver. **Lab. Invest.** 34: 141-149.





## **CHAPTER VII**

### **MAGNETIC RESONANCE IMAGE ANALYSIS OF ESTROGEN-INDUCED PITUITARY LESIONS IN RATS USING T1 AND T2 WEIGHTED INTENSITIES**

Joop H.J. van Nesselrooij, Nikolaus M Szeverenyi and Gwen M. Tillapaugh-Fay.

Magnetic Resonance in Medicine, submitted.



## Magnetic Resonance Image Analysis of Estrogen-Induced Pituitary Lesions in Rats Using T1 and T2 Weighted Intensities

Joop H.J. van Nesselrooij<sup>1,2</sup>, Nikolaus M Szeverenyi<sup>1</sup> and Gwen M. Tillapaugh-Fay<sup>1</sup>

<sup>1</sup>Nuclear Magnetic Resonance Research Laboratory, Department of Radiology, Health Science Center at Syracuse, Syracuse, New York 13210, USA.

<sup>2</sup>Laboratory of Pathology, Department of Biological Toxicology, TNO Toxicology and Nutrition Institute, 3704 HE Zeist, The Netherlands.

### ABSTRACT

Estrogen treated male rats provide a model of pituitary disease, generating a wide variety of pituitary lesions. Changes in the pituitaries of these animals were detected as early as 7 days post estrogen stimulus through the analysis of MR image intensities. T1 and T2 weighted axial images of the rat head at the level of the pituitary were obtained at 2 Tesla. The intensities of the pituitary (pars distalis) were plotted in a two dimensional scatterplot which was referenced to a similar scatterplot of a region in adjacent brain. The pars distalis was observed to have a larger distribution of intensities within an image (more texture) than the surrounding hypothalamic areas. T2 weighted image intensities of the pars distalis were found to increase relative to the surrounding hypothalamic areas at 7 days post estrogen stimulus. No changes in intensity for the pars distalis were noted on T1 weighted images following estrogen treatment.

### INTRODUCTION

In previous studies (1, 2) we have demonstrated that pituitary hypertrophy in an estrogen-induced rat pituitary tumor model could be detected on an MR image approximately 9 days post estrogen stimulus. Since one can detect cellular changes via histopathological and immunohistochemical techniques as early as 2 to 4 days post estrogen stimulus (3), the question was asked whether there is a concomitant change in "some" MR imaging property of the pituitary gland at this time. The present study was carried out to answer this question. To detect subtle intensity changes on MR images, computer generated 2 dimensional scatterplots were used to analyze the rat pituitary gland MR data.

### MATERIAL AND METHODS

#### Animals and diet

A group of 5 (3 week old) male Sprague Dawley rats was obtained from Harlan Sprague Dawley, Inc., Indianapolis, IN. The rats were kept in stainless steel wire-mesh cages, with the three experimental animals (A, B, and C) housed separately from control animals (D and E). The animal housing room was well ventilated, thermostated at 20°C with relative humidity 40-70%, and provided 12 hours of lighting per day. The animals had free access to food (Purina Formulab Chow 5000, Purina Mills Inc., St. Louis, MO) and tap water.

#### Estrogen treatment

A 25 mg estradiol-17 $\beta$  pellet (Organon, The Netherlands) was implanted subcutaneously between the scapulae of three rats under ether anesthesia. Two control rats were sham-operated in an identical manner, but without the deposition of a pellet. All 5 animals were treated under a protocol and housing arrangement approved by the Institutional Committee for the Humane Use of Animals.

#### Imaging

Images of the rat head were obtained using a 31 cm diameter horizontal bore, 2 Tesla, chemical shift/imaging NMR instrument (General Electric, Fremont, CA). The rats were immobilized on a board and a (4 cm diameter) dual pancake coil NMR probe was used for both radiofrequency transmission and detection. Data acquisition parameters for the T1 and T2 weighted spin echo images were as follows: single slice (axial 2 mm slice thickness), TR/TE of 450/27 and 2000/80, 4 excitations, 40 mm field of view (with a 425 Hz/mm readout gradient), 2.5 ms (5 lobed sinc) radiofrequency pulses, 256 complex sampling points and 256 phase encoding increments.

To eliminate motion during the imaging period, rats were anesthetized with sodium pentobarbital (Nembutal, Abbott Laboratories, North Chicago, IL, USA) 5mg/100g body weight i.p. Each animal was imaged on five different days (2, 4, 7, 9, 10 days post estrogen stimulus) to provide 25 sets of congruent T1 weighted and T2 weighted images.

#### Data Analysis -- Scatterplots

Images were transferred to and analyzed on a SUN 4/330 workstation running IMAGE software (New Methods Research, Inc., Syracuse, NY). Pixel intensities from "regions of interest" (ROI's) in congruent T1 weighted and T2 weighted images were plotted as two dimensional scatterplots. The horizontal axis of the scatter plot corresponds to intensity on the T1 weighted image and the vertical axis corresponds to intensity on the T2 weighted image. The regions of interest examined in this study were the pars distalis of the pituitary and a hypothalamic reference area in the adjacent brain (Figs. 1a and 1b).

The region of analysis was limited to only the pars distalis rather than the entire pituitary gland, since the analysis of the entire structure reduced the sensitivity of the technique and it is known that the pars distalis is the only portion of the gland affected in this estrogen model (1,2,3). Scatterplots were generated for both tissue regions for all five time points post estrogen implantation and were inspected visually for differences in the clustering of data points. The average number of pixels comprising the reference hypothalamic area was 160, whereas the region selected as pars distalis consisted of approximately 150 pixels. Scatterplots for each tissue (pars distalis and hypothalamus) were scaled and plotted in an identical manner so as to produce graphic representations which when printed could be superimposed on a light box. This method provided a convenient way to detect changes in the pars distalis intensities compared to the reference hypothalamus. The technique is independent of receiver sensitivity and display window settings. Correlated intensity information contained in two MR images is available for each ROI in one presentation. Subtle changes in pituitary intensity were detected as changes in the distribution of the data points for the pars distalis when superimposed on the corresponding scatter plot of surrounding brain.

#### Statistics

The mean relative difference between the hypothalamus and the pituitary T2 intensity was calculated by subtracting the mean of the hypothalamus from the mean of the pituitary and

this was divided by the mean of the hypothalamus. For each rat on each day the relative difference between hypothalamus and pituitary T2 intensities were subjected to ANOVA with linear trend analysis and multiple comparison tests using Bonferroni adjustments (P7D program of BMDP Statistical Software; Dixon, 1988) (6).

## RESULTS

The largest cross sectional area for the pars distalis is observed on images obtained in the axial plane (Figs. 1a and 1b). The various components of the gland are well visualized in the axial plane and small alignment errors do not significantly alter the gland's appearance. Scatterplots were obtained from these axial images, the location of each dot in the scatterplot represents the intensity of a pixel on both the T1 and T2 weighted image. Figures 2a and 2b are scatterplots for a control rat's hypothalamus and pars distalis, respectively. Brightness of a pixel in the T2 weighted image is represented as an upward displacement on the vertical axis while brightness of the congruent pixel on the T1 weighted image is represented by location on the horizontal axis. The tight clustering of pixel intensities in the plot for the hypothalamus suggests that this tissue is homogeneous at the resolution of the pixel size used in these experiments. The pars distalis produced a wider range of intensities on both T1 and T2 weighted images which resulted in a correspondingly more diffuse distribution on the scatterplot. Noise in the MR instrument (receiver) is to some degree responsible for the spread observed in all scatterplots, but this contribution is constant for both tissues.

Images of all animals produced scatterplots of the pars distalis having a much wider range of intensities on both the T1 and T2 images than did the reference region of hypothalamus. (Figures 2 through 4, comparing panel "a" with panel "b"). Control animals displayed a distribution of intensities for pars distalis on both T1 and T2 images that was lower than that observed for the corresponding reference region of hypothalamus. The scatterplots were very similar among test animals and for all imaging time points in the control animals. Figures 2a and 2b are representative plots obtained for a control animal on day 7. The three experimental animals examined at the two early time points (days 2 and 4) produced scatterplots similar to the control animals, but the scatterplots for pars distalis in these animals moved towards higher T2 intensities

relative to the hypothalamus when examined on days 7, 9, and 10. Scatterplots shown in Figures 3a and 3b were obtained from an experimental animal, rat B, 4 days post estrogen treatment. Scatterplots (Figs. 4a and 4b) were generated from images of an experimental animal rat B, 9 days post estrogen. These data is summarized in Table 1. No conclusions were made based on the intensity variations observed in the T1 weighted images. Intensity varied widely for the pars distalis in these images, and it is known that eventually the hypertrophic pituitary in the estrogen induced animals produces a visibly mottled appearance on T1 weighted images (1).

On the scatter plots of day 2 the intensity distribution of the pars distalis of the estrogen implanted rats was statistically significantly lower than the intensity of the pars distalis of the control rat. On day 4 the pars distalis of rat B and C (Fig. 5) displayed a significantly higher intensity while the pars distalis of rat A was significantly lower compared to the control rat. From day 7 onwards the pars distalis of the pituitaries of all treated rats was higher in intensity as compared to the pars distalis of the control rat. It may be stressed that the pars distalis of the control rat at day 2 had a significantly higher intensity level than the pars distalis of the estrogen treated rats (Fig. 5).

Table 1. Pixel intensities of adeno-pituitary compared with pixel intensities of a part of the hypothalamic area in the same rat.

Pituitary	Days after estrogen implantation				
	2	4	7	9	10
Rat A					
T1	equal	equal	equal	equal	equal
T2	lower	lower	equal	equal	equal
Rat B					
T1	equal	equal	equal	equal	equal
T2	lower	lower	lower	equal	equal
Rat C					
T1	equal	equal	equal	equal	n.o.
T2	lower	lower	equal	equal	n.o.
Rat D					
T1	equal	equal	equal	equal	n.o.
T2	lower	lower	lower	lower	n.o.
Rat E					
T1	equal	equal	equal	equal	equal
T2	lower	lower	lower	lower	lower

A, B and C are estrogen implanted rats.  
D and E are control rats

lower = Pituitary is lower in intensity than Hypothalamic area  
equal = Pituitary is equal to intensity of Hypothalamic area

n.o. = no observations

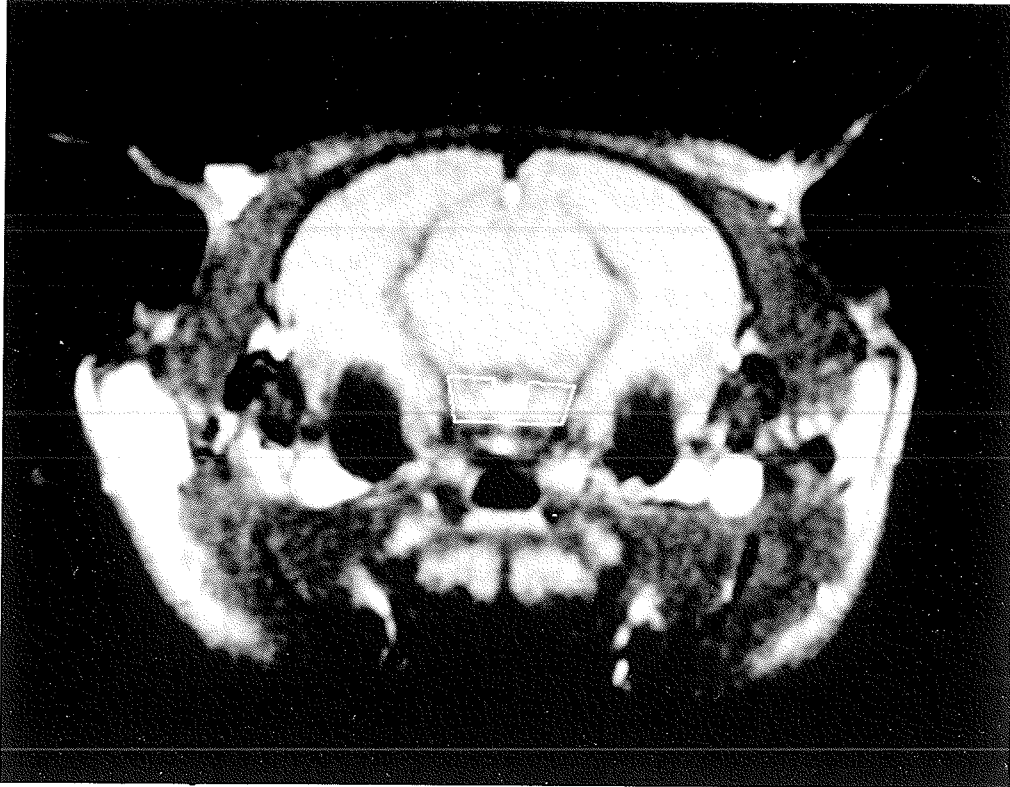


**Fig. 1a** -- An axial T1 weighted image (450/27) of a rat head obtained at a level cutting through the pituitary. The rat was a control animal, 4 days post estrogen stimulus. The regions of interest (pars distalis and hypothalamus) used in the scatterplot analysis are outlined with a white tracing. The dumbbell-shaped area outlined at the bottom of the brain is pars distalis.

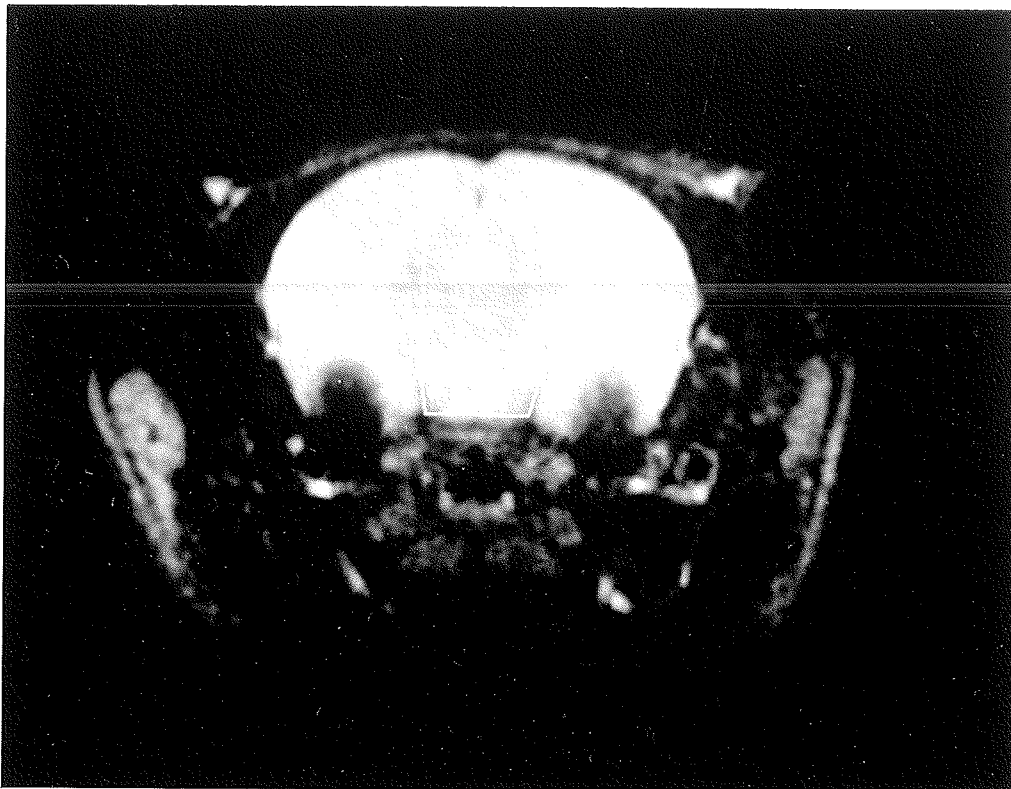


**Fig. 1b** -- A T2 weighted image (2000/80) congruent to Figure 1a. The regions of interest used in the scatterplots are traced in white.

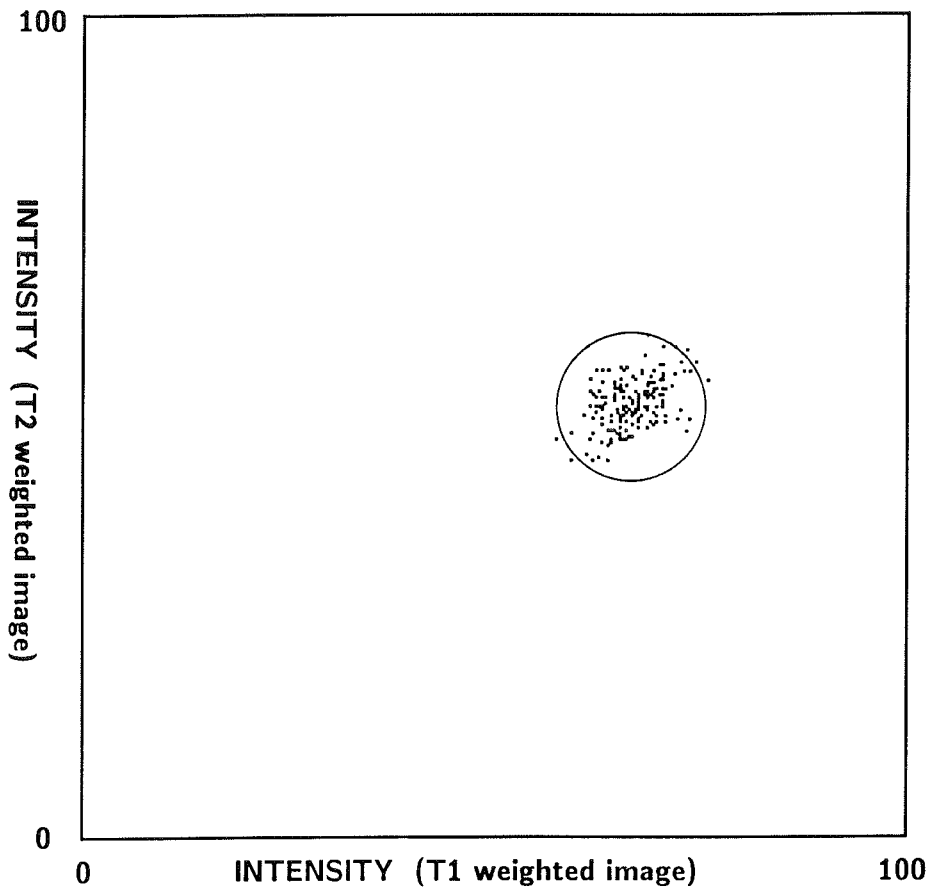


**Fig. 2a** -- The scatterplot of image intensities for the hypothalamic reference area in a control rat 7 days post estrogen treatment. A circle was added to the figure depicting the location of data points in order to facilitate comparison between scatterplots.

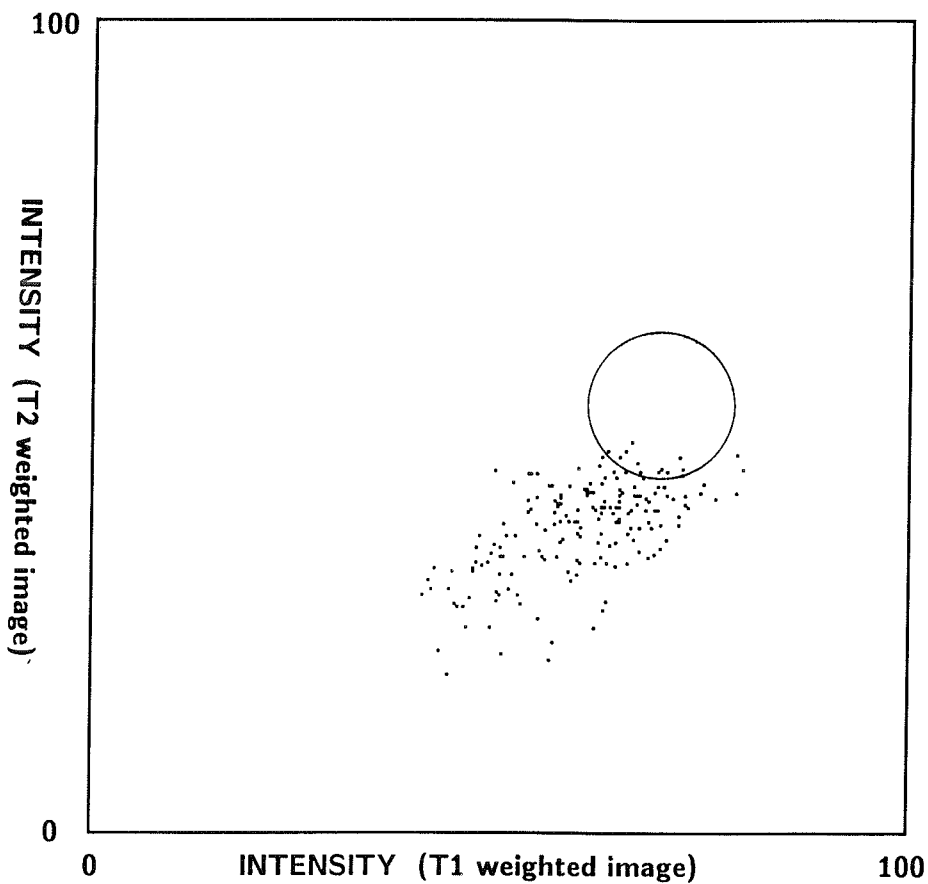


**Fig. 2b** -- The corresponding scatterplot to Figure 2a plotting image intensities from the pars distalis region of the pituitary. The circle represents the location of the data from Figure 2a.

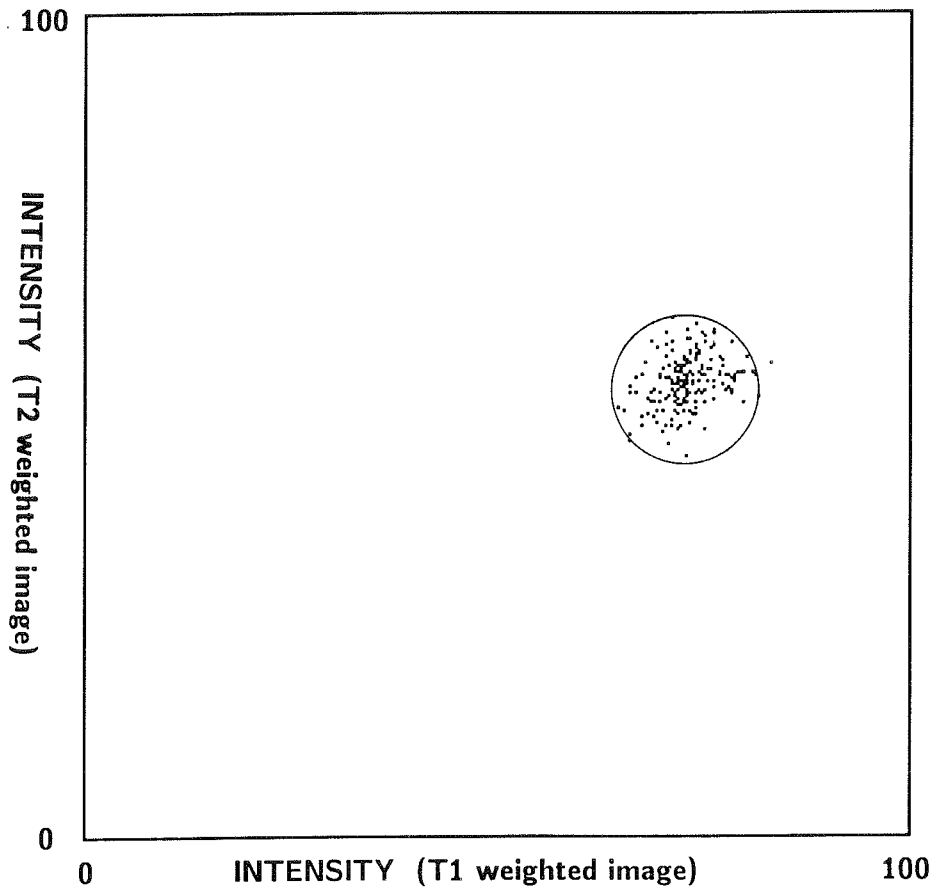


**Fig. 3a** -- The scatterplot of image intensities for the hypothalamic reference area in experimental rat B, 4 days post estrogen stimulus.

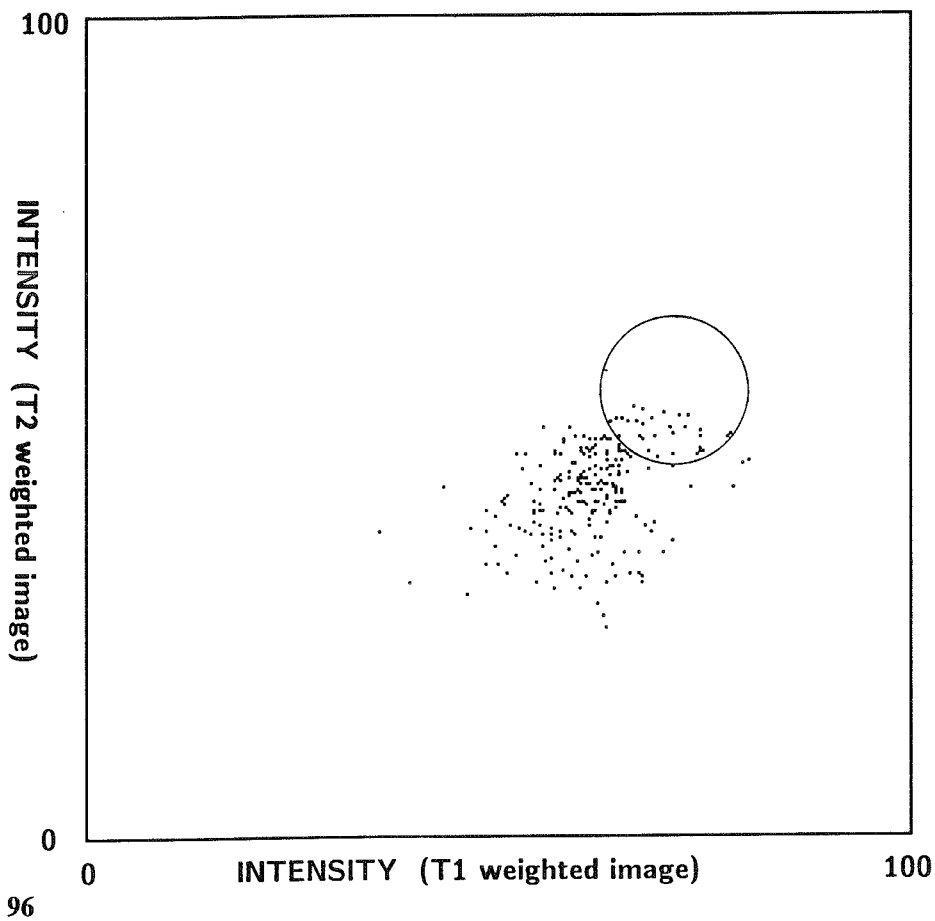


**Fig. 3b** -- The corresponding scatterplot to Figure 3a plotting image intensities from the pars distalis region of the pituitary. The circle represents the location of the data from Figure 3a.



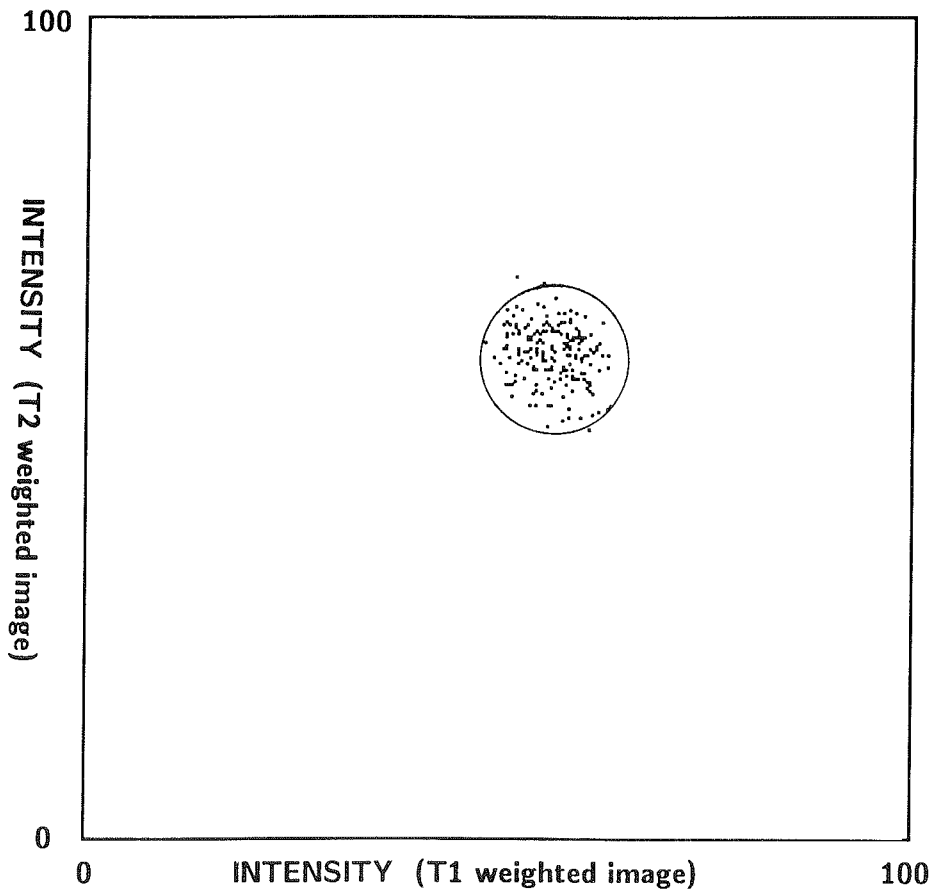


Fig. 4a -- The scatterplot of image intensities for the same experimental rat B as in Fig. 3a+b, 9 days post estrogen stimulus.

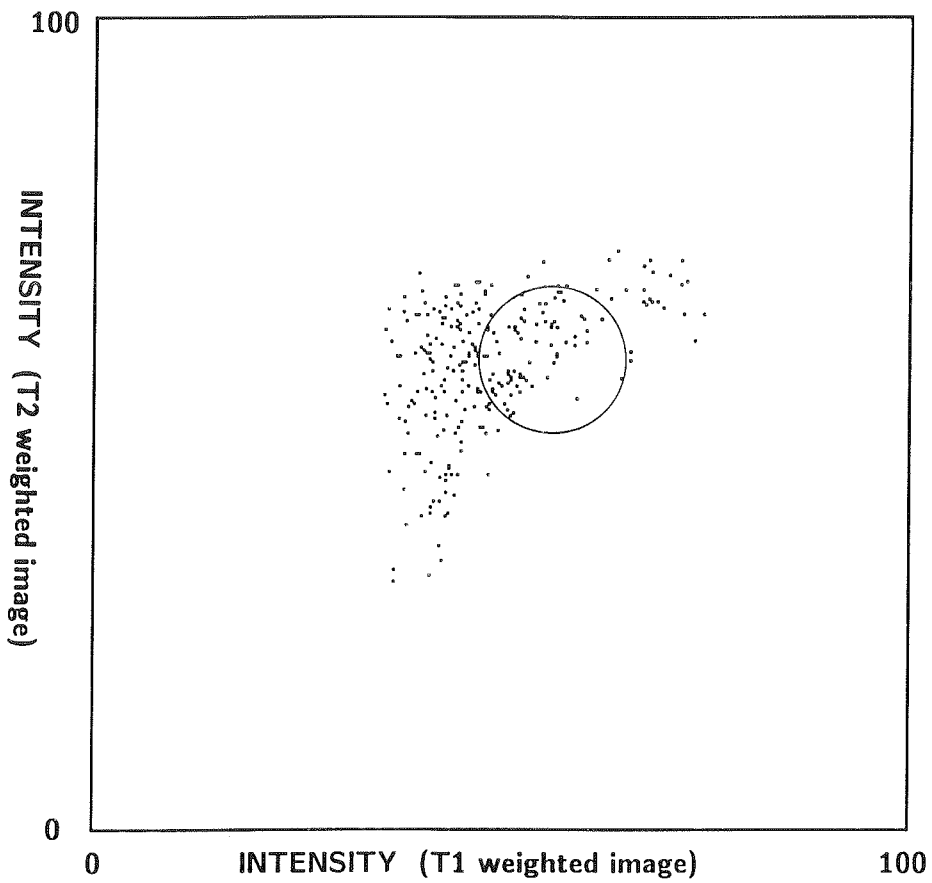


Fig. 4b -- The corresponding scatterplot to Figure 4a plotting image intensities from the pars distalis region of the pituitary. The circle represents the location of the data from Figure 4a.

Mean Relative differences between Pituitary and Hypothalamus T2 at Days 2 to 10

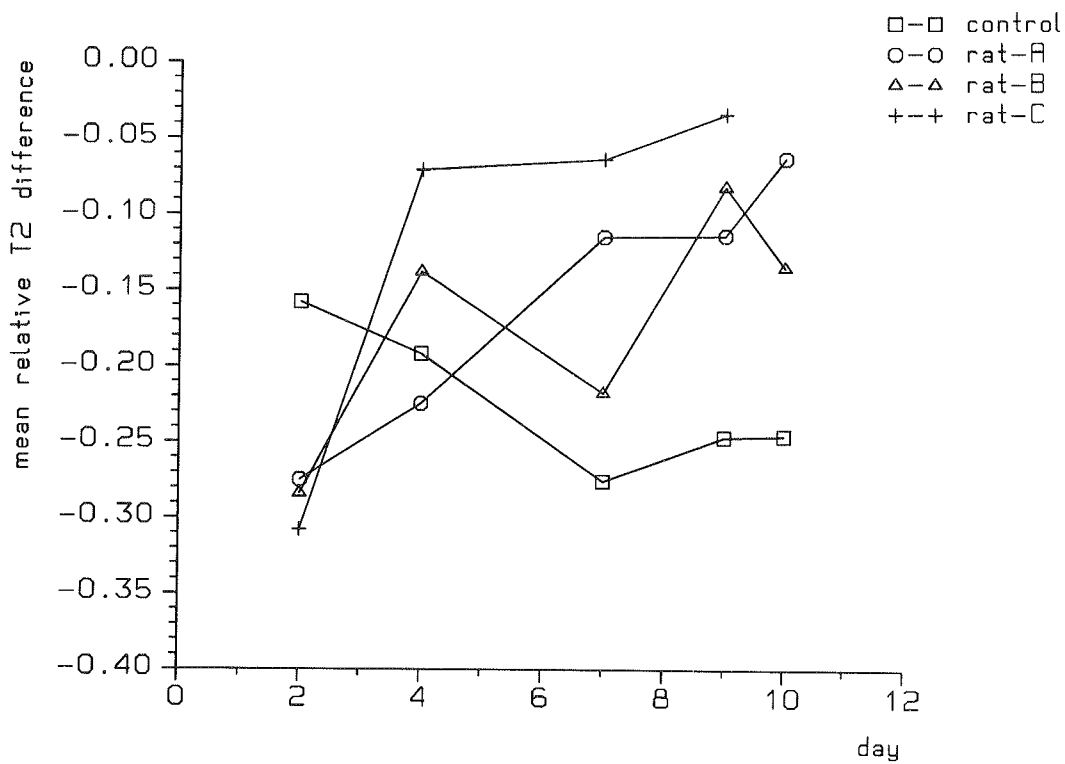


Fig. 5 -- Mean relative difference between hypothalamus and pituitary T2 intensities ranging from day 2 - 10.

**DISCUSSION**

In previous MR imaging studies we found that the earliest time point for detection of pituitary lesions in the estrogen induced rat model was at day 9. These changes were characterized by both anatomical (shape) differences as well as slight intensity variations (1, 2, 3). It was the goal of this investigation to determine if a more critical examination of the MR intensity variations could detect these changes at an even earlier point in time.

It is difficult to use absolute pixel intensity for comparative studies between animals since image intensity is related to many instrumental variables as well as the actual properties of the tissue under examination. Notably, the NMR probe sensitivity, amplifier gains, and magnet homogeneity vary with time and also with individual animal. A common approach is to compare relative intensities of a tissue under investigation (pituitary) with a reference tissue that is assumed to appear with reproducible intensity (hypothalamus). This treatment was combined with the use of a

scatterplot analysis to produce a graphic representation of variations in pixel intensity, one that provides more information than the simple average of intensity values in a ROI on a T1 or T2 weighted image.

A scatterplot provides more information than just a simple histogram of intensities from a ROI. Statistical analysis of the scatterplots revealed that at day 4 pituitaries of two treated rats (B and C) had a significantly elevated T2 intensity level compared to that of the control pituitary. This early difference was not visible on the scatterplots as such. The statistical analysis of the scatterplots of days 7, 9 and 10 showed a higher intensity for the pars distalis of the pituitary in treated rats than in the control rat. On day 7 the pars distalis of rat B showed no intensity elevation in the scatterplot analysis; this was confirmed by the statistical analysis revealing a minor elevation of intensity. The remarkably low intensity on day 2 of the pars distalis of the implanted rats is probably caused by an acute effect of the estrogen treatment on the pituitary.

A difficulty in this rat study was that the entire

pituitary gland was not affected uniformly by estrogen. The anterior part of the pituitary is known from a previous histopathological study (3) to be the only part affected. MR intensity measurements on the entire gland, therefore, result in an unnecessary dilution of detection sensitivity. The pars nervosa is not involved in pituitary tumor development and has been reported to give a high and variable MR image intensity (3, 4). Our preliminary study using the scatterplot approach (5) examined the entire gland and resulted in generally higher intensities on the T2 weighted images than those found in the present study. Scatterplots in the previous study also displayed less T2 intensity change as a result of estrogen treatment. Both studies generated a wider distribution of intensities in both the T1 and T2 weighted images for the pars distalis region relative to reference hypothalamus area. The center of the intensity distribution on T2 weighted images for the pars distalis was lower than that for the hypothalamus in both studies.

The measurement of pixel intensity fluctuations can be described as image texture. The hypothalamus appears with less intensity fluctuations than the pars distalis, perhaps as a result of the types of tissue and extent of vascularization. When the variation in intensity of pixels on an image is extensive and these pixels are clumped in groups, the tissue is said to have a mottled appearance. The tissue gives rise to a wide pattern on the scatterplot. It is worth noting that the texture does not significantly change in the estrogen treated animals although the T2 intensities increase.

## CONCLUSION

The use of scatterplots incorporating the intensity information from both T1 and T2 weighted images provides a means of identifying changes in the pituitary in this rat model. Large dispersion and variations in the intensities of the pars distalis are observed on T1 weighted images and affect both control and experimental animals. No pattern was identified in these changes and we suggest that T1 weighted image intensities are not a good indicator of disease in this animal model. Image intensity on T2 weighted images, however, does correlate with pituitary pathology, provided that the region of examination is limited to just the pars distalis section of the gland and that the intensity measurements are referenced to another external tissue intensity. Changes in the T2 weighted intensities can be detected as early as 7 days post estrogen treatment. This technique seems

to allow a somewhat earlier detection of pituitary changes compared to the previously reported MR imaging technique relying on changes observed in midsagittal MR images of this gland.

## ACKNOWLEDGEMENTS

We thank Drs. A. Zwart and A.J.M. Hagenars for the helpful assistance with the statistical analysis. This work was supported in part by Grant CIVO 87-2 from the Dutch Cancer Society (KWF).

## REFERENCES

1. J.H.J. van Nesselrooij, N.M. Szeverenyi and M.J. Ruocco, *J. Mag Res. Med.*, **11**, 161 (1989).
2. J.H.J. van Nesselrooij, N.M. Szeverenyi, G.M. Tillapaugh-Fay and F.G.J. Hendriksen, *Mag. Res. Imag.*, **8**, 525 (1990).
3. J.H.J. van Nesselrooij, J.P. Bruijntjes, A. van Garderen-Hoetmer, G.M. Tillapaugh-Fay, and V.J. Feron, *Carcinogenesis*, **12**, 289 (1991).
4. S.M. Wolpert, M. Osborne, M. Anderson, and V.M. Runge, *AJNR*, **9**, 1 (1988).
5. J.H.J. van Nesselrooij, N.M. Szeverenyi, G.M. Tillapaugh-Fay, *Works in Progress, SMRM Eighth Annual Meeting, Amsterdam* (1989).
6. W.J. Dixon, *BMDP statistical software* University of California Press Berkely, 1988.



## **CHAPTER VIII**

### **RAT PITUITARY CHANGES OBSERVED WITH MAGNETIC RESONANCE IMAGING FOLLOWING REMOVAL OF ESTROGEN STIMULUS: CORRELATION WITH HISTOPATHOLOGY AND IMMUNOHISTOLOGY**

Joop H.J. van Nesselrooij, Nikolaus M Szeverenyi, Cathy Ritter-Hrncirik,  
Gwen M. Tillapaugh-Fay and Victor J. Feron.

Carcinogenesis 13: 277-282, 1992.



# Rat pituitary changes observed with magnetic resonance imaging following removal of estrogen stimulus: correlation with histopathology and immunohistology

Joop H.J. van Nesselrooij<sup>1,2</sup>, Nikolaus M. Szeverenyi<sup>2</sup>, Cathy Ritter-Hrncirik<sup>2</sup>, Gwen M. Tillapaugh-Fay<sup>2</sup> and Victor J. Feron<sup>1</sup>

<sup>1</sup>Laboratory of Pathology, Department of Biological Toxicology, TNO Toxicology and Nutrition Institute, 3704 HE Zeist, The Netherlands and <sup>2</sup>Nuclear Magnetic Resonance Research Laboratory, Department of Radiology, State University of New York, Health Science Center at Syracuse, Syracuse, NY 13210, USA

The effect of estrogen withdrawal on pituitary glands of rats treated with estradiol-17 $\beta$  for various lengths of time was monitored by magnetic resonance imaging (MRI) and histological examination. Estrogen pellets were removed at seven different time points ranging from 4 to 206 days after pellet implantation. High-resolution mid-sagittal MR images of the rat head were made 1 day before pellet implantation, immediately following pellet withdrawal, and 14 and 28 days after pellet withdrawal. Twenty-eight days after pellet withdrawal pituitary glands were fixed and processed for histological examination. Enlarged pituitaries were detected by MRI from 16 days after implantation and onwards. Twenty-eight days after estrogen withdrawal the typical triangular shape of the normal pituitary had returned and pituitary morphology was indistinguishable from that of normal pituitaries in all rats that had been treated with estrogen for up to 114 days. Pituitaries of rats that had received estrogen for 186 days had a normal MR image 28 days after estrogen withdrawal, but microscopic examination revealed multifocal hyperplasias of prolactin-positive cells throughout the pars distalis. MRI of rats treated for 206 days showed tumourously enlarged pituitaries. There was no evidence of tumor regression in these rats 28 days after pellet removal. It was concluded that hypertrophic pituitaries regained a normal size, shape and morphology after estrogen withdrawal, except for a remarkable type of hyperplasia following estrogen treatment for 186 days and a recovery period of 28 days. In tumorous pituitaries no regression of lesions was noticed.

## Introduction

Estrogen-induced pituitary tumors in rats have been extensively studied as a model for spontaneous pituitary tumors in both humans and rodents (1–6). Treip (6) reported regression of estradiol-induced pituitary tumors in rats treated with estradiol for 110–150 days followed by a recovery period of 120–220 days after estradiol withdrawal.

Magnetic resonance imaging (MRI\*) has been demonstrated to be an effective and sensitive technique to study changes in pituitary size, shape and structure (7–9). We have successfully

used MRI to follow the development of estrogen-induced pituitary hypertrophy and neoplasia in individual rats. MRI has the advantage that it is non-invasive, minimizing the need for interim sacrifices and consequently reducing the number of animals required for these sorts of studies (9).

The purpose of the present investigation was to monitor the response (growth or shrinkage) of the rat pituitary gland following discontinuation of estrogen stimulus. Pituitary appearance was studied as a function of the duration of stimulus as well as a function of time after estrogen discontinuation. MRI was used extensively throughout the study with correlation to histopathology at the final day for each treated animal.

## Materials and methods

### Animals and treatment

A 25 mg estradiol-17 $\beta$  pellet (Organon, Oss, The Netherlands) was implanted s.c. in 14 4-week old male Sprague–Dawley rats obtained from Harlan Sprague–Dawley, Indianapolis, IN, USA. The estrogen pellet was removed, each time from two animals, at 4, 8, 16, 81, 114, 186 and 206 days after pellet implantation.

Rats were housed in wire-mesh cages in a well-ventilated room at 20°C with relative humidity 40–70% and 12 h lighting per day. Animals had free access to food (Purina Formulab Chow 5000, Purina Mills, Inc., St Louis, MO, USA) and tap water and they were checked daily. The animals were treated under a protocol and housing arrangement approved by the institutional Committee for the Humane Use of Animals.

### Imaging

High-resolution MR images of the rat cranium were made 1 day before pellet implantation, immediately following pellet withdrawal, and finally at 14 and 28 days after pellet withdrawal. A 2 Tesla 31 cm bore (General Electric, Fremont, CA) research imaging instrument was used to obtain T1 weighted spin echo images with a TE of 28 ms and a TR of 450 ms. Using an in-house manufactured 4 cm diameter double pancake coil, 2 mm thick sagittal mid-line slices were obtained since these were found to produce the most clear and reproducible results (7–9). Data collection matrix size was 256  $\times$  256 (complex) with four or eight excitations averaged to give adequate signal to noise ratio. In order to minimize animal motion during the image data acquisition, rats were anesthetized with sodium pentobarbital, 5 mg/100 g body wt.

### Histopathology and immunohistochemistry

At necropsy, pituitary glands were removed and fixed in a 4% buffered formaldehyde solution. The pituitaries were processed to Paraplast and 10.5  $\mu$ m

Table 1. Pituitary size before and after estrogen stimulus withdrawal

Days of estrogen stimulus	Days after estrogen withdrawal		
	0	14	28
4	N	N	N
8	N	N	N
16	EL	N	N
81	EL	N	N
114	EL	N	N
186	EL	EL	N
206	TEL	TEL	TEL

N, normal pituitary; EL, enlarged, normal triangular shape of the pituitary changes into enlarged rounded structures; TEL, tumourously enlarged, expansion of the tumorous pituitary structure into the brain with areas with a high degree of variability of signal intensity.

\*Abbreviations: MRI, magnetic resonance imaging; PRL, prolactin.

thick step sections were made of each gland, one of which was stained with H&E while the others were used for immunohistochemistry. Using rabbit anti-rat antiserum (UCB Bioproducts, Brussels, Belgium) a direct/indirect immunoperoxidase technique was used to stain sections for prolactin (PRL).

Swine anti-rabbit total immunoglobulin (Sanbio, Nistelroode, The Netherlands) was used as a bridge between the primary antibody and the rabbit peroxidase-antiperoxidase (Dako, Amsterdam, The Netherlands). 3,3-Diaminobenzidine-tetrahydrochloride (Sigma) was used as a substrate to visualize the product. The sections were counter-stained with Gill's type II hematoxylin.

The following criteria were used to differentiate between foci of hyperplastic cells and tumors. In comparison with normal pituitary tissue, in hyperplastic cell foci nuclear density was higher, cells were smaller, and cytoplasm was hyperbasophilic. Hyperplastic cell foci were distinguished from tumors on the basis of growth pattern and cytomorphology. Lesions with hemorrhagic areas and/or cellular and nuclear pleomorphism were classified as neoplasm, and lesions with neither pleomorphism nor hemorrhagic areas as hyperplastic cell foci. Compression, demarcation and encapsulation were not used as criteria to distinguish

hyperplastic cell foci from tumors because the degree of demarcation was highly variable even for large lesions, and some compression was occasionally found even with very small lesions; capsule formation never occurred.

## Results

### MRI

A summary of the pituitary sizes at the various time points before and after estrogen withdrawal is given in Table I.

In T1-weighted mid-line sagittal images the normal pituitary appeared triangular with sharply defined margins. Before pellet implantation, this characteristic pituitary shape was present on initial imaging of all 14 rats. No change in the triangular shape of the pituitary or image intensity was seen on days 4 and 8 after

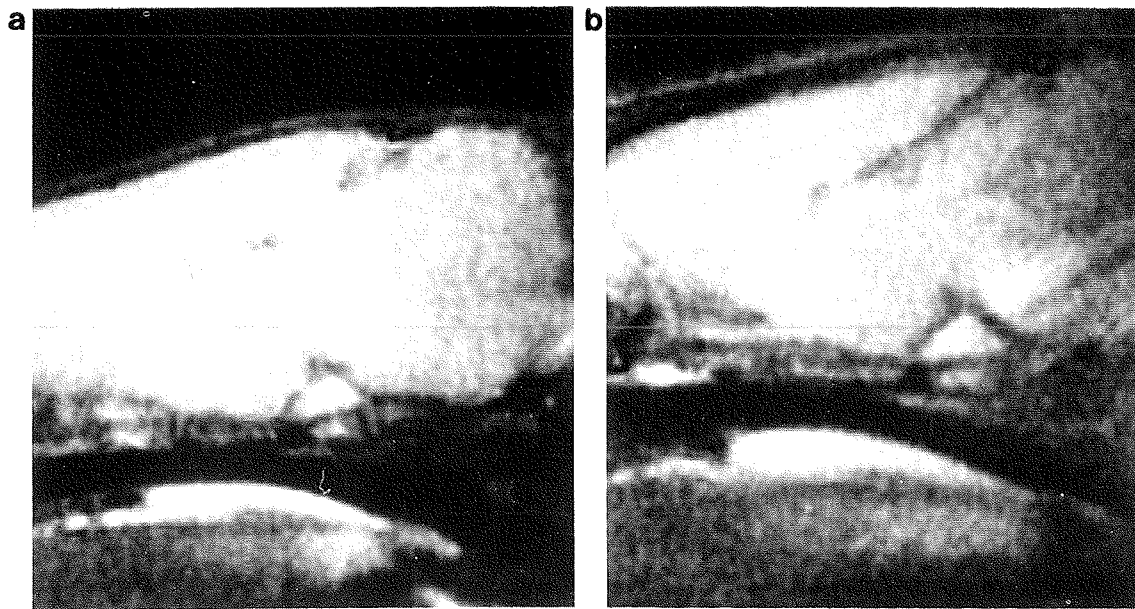


**Fig. 1.** (a) T1 weighted mid-sagittal image after 4 days of estrogen implantation. The typically triangular shape of the pituitary is unchanged. (b) T1 weighted mid-sagittal image 28 days after estrogen withdrawal. The triangular shape of the pituitary remained the same.

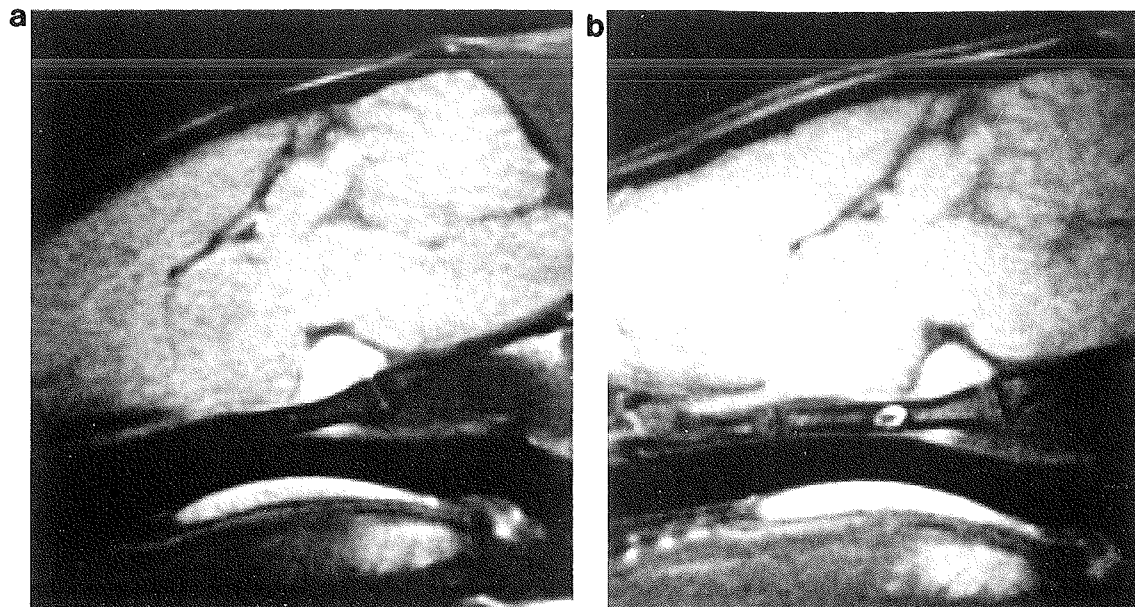


**Fig. 2.** (a) T1 weighted mid-sagittal image after 81 days of estrogen implantation. The pituitary is enlarged and the pars nervosa is squeezed upwards by the enlarged pars distalis. (b) T1 weighted mid-sagittal image 28 days after estrogen withdrawal. The pituitary returned to its normal triangular shape.



initiation of the estrogen treatment, and after estrogen withdrawal on days 14 and 28 (Figure 1a and b).

On day 16 after implantation, there was a slight rounding of the margins of the pituitary, and the subarachnoid space between gland and diencephalon and the space between pituitary and pons were narrowed when viewed in the sagittal image planes. Signal intensity was variable 14 and 28 days after estrogen withdrawal, but the typical triangular shape of the pituitary and its normal signal intensity had returned.

On day 81 after estrogen implantation, the pituitary was distinctly enlarged, and the pars nervosa was squeezed upwards by the enlarged pars distalis. Pituitary signal intensity was hyperintense compared to brain; pars nervosa signal intensity was

more hyperintense than that of the pars distalis (Figure 2a and b). Similar pituitary images were obtained on day 114 after pellet implantation (Figure 3a and b). Images made 14 and 28 days after estrogen withdrawal showed a complete return of the pituitary to its normal triangular shape.

On day 186 after implantation, the enlarged pituitary had expanded into the brain and image signal intensity was lighter than brain but uniform (Figure 4a and b). Fourteen, and particularly 28 days after pellet removal, the pituitaries of these animals had completely returned to their normal shape. However, the pars nervosa was still slightly squeezed upwards by a slit-like space between pars nervosa and pars distalis.

After 206 days of estrogen treatment, images of the treated

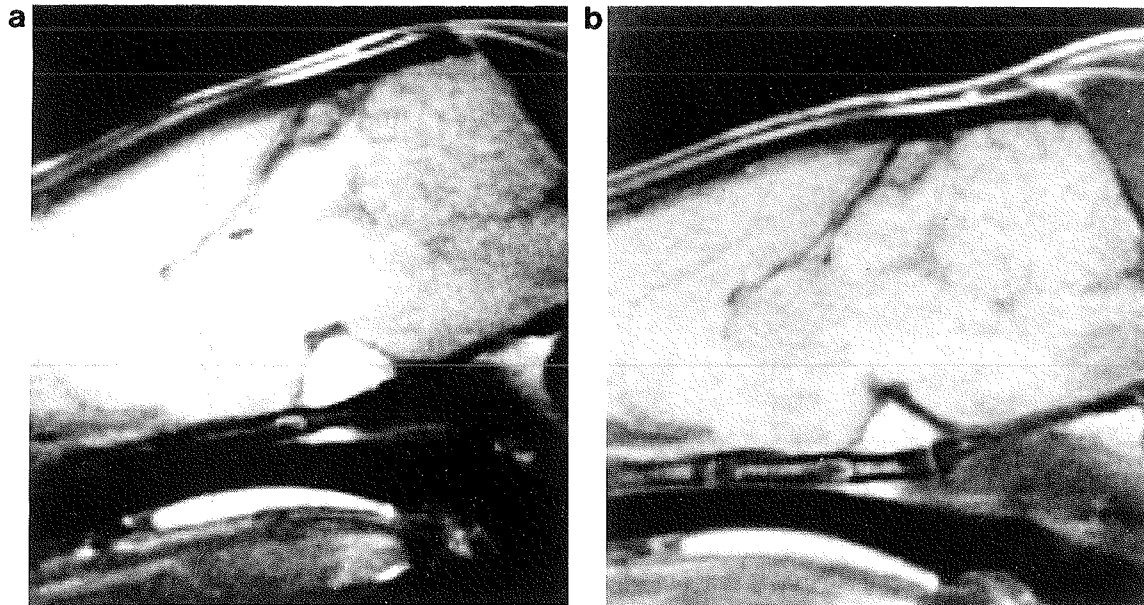


Fig. 3. (a) T1 weighted mid-sagittal image after 114 days of estrogen implantation. The pituitary is distinctly enlarged. (b) T1 weighted mid-sagittal image 28 days after estrogen withdrawal. The pituitary returned to its normal triangular shape.

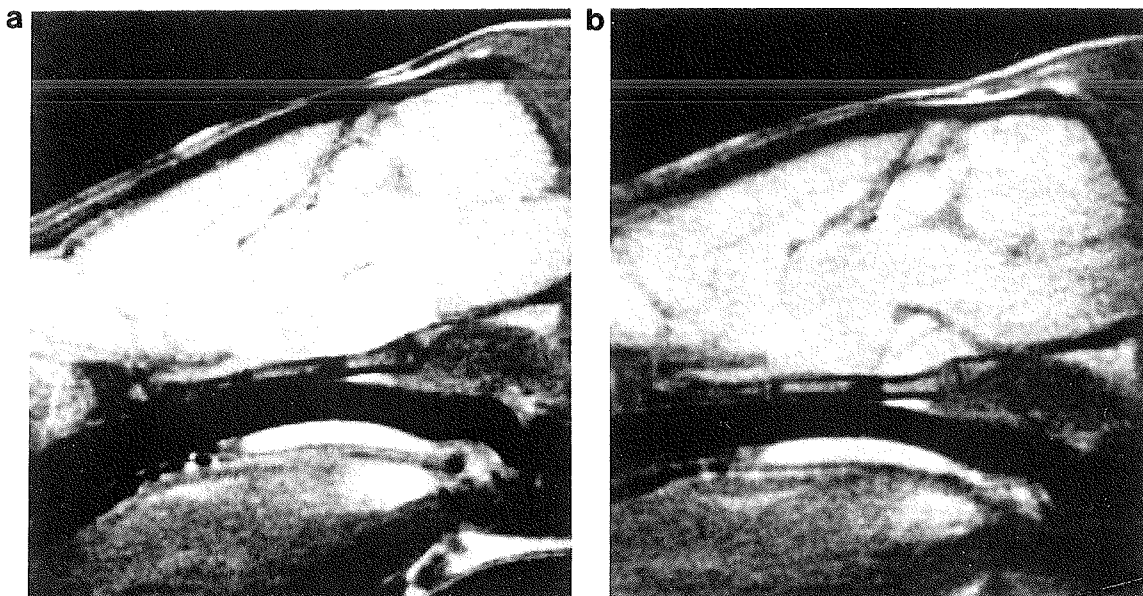
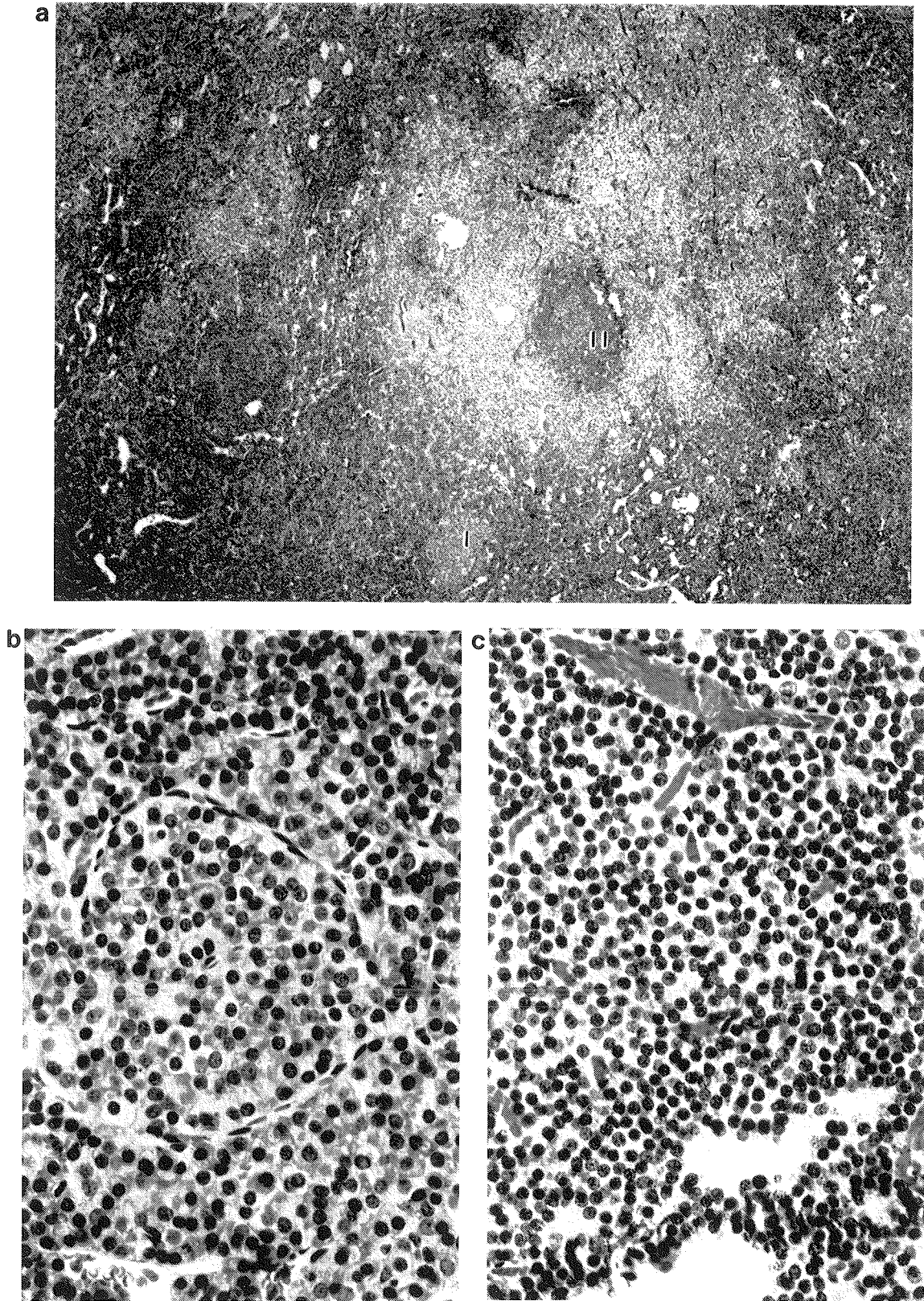
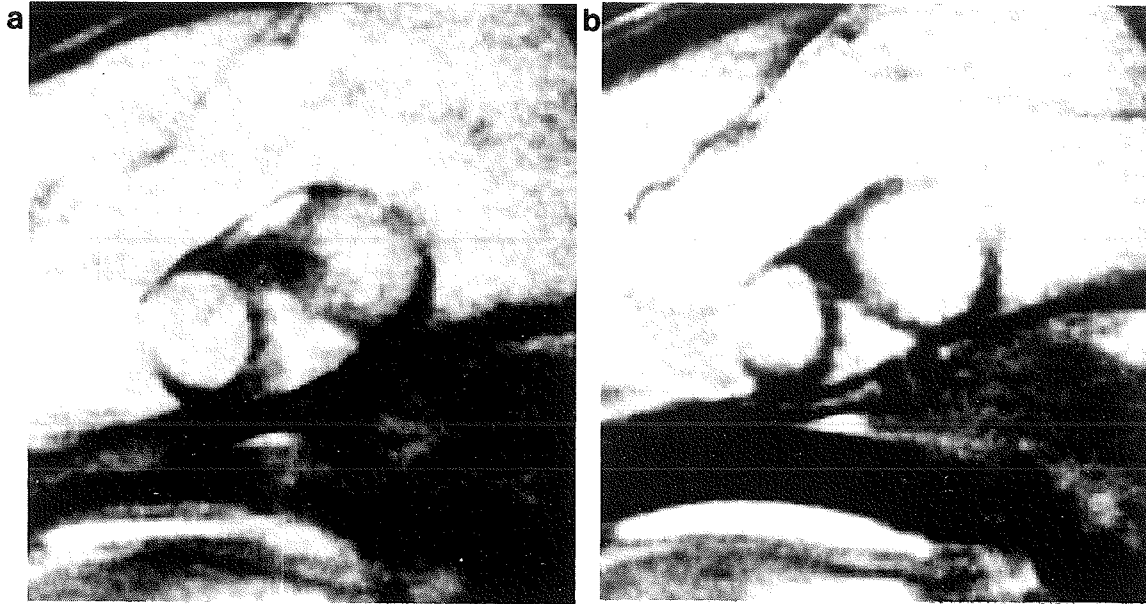


Fig. 4. (a) T1 weighted mid-sagittal image after 186 days of estrogen implantation. The enlarged pituitary expands into the brain and signal intensity is brighter than surrounding brain tissue but uniform. (b) T1 weighted mid-sagittal image 28 days after estrogen withdrawal. The pituitary returned to its normal triangular shape. However, the pars nervosa is still squeezed upwards by a slit-like space between the pars nervosa and the pars distalis.



**Fig. 5.** (a) Pituitary of a rat treated with estrogen for up to 114 days following a recovery period, showing multifocal hyperplasia. Two distinct forms of focal hyperplasias can be observed. One type consists of hypertrophic cells surrounded by a zone of cells with abundant cytoplasm not staining with H&E (area I) and the other type consists of small cells with very little cytoplasm (area II). Between the hyperplastic foci scattered slightly hypertrophic and normal pituitary cells can be seen. H&E staining,  $\times 100$ . (b) Area I: hypertrophic cell hyperplasia. This consists of cells with pale, vacuolated cytoplasm that is slightly more abundant than in normal pituitary cells. Nuclei are uniform and foci are not well demarcated. H&E staining,  $\times 250$ . (c) Area II: small cell hyperplasia. This consists of cells with little cytoplasm that do not stain with H&E. Nuclei are uniform and foci are not well demarcated. H&E staining,  $\times 250$ .



**Fig. 6.** (a) T1 weighted mid-sagittal image after 206 days of estrogen implantation. The markedly enlarged pituitary shows a great variability in signal intensity ranging from hypo-, iso- to hyperintense areas relative to surrounding brain tissue. (b) T1 weighted mid-sagittal image 28 days after estrogen withdrawal. No regression of this markedly enlarged pituitary is seen except for some minor changes in the signal intensities.

rats showed markedly enlarged pituitaries with great variability in signal intensity ranging from hypo-, iso- to hyperintense relative to surrounding brain tissue (Figure 6a). No indication of regression of this enlargement was obtained in these animals after pellet removal except for some minor changes in signal intensities (Figures 6b).

#### *Histopathology and immunohistochemistry*

Pituitaries from rats treated with estrogen for up to 114 days and followed by a recovery period of 28 days were histologically indistinguishable from pituitaries of untreated rats. Indeed, the number and distribution of PRL-positive cells in these pituitaries were completely normal.

The pituitaries of rats that had received estrogen for 186 days followed by a 28 day estrogen withdrawal period had multifocal hyperplasia, scattering throughout the pars distalis. Two distinct forms of focal hyperplasias were observed: one type consisted of small cells and the other type of hypertrophic cells (Figure 5a, bI, cII). The cells in small cell hyperplasias (Figure 5cII) had little cytoplasm that did not stain with H&E. The nuclei were uniform and no mitotic figures were seen. These focal hyperplasias were not well demarcated, and several of these foci were surrounded by a zone of cells of ordinary size but with abundant cytoplasm that did not stain with H&E. Hyperplasias of hypertrophic cells (Figure 5bI) consisted of cells with pale, vacuolated cytoplasm that were slightly larger than normal pituitary cells. Their nuclei were uniform and mitotic figures were not seen. These foci were not well demarcated and were surrounded by normal pituitary cells. Between these two types of hyperplastic foci, scattered slightly hypertrophic and normal cells were present. Cells in both types of hyperplasia were PRL positive. Some sinusoids in hyperplastic foci appeared slightly compressed but no compression of surrounding tissue was observed.

Pituitaries of rats that had recovered for 28 days following 206 days of estrogen treatment had tumors that were characterized by the presence of hemorrhagic as well as solid areas and cysts.

Hemorrhagic areas consisted of cells arranged in cords, one to several cell layers thick, with cleft-like sinusoids on one side and blood-filled cyst-like structures lined by epithelial cells on the other side as described previously (9). Solid areas consisted of clusters of cells without a specific growth pattern and sparse sinusoids.

#### **Discussion**

Two different stages in the development of estrogen-induced pituitary tumors in rats have been identified in previous MRI studies (7–9): pituitaries with the normal triangular shape changed into hypertrophic pituitaries with a rounded, enlarged structure (stage 1); and tumorously enlarged pituitaries characterized by expansion of the pituitary structure into the brain and by areas with a high degree of variability of signal intensity (stage 2). To determine reversibility of these stages in pituitary tumorigenesis, in the present study the estrogen stimulus was withdrawn at different times after the start of estrogen treatment. Hypertrophic pituitaries developed between 16 and 114 days of estrogen treatment, which returned to the normal triangular shape within 28 days after cessation of estrogen-treatment. Tumorous pituitaries were seen after 206 days of estrogen treatment, and their MR images remained unchanged after estrogen withdrawal except for some minor changes in signal intensity. These results are at variance with those of Treip (6) who reported pituitary tumor regression determined as a decrease in pituitary weight 110 days after withdrawal of the estrogen stimulus following 220 days of treatment. Possible explanations for these contrasting results are differences in duration of follow-up period, rat strain and methodology used (namely pituitary weights versus MRI and histopathology). Moreover, it may be possible that in the study by Treip (6) the induced pituitary lesions were still in the hypertrophic phase (stage 1) since the description of pituitary tumors by Treip (6) better resembles pituitary hypertrophy than pituitary neoplasia.

Estrogen withdrawal after 186 days of treatment resulted in

a complete return of the hypertrophic pituitaries to the normal triangular shape within 28 days. A possible explanation for the still slightly enlarged pituitary seen at this time point by MRI is a cystic enlargement of Rathke's pouch, which is located between the pars distalis and the pars intermedia, perhaps in combination with multifocal hyperplasia in the pars distalis. However, light microscopic examination at this time point revealed an unexpected pituitary morphology. In contrast to the diffuse hypertrophy and hyperplasia of PRL-containing cells throughout the enlarged pars distalis in rats continuously exposed to estrogen (1,7–9), 28 days following withdrawal of the estrogen stimulus, multifocal hyperplasias consisting of small or hypertrophic cells were observed. These hyperplasias *per se* could not be detected by MRI, since their presence did not result in changes in MRI signal intensity. To our knowledge, hyperplasias with this morphological appearance have never been described in estrogen-treated rats. In an autopsy study of old men treated with diethylstilbestrol, Scheithauer *et al.* (10) described pituitaries with hyperplasias of uniform PRL cells that occurred in diffuse as well as nodular patterns.

Pituitary hyperplasias and tumors occur spontaneously in aging rats (11–14). The small cell hyperplasias seen in this study morphologically resemble spontaneous rat pituitary hyperplasias. Thus, withdrawal of the estrogen stimulus after ~6 months of estrogen treatment results in the occurrence of focal pituitary lesions that occur in untreated rats only beyond 18 months of age. However, since recovery from estrogen treatment beyond 28 days was not studied, the further fate of these lesions remains unknown. Several of the small cell hyperplasias in the present study occurred within areas of diffusely arranged, enlarged cells, which may suggest that these hypertrophic cells are precursors of the small cell hyperplasias.

In conclusion, estrogen withdrawal in the early stages of pituitary tumor development induced by estrogen (hypertrophic pituitaries) results in a return to a pituitary of normal size and shape, whereas withdrawal of estrogen stimulus once tumorous pituitaries have developed does not lead to tumor regression. The effect of recovery from estrogen treatment for periods >28 days on pituitary tumors remains to be determined. Nevertheless, the results of this study suggest that estrogen-induced pituitary tumors are autonomous and estrogen-independent neoplastic processes. Again MRI proved to be an effective technique to display changes in pituitary shape, size and structure, though multifocal hyperplasias were not detected.

### Acknowledgements

The authors wish to thank Dr M.C. Bosland, Institute of Environmental Medicine, New York University Medical Center, New York, NY, for his helpful comments. This work was supported in part by grant CIVO 87-2 awarded by the Dutch Cancer Society (Koningin Wilhelmina Fonds).

### References

- Lloyd, R.V. (1983) Estrogen-induced hyperplasia and neoplasia in the rat anterior pituitary gland, an immunohistochemical study. *Am. J. Pathol.*, **113**, 198–206.
- Wiklund, J., Wertz, N. and Gorsky, J. (1981) A comparison of estrogen effects on uterine and pituitary growth and prolactin synthesis in F344 and Holtzman rats. *Endocrinology*, **109**, 1700–1707.
- Herbert, D.C., Cisneros, P.L. and Rennels, E.G. (1977) Morphological changes in prolactin cells of male rats after testosterone administration. *Endocrinology*, **100**, 487–495.
- Furth, J., Clifton, K.H., Gadsen, E.L. and Buffett, R.F. (1956) Dependent and autonomous mammatropic pituitary tumors in rats: their somatotrophic features. *Cancer Res.*, **16**, 608–616.
- Clifton, K.H. and Meyer, R.K. (1956) Mechanism of anterior pituitary tumor induction by estrogen. *Anat. Rec.*, **125**, 65–81.
- Treip, C.S. (1983) The regression of oestradiol-induced pituitary tumours in the rat. *J. Pathol.*, **14**, 29–40.
- Van Nesselrooij, J.H.J., Szeverenyi, N.M. and Ruocco, M.J. (1989) Magnetic resonance imaging of estrogen-induced pituitary hypertrophy in rats. *Magn. Reson. Med.*, **11**, 161–171.
- Van Nesselrooij, J.H.J., Szeverenyi, N.M., Tillapaugh-Fay, G.M. and Hendriksen, F.G.J. (1990) Gadolinium-DTPA enhanced and digitally subtracted magnetic resonance imaging of estrogen induced pituitary lesions in rats: correlation with pituitary anatomy. *Magn. Reson. Imag.*, **8**, 525–533.
- Van Nesselrooij, J.H.J., Bruijntjes, J.P., van Garderen-Hoetmer, A., Tillapaugh-Fay, G.M. and Feron, V.J. (1991) Magnetic resonance imaging compared with hormonal effects and histopathology of estrogen-induced pituitary lesions in the rats. *Carcinogenesis*, **12**, 289–297.
- Scheithauer, B.W., Kovacs, K.T., Randall, R.V. and Ryan, N. (1989) Effects of estrogen on the human pituitary: a clinico pathologic study. *Mayo Clin. Proc.*, **64**, 1077–1084.
- Berkvens, J.M., Van Nesselrooij, J.H.J. and Kroes, R. (1980) Spontaneous tumors in the pituitary gland of old Wistar rats: a morphological and immunocytochemical study. *J. Pathol.*, **130**, 179–191.
- Kroes, R., Berkvens, J.M., de Vries, T. and Van Nesselrooij, J.H.J. (1982) Histopathological profile of a Wistar rat stock including a survey of the literature. *J. Gerontol.*, **36**, 259–279.
- Trouillas, J., Girod, C., Claustrat, B., Cure, M. and Dubois, M.P. (1982) Spontaneous pituitary tumors in the Wistar/Furth/Ico rat strain. *Am. J. Pathol.*, **109**, 57–70.
- Van Nesselrooij, J.H.J., Kuper, C.F., Bosland, M.C. Bruijntjes, J.P. and Kroes, R. (1985) Spontaneous pituitary lesions and plasma prolactin levels in rats. In Auer, L.M. (ed.), *Prolactinomas: An Interdisciplinary Approach*. De Gruyter, Berlin/New York, pp. 85–87.

Received on August 28, 1991; revised on October 15, 1991; accepted on October 17, 1991





## SUMMARY AND CONCLUSIONS





## SUMMARY AND CONCLUSIONS

Proliferative pituitary lesions (hyperplasias and tumors) are common in aging man and rodents. In humans, such lesions frequently pose a serious diagnostic problem, because measurement of hormone levels does not permit detection of pituitary hyperplasia and is of doubtful value for detecting pituitary tumors. Magnetic Resonance Imaging (MRI) is a powerful new technique for the detection and diagnosis of such pituitary lesions in man.

The objective of the investigations described in this thesis were

- To develop a classification system for the entire spectrum of hyperplastic and neoplastic lesions of the rat pituitary.
- To evaluate the suitability of MRI as a non-invasive method for the detection and characterization of rat pituitary lesions induced by estrogen.
- To compare MR images of the pituitary lesions with their light and electron microscopic morphology and with diagnostic information derived from plasma levels of pituitary hormones.

Spontaneous pituitary lesions in aged rats were classified on the basis of their light microscopic morphology as foci of hypertrophic or hyperplastic cells, and hemorrhagic, pleomorphic or spongicytic tumors in CHAPTER II. In addition, the predictive value of elevated plasma prolactin (PRL) concentrations for the presence of spontaneous pituitary lesions was evaluated. The pituitaries were examined by light microscopy and stained for PRL using immunohistochemical techniques. Plasma PRL concentrations were measured by radioimmunoassay. The morphologic criteria developed to distinguish spontaneous hypertrophic, hyperplastic and neoplastic lesions of the rat pituitary corresponded well with their PRL immunoreactivity and/or ability to elevate plasma PRL concentration. Thus, the criteria constitute a biologically meaningful classification system for spontaneous pituitary lesions in rats.

In CHAPTER III MRI was evaluated as a method for the early detection of estrogen-induced pituitary enlargement in rats. Following subcutaneous implantation of an estrogen-containing pellet in male rats, differences in the MR images of the pituitary gland between implanted and control rats were first detected after 16 days. The gland in the implanted rats was diffusely enlarged with rounded margins, when viewed in sagittal, T1 weighted images. Additionally, signal intensity was not uniform in the enlarged pituitary of estrogen-implanted rats, while uniform signal intensity was common in control rats. A parallel study demonstrated that pituitary weights in estrogen-treated rats were statistically significantly increased after implantation from 18 to 35 days onwards. Midline sagittal T1 weighted images proved to be the most effective and reproducible technique to visualize the shape of the rat pituitary gland.

The development of estrogen-induced pituitary lesions was studied in a time-sequence experiment using MRI, plasma hormone determinations, and light microscopy (CHAPTER IV). Measurements were made at 15 time points, ranging from 1 hour to 272 days after subcutaneous implantation of an estrogen pellet. The first histopathological pituitary changes were seen on day 2. Acidophilic cells were enlarged and contained an increased number of vacuoles. On day 4 the first immunohistochemical changes were seen as an increase in the number of PRL-positive cells. Significantly increased PRL levels in plasma occurred from day 9 onwards. Gradual enlargement of the pituitary caused by hyperplasia of hypertrophic PRL-positive cells could be followed by MRI from day 9 onwards. From day 186 onwards pituitary tumors were present as determined by light microscopy. Their MR images were heterogeneous due to great differences in signal intensity ranging from hypo- or iso- to hyperintense. Signal intensities of hemorrhagic tumor areas varied widely, probably due to variation in the blood flow in these areas. The sensitivity of MRI was insufficient to detect small intraparenchymal hemorrhages which developed during the first 5-6 months following estrogen implantation, or small numbers of these hemorrhages. In conclusion, MRI appeared to be a

powerful tool for detecting pituitary enlargement and tumors of the pituitary, allowing the development of such lesions to be followed in the same animal. Small focal lesions as intraparenchymal hemorrhages, however, cannot readily be detected.

In an attempt to explain the widely varying signal intensities of hemorrhagic tumor areas, the paramagnetic relaxation contrast agent Gadolinium-DTPA (Gd-DTPA) was used to improve the detection and characterization of these hemorrhagic areas (CHAPTER V). Gd-DTPA is a very stable, chelate complex that acts by enhancing T1 and T2 relaxation rates for water. This complex can be administered intravenously in concentrations sufficient to cause reduction of longitudinal magnetization relaxation times in specific tissues. These tissues then appear with enhanced intensity on T1 weighted images. The pituitary is an endocrine organ with a rich blood supply and a dense network of sinusoids. Assuming that Gd-DTPA after distribution in the intravascular compartment rapidly passes into the interstitial compartment, it is likely that this contrast agent appears in the pituitary in a matter of minutes following injection. Indeed, in normal rats and in rats with an estrogen implant for less than 87 days image enhancement by Gd-DTPA was immediate. Hypertrophic pituitaries displayed uptake of contrast, but the distribution of contrast agent was nonuniform and the image was mottled. Histological slides in the same anatomical plane as the MR images were obtained, allowing identification of individual lesions. Cystic areas within tumors were found to give strong contrast enhancement in less than five minutes after injection. Solid and hemorrhagic areas of the pituitary tumor were hypo- to isointense relative to surrounding brain tissue, and they did not take up contrast agent. Histopathological analysis demonstrated that solid areas in the pituitary tumors lack sinusoids, which explains why little or no enhancement occurred. Hemorrhagic areas, however, consisted of sinusoids and cyst-like formations filled with red blood cells which accounted for the bulk of the tumor volume. Significant perfusion apparently did not occur in these areas.

The lack of Gd-DTPA in the hemorrhagic areas of the pituitary tumors led us to examine the formation of the blood-filled cavities in developing tumors of the anterior pituitary of estrogen-treated

rats (CHAPTER VI). At 15 time points ranging from 7 to 272 days after subcutaneous implantation of an estrogen pellet, pituitaries were examined using light and electron microscopy. In chronological order the following changes were seen: swelling and arrangement in trabeculae of epithelial cells which contained increased amounts of rough endoplasmic reticulum, Golgi structures, and electron dense secretory vacuoles; arrangement of epithelial cells in islands and endothelial degeneration; distended sinusoids, as well as sinusoids compressed by swollen epithelial cells; endothelial degeneration and necrosis; loss of basement membranes as well as focal occurrence of multiple basement membranes; and scattered necrotic and immature epithelial cells of reduced size. The endothelial necrosis, loss of basement membrane, and both distended and compressed sinusoids became increasingly more prominent, finally resulting in blood-filled cavities partially lined by epithelium. Thus local compression of sinusoids due to epithelial cell swelling (and perhaps also compression of pituitary surface veins due to a volume increase of the gland) is likely to play a primary role in the development of ischemic endothelial damage leading to loss of endothelial lining and basement membrane, and eventually to the formation of blood-filled spaces partially lined by epithelial cells. No signs of stasis were found in the hemorrhagic areas. Probably only a very slow blood flow was maintained in these hemorrhagic tumor areas, which may explain the lack of signal enhancement in these areas early after administration of the contrast agent Gd-DTPA and observed in an earlier study (Chapter V).

The study described in Chapter IV demonstrated that the first histopathological pituitary changes were seen on day 2 after initiation of estrogen-treatment and the first changes in staining for PRL on day 4. The first MRI changes however, were not apparent until day 9. In CHAPTER VII detection of changes at an earlier time using more in depth analysis of the MR intensity variation has been described. To detect subtle intensity changes, computer generated 2 dimensional scatterplots of MR images were used to analyze the pituitary MRI data of estrogen-treated rats. T1 and T2 weighted axial images of the rat head at the level of the pituitary were obtained. The intensities of the pituitary (pars distalis) were plotted in a 2 dimensional scatterplot which was referenced to a similar scatterplot of a region in adjacent brain (hypothalamus). The pars distalis had more texture in these plots than the

surrounding hypothalamic area. T2 weighted image intensity of the pars distalis increased relative to the adjacent hypothalamic area as early as on day 4 after estrogen implantation, whereas no change in intensities of the pars distalis was noted on the T1 weighted images. Large dispersion and variation in the intensity of the pars distalis were observed on T1 weighted images in both control and experimental animals. No consistent pattern was identified in these changes and therefore we conclude that T1 weighted image intensities do not provide useful information in this animal model. Image intensity on T2 weighted images, however, corresponded with pituitary pathology, provided that the region of examination was limited to the pars distalis, and that the measurements were referenced to an external tissue, i.e., brain. In conclusion, the use of scatterplots incorporating the intensity information from both T1 and T2 weighted images provides a highly sensitive means of identifying very early changes in the pituitary in this rat model. This technique possibly detects pituitary changes earlier after estrogen implantation than MRI which relies on changes in shape detected in midsagittal MR images of the pituitary in estrogen-treated rats.

In CHAPTER VIII growth or shrinkage of the estrogen-induced enlarged rat pituitary gland was monitored after withdrawal of the estrogen stimulus using MRI and histopathological and immunohistochemical examination. The estrogen pellet was removed at 4, 8, 16, 81, 114, 186 and 206 days after pellet implantation. High resolution mid-sagittal MR images of the rat heads were made one day before pellet implantation, immediately following pellet removal, and at 14 and 28 days after pellet withdrawal. The animals were killed 28 days after pellet withdrawal and pituitaries were collected fixed in formalin and subsequently processed for histological and immunohistochemical investigation. MRI detected hypertrophic pituitaries from day 16 after implantation onwards. Histological evidence of diffuse cellular hypertrophy and hyperplasia was evident from 9 days of estrogen exposure onwards. Twenty eight days after estrogen withdrawal the typical triangular shape, characteristic for the MR image of the normal pituitary, had returned in all rats treated with estrogen for 16 up to 186 days. Light microscopic appearance was back to normal in rats treated for 4 up to 114 days. Rats that received estrogen for 186 days had multiple focal hyperplasias of PRL-positive cells throughout the pars distalis 28 days after estrogen withdrawal. These multiple focal hyperplasias have not

previously been described in estrogen-treated animals. After 206 days of estrogen treatment pituitaries of treated rats were tumorously enlarged with a great variability in MRI signal intensity, ranging from hypo-, iso- to hyperintense relative to surrounding brain tissue. There was no tumor regression obtained in these animals after pellet removal for 28 days as determined by MRI and light microscopy. In conclusion, estrogen withdrawal in the early stages of pituitary tumor development induced by estrogen (hypertrophic pituitaries) results in a return to a normal pituitary size and shape, whereas withdrawal of estrogen stimulus once tumorous pituitaries have developed does not lead to tumor regression. After 186 days of estrogen treatment followed by a 28-day non-treatment period, focal hyperplasias have developed in the hypertrophic pituitary that do not regress following estrogen withdrawal. These hyperplastic lesions were not visible by MRI. Thus MRI proved to be an effective technique to display changes in pituitary shape, size, and structure although small focal hyperplasias were not detected.

## GENERAL CONCLUSIONS

The following conclusions can be drawn from the research described in this thesis:

- I. The shape and signal-intensity of small organs in the rat such as the pituitary gland, can be excellently visualized by MRI. Even smaller structures than the pituitary, such as the cranial nerves III and VI could be visualized.
- II. Since the pituitary gland is fixed within the cranium, changes in rat pituitary shape caused by, e.g. glandular hypertrophy, cysts, and neoplasia can be nicely visualized and followed over time by MRI. Thus, the pituitary, together with tissues such as brain, is an excellent model tissue for MRI studies.
- III. Focal, microscopic-size hyperplasia in the rat pituitary cannot be detected using MRI.
- IV. MR images of normal and hypertrophic pituitaries, but not pituitary tumors, in the rat can be intensified using the contrast-enhancing compound Gadolinium-DTPA.
- V. Slight changes in signal intensity of MR images can be analyzed and interpreted using two-dimensional scatterplots and sensitive statistical analysis thereof.

The studies described in this thesis also allow the following remarks:

- The estrogen-induced pituitary tumor model in the rat used appeared very suitable for studying the pathogenesis of proliferative pituitary lesions such as the focal hyperplasia observed 4 weeks after cessation of 6 months-long estrogen treatment.
- This animal model can be further refined by integration of MRI and histopathology data on spontaneous pituitary changes in the characterization of the estrogen-induced pituitary lesions.
- MRI is a potentially useful tool for the testing of therapeutic regimens for pituitary tumors in this animal model.
- Metabolism studies in rat pituitary tissue using localized MRI spectroscopy is a potential future application of these powerful non-invasive techniques.
- Application of MRI techniques can contribute to a marked reduction of the number of experimental animals, because development of tissue changes can be followed over time without the need for interim sacrifices. In addition, in life lesion development can be followed and optimal sacrifice times can be selected leading to increased quality of experimental results.





## **SAMENVATTING**





## SAMENVATTING

In de adenohipofyse van oude ratten worden vaak hyperplastische en neoplastische veranderingen aangetroffen. Vergelijkbare afwijkingen komen voor bij de mens. In veel gevallen wijst een verhoogde prolactinespiegel op de aanwezigheid van een hypofysetumor. Voor hyperplasieën en sommige tumoren van de hypofyse geldt dit echter niet. Magnetic resonance imaging (MRI) is een nieuwe techniek voor detectie en diagnose van zulke hypofyse-lesies bij de mens<sup>1</sup>.

Het hoofddoel van het onderzoek beschreven in deze dissertatie was het beoordelen van MRI technieken op hun bruikbaarheid voor het opsporen van hypofyseveranderingen bij de rat. Hiertoe werd een classificatiesysteem voor hypofyselesies bij de rat ontwikkeld, en werden MR beelden van hypofyzen vergeleken met histologische beelden en met veranderingen in hypofysehormoonspiegels in het bloed.

In **HOOFDSTUK II** wordt onderzoek beschreven naar de voorspellende waarde van plasmaprolactine (PRL)-spiegels voor het voorkomen van spontane lesies in de pars distalis van de hypofyse bij de rat. Een breed scala aan lesies werd waargenomen variërend van foci van hypertrofe cellen en focale hyperplasieën tot en met tumoren. De aanwezigheid van foci van hypertrofe cellen of van focale hyperplasieën ging niet gepaard met afwijkende PRL-spiegels in bloed plasma. Afgezien van een enkele vals negatieve waarneming bleken verhoogde PRL-spiegels te correleren met de aanwezigheid van hypofysetumoren bij zowel mannelijke als vrouwelijke ratten. Met behulp van multivariantie-analyse werden significante positieve correlaties gevonden tussen plasma PRL-spiegels en aanwezigheid, omvang en mate van PRL immunopositiviteit in hypofysetumoren. Echter de aanwezigheid van focale hyperplasieën (immunopositief voor PRL) en van foci van hypertrofe cellen (immunonegatief voor PRL) ging niet gepaard met afwijkende plasma PRL spiegels. De morfologische criteria die voor het

onderscheiden van de hypofyselesies werden gebruikt bleken derhalve goed te correleren met de mate van PRL immunoreactiviteit van de lesies en/of met hun vermogen om de PRL-spiegels te verhogen. Hiermee heeft het gebruikte classificatiesysteem een biologische basis. De beperkte diagnostische betekenis van verhoogde plasma PRL spiegels voor de aanwezigheid van hypofysetumoren bij de rat komt overeen met de situatie bij de mens.

Het onderzoek in **HOOFDSTUK III** heeft aangetoond dat het mogelijk is om met MRI in een vroeg stadium hypofyselesies bij de rat op te sporen. Nadat bij mannelijke ratten oestrogeen pellets subcutaan waren geïmplanteed, werden de veranderingen in de vorm van de hypofyse met behulp van MRI in de tijd gevolgd en gekarakteriseerd. MR-beelden werden onder verschillende hoeken gemaakt. Een mid-sagittale doorsnede van de hypofyse bij een controle rat laat een driehoekig profiel zien. Reeds 16 dagen na de oestrogeen pellet implantatie waren veranderingen in de vorm van de hypofyse zichtbaar. De craniale zijde van de driehoek was licht opgebold en de hoeken vertoonden enige ronding. Tevens was de intensiteit van het beeld van de hypertrofe (vergroete) hypofyse niet meer homogeen. Uit een parallelstudie bleek dat de hypofysegewichten van de met oestrogeen behandelde ratten voor het eerst significant toe waren genomen tussen dag 18 en 35 na pelletimplantatie. Geconcludeerd werd dat een sagittale MRI doorsnede door het midden van de ratte kop de meest reproduceerbare beelden oplevert ten behoeve van het opsporen van hypertrofe hypofyzen.

In een volgende studie (**HOOFDSTUK IV**) werd de ontwikkeling van hypofysetumoren bij de rat bestudeerd door MR-beelden van de hypofyse te vergelijken met hormoonspiegels in het bloed en met de histopathologie van de hypofyse. Op 15 tijdstippen variërend van 1 uur tot 272 dagen na oestrogeen implantatie werden MR-opnamen van

<sup>1</sup> Een korte uitleg van deze techniek is opgenomen als addendum bij deze samenvatting (pagina 125)

de hypofyse gemaakt en werd de hypofyse histopathologisch en immunohistochemisch bestudeerd, terwijl tevens de plasmaspiegels van een aantal hypofysehormonen werden bepaald. Twee dagen na het begin van oestrogentoediening werden voor het eerst histopathologische veranderingen in de hypofyse gezien. De acidofiele cellen waren vergroot en hun cytoplasma bevatte veel vacuolen. Vanaf dag 4 was een toename van het aantal PRL-positieve cellen te zien. PRL spiegels in het bloed waren significant verhoogd vanaf dag 9, terwijl op deze dag ook voor het eerst veranderingen in het MR beeld van de hypofyse waren te zien. Een geleidelijke vergroting van de hypofyse, veroorzaakt door hyperplasie van de hypertrofe PRL-positieve cellen kon met MRI worden gevolgd. Ook het ontstaan en de verdere ontwikkeling van hypofysetumoren konden met MRI goed worden gevolgd. De MR signaalintensiteit van de verschillende gebieden in de tumoren varieerde per dier van hypointens (donker) via isointens (gelijk aan omliggend weefsel) tot hyperintens (licht). Deze gebieden met sterk wisselende intensiteit bleken overeen te komen met de histologisch waargenomen haemorrhagische gebieden in hypofysetumoren. De wisselende intensiteit van deze haemorrhagische gebieden werd toegeschreven aan verschillen in de mate van bloeddorstrooming. Geringe histopathologische veranderingen zoals intraparenchymale bloeddinkjes of kleine hyperplasieën konden niet met MRI worden waargenomen. Niettemin kan worden geconcludeerd dat MRI een gevoelige techniek is voor het opsporen van hypofysevergroting en hypofysetumoren bij de rat. Deze techniek maakt het mogelijk zulke hypofyseveranderingen in de tijd te volgen in hetzelfde dier; hierdoor vermindert de behoefte aan tussentijds opofferen van dieren met als gevolg dat er voor dit soort experimenten minder dieren nodig zijn.

De sterk wisselende signaalintensiteiten van haemorrhagische hypofysetumoren vormden de aanleiding voor een studie naar de doorbloeding van deze hypofyselesies waarbij ten behoeve van het MRI-onderzoek het contrastmiddel Gadolinium-DTPA (Gd-DTPA) werd toegepast (**HOOFDSTUK V**). Gd-DTPA is een paramagnetische stof die na intraveneuze toediening een hoge signaalintensiteit (sterke oplichting) veroorzaakt op de plaats waar het terecht komt. Opname van Gd-DTPA door hypertrofe hypofyzen was reeds enkele minuten na toediening zichtbaar op de MR-beelden. Dit is niet opzienbarend omdat de hypofyse als endocriene

klier over een rijk netwerk van bloedvaatjes beschikt. Het MR beeld van de hypertrofe hypofyse was niet uniform en vertoonde een licht-en-donker stippeling hetgeen wijst op een onregelmatige verspreiding van het contrastmiddel in de hypofyse. Hypofysetumoren vertoonden een ander beeld: slechts zeer kleine gebiedjes toonden een verhoogde intensiteit; kennelijk was het contrastmiddel slechts in zeer beperkte mate opgenomen. De resterende delen van de tumor bleven donker of hadden dezelfde intensiteit als het omliggende hersenweefsel, zelfs een uur na toediening van het contrastmiddel. Histologisch onderzoek van de hypofysetumoren liet zien dat de in helderheid toegenomen gebiedjes cysten waren. De haemorrhagische en solide delen waren niet of soms in zeer geringe mate in helderheid toegenomen. Dat solide gebieden dit contrastmiddel niet opnemen is niet verwonderlijk omdat histopathologisch onderzoek heeft uitgewezen dat deze gebieden weinig of geen bloedvaatjes bezitten. Daarentegen wekt het wel verbazing dat de haemorrhagische gebieden nauwelijks contrastmiddel hadden opgenomen. Deze gebieden bevatten namelijk veel bloedvaatjes en cysteuze structuren gevuld met bloed en vormden daarmee het overgrote deel van de haemorrhagische gebieden in de hypofysetumoren.

Omdat geen verklaring kon worden gegeven voor de afwezigheid van Gd-DTPA in de bloedrijke gebieden van de hypofysetumoren werd onderzoek uitgevoerd naar de pathogenese van deze haemorrhagische gebieden (**HOOFDSTUK VI**). Met behulp van lichtmicroscopie en transmissie electronenmicroscopie werd op 15 tijdstippen, variërend van 7 tot 280 dagen, na implantatie van de oestrogeen pellet de hypofyse onderzocht. In chronologische volgorde werden de volgende veranderingen geconstateerd: (1) proliferatie van hypertrofe epitheelcellen die veel ruw endoplasmatisch reticulum, Golgi-systemen en secretoire vacuolen bevatten; (2) deze cellen rangschikken zich vervolgens in rijen en vormen allengs steeds groter wordende eilandjes; (3) tegelijkertijd treedt er enerzijds verwijding en anderzijds compressie van bloedvaten op; (4) endotheelcellen gaan degeneratieve veranderingen vertonen en basaalmembranen verdwijnen, waarschijnlijk tengevolge van mechanische schade door de steeds in omvang toenemende eilandjes en compressie van bloedvaatjes hetgeen tot lokale ischemie leidt; (5) dit veroorzaakt verlies van endotheelcellen en basaalmembranen waardoor de met bloed gevulde holten ontstaan die bekleed zijn

met epitheelcellen en die de uiteindelijke haemorrhagische gebieden vormen in de hypofysetumoren. In de haemorrhagische tumorgebieden werden geen tekenen van stasis gevonden; waarschijnlijk is er een zeer geringe en langzame bloeddorstrooming hetgeen de afwezigheid van zowel het contrastmiddel Gd-DTPA als tekenen van stasis zou kunnen verklaren.

Uit het onderzoek beschreven in hoofdstuk IV bleek dat reeds op de dagen 2 en 4 na oestrogeentoediening bij de rat histopathologische en immunohistochemische veranderingen in de hypofyse konden worden aangetoond. In **HOOFDSTUK VII** is beschreven of dit soort vroege veranderingen met behulp van MRI te detecteren is. Om veranderingen in de hypofyse waar te nemen voordat de anatomie verandert, werden computer gegenereerde 2 dimensionale scatterplots gemaakt van de pars distalis en van een deel van de hypothalamus dat als referentiegebied diende. Met T1 en T2 gewogen axiale beelden van de rattekop konden de intensiteitsverschillen in de scatterplots tussen de hypofyse en het referentiegebied bestudeerd worden. Na 7 dagen oestrogeen toediening bleek de intensiteit van de hypofyse ten opzichte van de hypothalamus in T2 gewogen beelden toe te nemen terwijl in T1 gewogen beelden geen verandering in intensiteit te zien was. Geconcludeerd werd dat scatterplots verkregen uit de intensiteitsinformatie van T1 en T2 gewogen beelden bruikbaar zijn voor het identificeren van hypofyselesies. Een grote spreiding en variatie in intensiteit van T1 gewogen beelden van de hypofyse waren op de scatterplots te zien waardoor T1 afvalt als mogelijke indicator. Daarentegen correleerde het intensiteitsverschil van T2 gewogen beelden goed met de geïnduceerde hypofyseveranderingen mits de metingen zich beperkten tot de pars distalis en mits in het omliggende weefsel steeds hetzelfde gebied als referentie werd gebruikt.

Het onderzoek beschreven in **HOOFDSTUK VIII** laat zien in hoeverre MRI bruikbaar is voor het vaststellen van progressie of regressie van oestrogeen geïnduceerde hypofyselesies bij ratten na verwijdering van de oestrogeenstimulus. De oestrogeenstimulus werd verwijderd op 7 verschillende tijdstippen variërend van 4 tot 206 dagen na implantatie van de oestrogeenpellet. MR beelden van de hypofyse werden gemaakt een dag voor pelletimplantatie, onmiddellijk na verwijdering van de pellet en

vervolgens 14 en 28 dagen later. Achtentwintig dagen na verwijdering van de pellet werden de ratten gedood en werd de hypofyse ook histopathologisch en immunohistochemisch bestudeerd. Vanaf dag 16 lieten MR-beelden een vergrote hypofyse zien. Tot en met dag 186 na pelletimplantatie bleken de MR-beelden van de hypofyse opgenomen na een herstelperiode van 28 dagen niet te onderscheiden van die van controle dieren. Een opvallende waarneming was dat bij dieren die gedurende 186 dagen met oestrogeen waren behandeld, na een herstelperiode van 28 dagen, in de hypofyse multiple focale hyperplasieën van PRL-positieve epitheelcellen voorkwamen. In andere studies waren hypertrofe en hyperplastische cellen altijd diffuus over de hypofyse verspreid. De betekenis van deze hyperplastische foci is voornamelijk onduidelijk. Tweehonderdzes dagen na implantatie van de oestrogeenpellet waren de hypofyzen tumorachtig veranderd en vertoonden de MR beelden de kenmerkende hypo-, iso- en hyperintense gebieden. Na verwijdering van de oestrogeenstimulus was er bij deze dieren geen sprake van regressie van de hypofyselesies; integendeel, de tumoren namen in omvang toe of bleven gelijk van grootte. Uit dit onderzoek werd geconcludeerd dat hypofyzen met hypertrofe veranderingen zich weer herstellen, terwijl neoplastische hypofyselesies blijven bestaan of progressief doorgroeien. Voorts bestaat er kennelijk een tussenvorm waarbij focale hyperplasieën ontstaan waarvan het gedrag op de lange termijn nog onbekend is. Opnieuw bleek MRI een geschikte techniek om het verloop van (bepaalde) hypofyselesies te volgen.

## ALGEMENE CONCLUSIES

Uit onderzoek beschreven in dit proefschrift kunnen de volgende conclusies worden getrokken:

- I. Vorm en intensiteit van kleine organen zoals de hypofyse bij de rat zijn met MRI goed zichtbaar te maken. Zelfs nog kleinere structuren zoals de craniale zenuwen III en VI konden worden gevisualiseerd.
- II. Omdat de hypofyse niet beweegt zijn veranderingen in vorm veroorzaakt door bijvoorbeeld hypertrofie, cysten of tumoren met MRI goed waar te nemen en is hun ontwikkeling goed te volgen.
- III. Focale, alleen microscopisch waarneembare hyperplasieën, kunnen met MRI niet worden

waargenomen.

- IV. Met behulp van het contrastmiddel Gadolinium-DTPA kunnen de MR-beelden van de normale en hypertrofe hypofyse worden geïntensiveerd.
- V. Geringe veranderingen in de intensiteit van de MR-beelden kunnen met behulp van twee dimensionale scatterplots en gevoelige statistische methoden worden geanalyseerd en geïnterpreteerd.

De beschreven studies geven voorts aan dat:

- Dit oestrogeen rattehypofysemodel zich goed leent voor het bestuderen van het ontstaan en de ontwikkeling van hypofyselesies, zoals bijvoorbeeld de focale hyperplasieën waargenomen na het wegnemen van de oestrogeenstimulus na zes maanden.
- Dit model verder verbeterd kan worden door nadere karakterisering van spontane hypofyselesies met behulp van MRI.
- MRI een belangrijke rol kan spelen bij het testen van de effectiviteit van geneesmiddelen in dit model.
- Met behulp van lokaal MRI-gestuurde spectroscopie, metabolisme onderzoek in hypofyselesies mogelijk lijkt te zijn.
- Toepassen van MRI in dit model proefdierbesparend werkt omdat bij het volgen van afwijkingen in de tijd tussentijds opofferen van de dieren wordt beperkt.

## ADDENDUM

MRI maakt gebruik van de eigenschappen van magnetisme, radiogolven en protonen. Aantrekkingskrachten tussen lichamen is al sinds de prehistorie bekend. De eerste die systematisch de aantrekkingskrachten onderzocht was de Griek Thales (640-564 v.Chr.) Thales noemde de ijzer aantrekkende materialen "Ho magnetes lithos" naar de plaats Magnesia waar deze stenen vandaan kwamen. Sindsdien is veel onderzoek aan magneten, zoals we die vandaag de dag noemen, en het fenomeen magnetisme gedaan. De elektromagneet is in 1823 ontwikkeld door de Engelsman William Sturgeon (1783-1850).

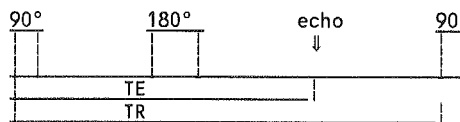
In 1946 verschenen de eerste publikaties omtrent Nuclear Magnetic Resonance (NMR) of te wel Kern Spin Resonantie (het lokaliseren en detecteren van atoomkernen die een magnetisch moment bezitten). De onderzoekers Bloch en Purcell publiceerden NMR waarnemingen die een eerdere suggestie van de Nederlander Gorter bevestigden. In de chemie en biochemie werd NMR vanaf die jaren een belangrijk hulpmiddel bij de structuuropheldering van organische en anorganische stoffen. Decennia later (rond 1973) waren het Lauterbur, Mansfield en Demedian die de afbeeldingstechnieken met behulp van NMR-technieken ontwikkelden: Magnetic Resonance Imaging (MRI) zoals dat tegenwoordig heet. Rond 1980 kwamen de eerste instrumenten op de markt. Een voorwaarde om met MRI verkregen beelden te kunnen beoordelen is dat de onderzoeker op de hoogte is van de fysische aspecten van het beeldvormende proces.

Het menselijk en dierlijk lichaam bestaat voor 80% uit water. Dit is te splitsen in waterstof, zuurstof en andere substantiële delen. Waterstofkernen bevatten protonen die een magnetisch moment bezitten. Wanneer een lichaam in een sterk magneetveld wordt geplaatst zullen de protonen reageren als kompasnaalden en evenwijdig aan het magneetveld gaan staan spinnen (denk aan snel draaien van een tol). Door een radiofrequentiepuls, die wel aan een bepaalde resonantiewaarde moet voldoen, is het mogelijk om de longitudinale magnetisering om te zetten (denk aan de tol die zeer snel draait) in transversale magnetisatie (dit komt overeen met de uitslag van een tol die heel langzaam draait). Een signaal, uitgezonden door de protonen, kan nu ontvangen worden. Dit gebeurt met behulp van een antenne en een FM radio ontvanger. De antenne is een in een aantal bochten gedraaide koperdraad in de vorm van onder andere een zadel, de zogeheten "saddle coil", die afgestemd moet worden op de

reeds eerder genoemde resonantievoorwaarden (de Lamor frequentie). De FM radio ontvanger is aangesloten op een computer zodat de ontvangen wisselstroompjes kunnen worden opgeslagen om later in een beeld te worden omgezet. De uiteindelijke gegenereerde hoeveelheid protonen is afhankelijk van de sterkte van de magneet en de hoeveelheid protonen die de afzonderlijke weefseldelen van het lichaam bevatten.

De tijdstippen en de duur waarop radiofrequentie-pulsen worden uitgezonden en wanneer signalen worden opgevangen worden bepaald door de TR en TE tijden in een te gebruiken pulssequentie. TE staat voor echotijd en is de tijd die gebruikt wordt tussen het genereren van een transversale magnetisering en het ontvangen van de echo. TR is de repetitietijd, dit is de tijd die ligt tussen een 90° puls tot het initiëren van een volgende 90° puls. De meest gebruikte pulssequentie vandaag de dag is de Spin Echo. In deze pulssequentie wordt een extra radiofrequentie puls (een refocuserende 180° puls) toegevoegd na de transversale magnetiseringspuls (de originele 90° puls). In schema ziet dat er als volgt uit:

Spin Echo, pulssequentie



Met het variëren van de TR en TE tijden wordt een bepaalde selectiviteit geïntroduceerd. Wanneer b.v. de TE heel kort is, zal alleen een signaal ontvangen worden van de protonen in weefsel die snel terugkeren naar de longitudinale magnetisering. Zo heeft ieder type normaal en pathologisch weefsel zijn eigen snelheid waarmee het terugkeert van de transversale naar de longitudinale magnetisering en zo kunnen met behulp van T1 gewogen beelden (zeer korte TE en TR) of met T2 gewogen beelden (lange TE en TR), de specifieke karakteristieken van weefsel soorten zichtbaar gemaakt worden. Deze imagingtechnieken werden toegepast in de MRI studies beschreven in de **Hoofdstukken III, IV, V, VII en VIII.**



## DANKWOORD/ACKNOWLEDGEMENTS

Het onderzoek beschreven in dit proefschrift is tot stand gekomen dankzij medewerking en hulp van velen die ik hiermee wil bedanken.

In het bijzonder wil ik Prof. Dr. Vic Feron danken die mijn promotor wilde zijn en als voormalig hoofd van de afdeling Biologische Toxicologie vertrouwen in mij stelde waardoor ik dit onderzoek kon uitvoeren. Je enthousiasme gaf mij altijd een veilig gevoel. Ook is het voor mij een bijzonder grote eer je eerste promovendus te mogen zijn.

Veel dank ben ik verschuldigd aan Prof. Dr. Bob Kroes als promotor en opleider, als ook aan Prof. Dr. Joost Ruitenbergh toenmalig hoofd van het Laboratorium voor Pathologie van het voormalige Rijks Instituut voor de Volksgezondheid (RIV). Jullie lieten mij destijds de vrijheid om te experimenteren en gaven richting aan mijn opleiding in de pathologie waarvan ik nu nog steeds de vruchten pluk.

Dank ben ik ook verschuldigd aan Prof. Dr. Steven Lamberts promotor van het eerste uur. Je deed mij inzien dat het hypofyseonderzoek waarmee ik wilde starten inhoudelijk de juiste wetenschappelijke vraagstelling bezat. De contacten die we hadden toen ik in de Verenigde Staten verbleef hielpen mij elke keer weer bij het volharden in mijn onderzoek.

Dr. Maarten Bosland: de lange discussies die we hadden over het hypofyse-onderzoek en de vele uren die jij gestoken hebt in de manuscripten zijn voor mij van onschatbare waarde geweest. Je inbreng bij het schrijven van het projectvoorstel was cruciaal. Ik heb veel van je geleerd. De vele telefonische contacten die we hadden toen ik in Syracuse werkte waren altijd plezierig en nuttig. Vele keren hebben jij en Marsha mij bij jullie thuis ontvangen toen ik op en neer reisde tussen Nederland en de Verenigde Staten. Heel veel dank voor jullie hulp en vriendschap.

Dank gaat ook uit naar Dr. Frieke Kuper, die met haar kritische blik zeer behulpzaam en een grote stimulans voor mij was.

De literatuurstudies die Drs. Bernadette van Nesselrooij en Drs. Pieter Deinum in het kader van hun wetenschappelijke stage uitvoerden, vormde een stevige basis voor het verrichtte onderzoek, veel dank hiervoor.

In mijn dank wil ik ook De Raad van Bestuur van TNO betrekken die de stage in de Verenigde Staten financieel ondersteunde uit het TNO fonds "innoverend onderzoek". De hulp van Ir. Bob de Lange, liaison postgraduate training, en van Drs. Robert Arlman, hoofd personeelszaken was hierbij onontbeerlijk.

Prof. Dr. Ir. Ruud Hermus, directeur van het Instituut voor Toxicologie en Voeding TNO (ITV-TNO), dank ik voor de gelegenheid die mij werd geboden om dit onderzoek uit te voeren.

Dr. A.P. de Groot, voormalig hoofd van de afdeling Biologische Toxicologie (ITV-TNO), veel dank voor de gelegenheid die ik kreeg om dit onderzoek uit te voeren.

Dank gaat ook uit naar Dr. Dolf Beems voormalig hoofd van de sectie Pathologie (ITV-TNO), die mij vanaf het begin binnen en buiten de afdeling ondersteunde in het promoten van het belang van MRI technieken bij toxicologisch onderzoek. Je hulp bij het uitzoeken van een locatie om mijn project te starten heb ik zeer gewaardeerd.

Prof. Dr. Peter van Bladeren, hoofd van de afdeling Biologische Toxicologie: veel dank voor de vrijheid die je me gaf en nog steeds geeft om dit type onderzoek voort te zetten.

Dr. Ruud Woutersen, hoofd sectie Pathologie: jij en Felice waren de eersten die ons kwamen opzoeken in de Verenigde Staten. We genoten daar erg van. Je hulp bij mijn verdere ontwikkeling wordt door mij zeer gewaardeerd; veel dank hiervoor.

Ik wil ook graag de medewerkers van de afdeling Biologische Toxicologie en met name van de sectie Pathologie bedanken. Veel werk hebben voor mij verzet: Lidy van Oostrum, Nel Hagemeyer, Erwin Schut, Hannie Jansen-de Ruiter, Greetje Stoepker, Truus Steenwijk-Krommendijk, Arda Vis-Löning, Wilma Stenhuis en Gerard Roverts.

Speciale dank gaat naar Joost Bruijntjes voor de vele immunoperoxidase kleuringen en naar Ferry Hendriksen voor het EM werk. Ook dank ik speciaal Annemarie van Garderen-Hoetmer die in mijn Amerikaanse periode de touwtjes op het thuisfront in handen had, en Marcel Nederhoff die zelfs overkwam naar de Verenigde Staten om een techniek uit te voeren die ter plaatse nog onbekend was.

Karin Hoefs en Jolanda de Bruin die ik ettelijke malen vroeg iets voor mij uit te typen; dank hiervoor.  
Rob van Rijn die de layout van het boekje voor zijn rekening nam en een fantastisch resultaat heeft bereikt; zeer bedankt.

Mijn kamergenoot Victor Hollanders die in de afgelopen periode heel wat te verduren heeft gehad maar alles laconiek over zich heen liet komen; veel dank.

Veel dank aan Gerrit de Kruyf, Ans van Tuyl en Gerard van Beek die mijn dieren op een voortreffelijke manier behandelden en verzorgden.

Bill Floor en Bert de Bie die alle RIA hormoonbepalingen hebben verricht; zeer bedankt.

I want to thank Prof. Stephen Kieffer M.D. and Prof. John McAfee M.D. for the temporary appointment they gave me as a visiting scientist in the Department of Radiology at the SUNY Health Science Center at Syracuse, New York, USA .

I especially want to express my thanks to Dr. Nick Szeverenyi for teaching me physics and the principles of MRI, for your hospitality and the place you gave me in your NMR research laboratory. Your collaborative spirit has resulted in many chapters of this thesis. You are a real friend and were a great help not only for me but also for my family. Also thanks to Gwen Tillapaugh-Fay and Cathy Ritter-Hrncirik for their technical support, you both are irreplaceable.

In het bijzonder wil ik mijn ouders bedanken die overtuigd waren dat ik zou promoveren, maar dit jammer genoeg niet kunnen meemaken. Hierin wil ik ook mijn familie en schoonfamilie betrekken die altijd zeer geïnteresseerd waren in het verloop van mijn studie en onderzoek.

Mijn paranimfen: Hanneke Garbis-Berkvens jij was niet alleen de grondlegster van het hypofyseonderzoek maar jij bracht mij ook de liefde voor het vak pathologie in de meest uitgebreide zin bij. Mijn broer Wiet die de omslag van dit boekje ontwierp waaruit zijn gefascineerdheid voor dit onderwerp mag blijken, heel veel dank. Carla, Iris en Vincent, ik vond deze periode zeer avontuurlijk en leerzaam. Ik weet dat jullie dit ook zo ervaren hebben. Ik dank jullie voor het vertrouwen, de inzet en de steun die mede tot een fantastische finale hebben geleid.







## CURRICULUM VITAE

De schrijver van dit proefschrift werd op 24 juli 1946 te Utrecht geboren. Vanaf 1964 was hij werkzaam bij het Laboratorium voor Pathologie van het Rijks Instituut voor de Volksgezondheid en Milieuhygiëne (RIVM), voorheen RIV, te Bilthoven. Het histopathologisch onderzoek in het kader van de toxicologische experimenten en het hypofyse onderzoek werden verricht onder leiding van Prof. Dr. R. Kroes en Prof. Dr. E. J. Ruitenbergh. Na de dienstplicht te hebben vervuld van '66-'68 werd in 1977 het HBO diploma behaald. Vanaf 1979 is hij bij de afdeling Biologische Toxicologie (Hoofd, Prof. Dr. P.J. van Bladeren) van het Instituut voor Toxicologie en Voeding TNO te Zeist (Directeur Prof. Dr. Ir. R.J.J. Hermus) werkzaam als experimenteel patholoog/projectleider. Van 1980 t/m 1986 is hij actief geweest in de OR van het Instituut voor Toxicologie en Voeding. Tijdens deze periode is hij tevens 2 jaar voorzitter van Groeps Ondernemingsraad van de Hoofdgroep Voeding en 2 jaar lid van de Centrale Ondernemingsraad van TNO geweest. Gedurende 2 jaar (van 1987 tot 1989) en parttime in 1990 werd MRI onderzoek verricht bij het NMR Research Laboratory, Dept. of Radiology, van de State University of New York, Health Science Center at Syracuse, Syracuse, NY, USA (Hoofd, Dr. N.M. Szeverenyi). In 1992 werd het HLO getuigschrift behaald. Gedurende de afgelopen 5 jaar gaf hij gestalte aan het MRI onderzoek binnen de afdeling Biologische Toxicologie van het Instituut voor Toxicologie en Voeding TNO te Zeist.









